Australian Government

Nuclear-based science benefiting all Australians

LITTLE FOREST BURIAL GROUND - GEOLOGY, GEOPHYSICS AND WELL INSTALLATION 2009-2010

Date of Issue	05 November 2012
Report No	E-781
ISBN	1 921268 22 0
ISSN	10307745

Stuart Hankin

Institute for Environmental Research

Summary

This document reports on a program of drilling at Little Forest Burial Ground undertaken in the period 2009-2010 under the supervision of the ANSTO's Nuclear Methods in Earth Systems (NMES) project.

Under this program, the following activities were undertaken:

- resistivity, ground penetrating radar and electromagnetic geophysical surveys to define the trench area and investigate stratigraphy;
- core and crushed soil/rock sampling by drilling (direct-push, solid flight auger and diamond core) at 0.5 metre intervals at 40 locations;
- installation and development of 18 groundwater observation wells;
- survey of new wells and trench boundary marks in MGA94 coordinates and AHD (Australian Height Datum).

This report presents:

- a summary of existing knowledge of the burial ground and neighbouring sites, including a detailed discussion of the geological setting (Chapter 1);
- the objectives for the work undertaken (Chapter 2);
- a detailed description of all methods used (Chapter 3);
- a discussion of geophysical, drilling and well construction results and observations of the campaign (Chapter 4);
- recommendations for further work (Chapter 5).

The appendices provide an extensive summary of the construction details of all operational wells at the site, including geological logs, survey coordinates and elevations. A brief evolution of the site as documented by aerial photography is included at Appendix C.

Interpretation of chemical/radiological data from the soil and water samples retrieved as a result of the drilling activities will be presented in separate reports.

Acknowledgements

The author wishes to thank Mat Johansen for guidance and mentorship during planning and execution of the field campaigns. Thanks also to Eve Chong, Matthew Dore, Jennifer Harrison, Cath Hughes, Mat Johansen, Tim Payne, Sangeeth Thiruvoth and Kerry Wilsher for contributions in the field. The author wishes to acknowledge Ander Guinea and Dioni Cendon in producing the electrical resistivity survey in 2011, and Mat Johansen for the contribution on soil moisture profiles. Thanks to Tim Payne, Cath Hughes and Mat Johansen for review of this document.

Table of Contents

See separate volume for appendices pages 93-178.

1 Introduction

Over 2009-2010, a program of drilling and well installation at the Little Forest Burial Ground (LFBG) was commissioned by the ANSTO Nuclear Methods in Earth Systems (NMES) project. At LFBG, the NMES project undertakes research into characterisation of radionuclide content and migration rate in the subsurface beneath and adjacent to the burial trenches through the groundwater pathway. Prior to this drilling project, adequate information on the transport of radionuclides from the trenches was not available because the existing LFBG wells were focused mainly on detection at the fence boundary, and because of the deterioration of some the older wells. The focus of this campaign was to obtain soil and rock samples, and to install observation wells at strategic locations determined to best achieve the multiple objectives of the project's research. Key objectives were:

- To characterise soils and lithofacies relevant to transport of contaminants from the trenches.
- To determine contaminant fluxes from the trenches laterally through surface soils, and downward through the underlying shale;
- Better understanding of contaminant transport in seepage/infiltration areas and the mixing of contaminants between LFBG and the adjacent Harrington's Quarry.

From this work:

- three types of geophysical data were acquired over the trench area
- 134 metres of intact rock core were retrieved by direct-push and diamond drilling methods at 31 locations to a maximum depth of 7 metres;
- 230 crushed rock samples were retrieved by auger drilling methods at 17 locations to a maximum depth of 9 metres;
- 18 observation wells were installed compliant with QNRM04027 (ARMCANZ, 2003) to a maximum depth of 20.5 metres.

Coring activities confirmed that the groundwater at the LFBG site does not conform to a typical shallow unconfined aquifer. But rather, much of the soil profile from 0 to 5 m is dry, with some relatively thin layers of saturation. During drilling, perched water was encountered at all drill locations within 5 metres of the trench area at approximately the same depth as the estimated base of the trenches. Dry weathered rock material was then encountered beneath the perched water zone. The presence of perched water at this depth suggests lateral water flow from the lower parts of the trenches, and hence also that the trenches may form a collection reservoir of input rainwater from the surface.

Four different design types of observation wells were installed (see Section 3.3). Type I and Type II shallow wells were designed to terminate within the upper weathered shale layer where the burial trenches lie. The Type I and II wells vary in design by hole and filter pack diameter, and Type I wells do not have a bottom seal below the filter pack. The Type III deep wells were designed to terminate only in the lower

sandstone layer. To ensure no contamination pathway was introduced to the lower sandstone, the Type III design specified a 2-stage installation process, in which a grout seal was first emplaced in a permanent outer casing in the base of the overlying shale. The Type III design required the seal to be proven watertight prior to continuation of drilling into the target sandstone. The seal was not able to be established to meet this design criteria, therefore the Type III wells were not completed into the sandstone in the trench area, and these wells were subsequently plugged by bentonite grouting. A Type IV angle well was installed at a 45 degree angle beneath trench 52.

Further drilling is recommended to complete installation of observation wells into the underlying sandstone beneath the trench area. However, a key feature of any wells penetrating the shale layer is an effective seal around the well casing that prevents seepage of contaminated water from above the shale downward into the underlying sandstone. Prior to commencing of future drilling, careful selection of suitable drilling equipment, personnel and methods are needed to ensure emplacement of an adequate seal.

1.1 Site background

The LFBG is located 1.5 km north of ANSTO (see **Figure 1**) and was used by the AAEC during the period 1960-1968 for the burial of low level radioactive waste. The site was first selected and investigated as a prospective burial site in 1957 due to its proximity to ANSTO and shale geology (Mumme, 1974). The site was chiefly used for disposal of contaminated solid laboratory waste and solidified sludge in packaging ranging from plastic bags to steel drums. Details of the waste contents may be found in AAEC, 1985, from which a summary table is included below at **Table 1**, although waste inventories are currently under review pending a thorough examination of the original AAEC Waste Operations records.

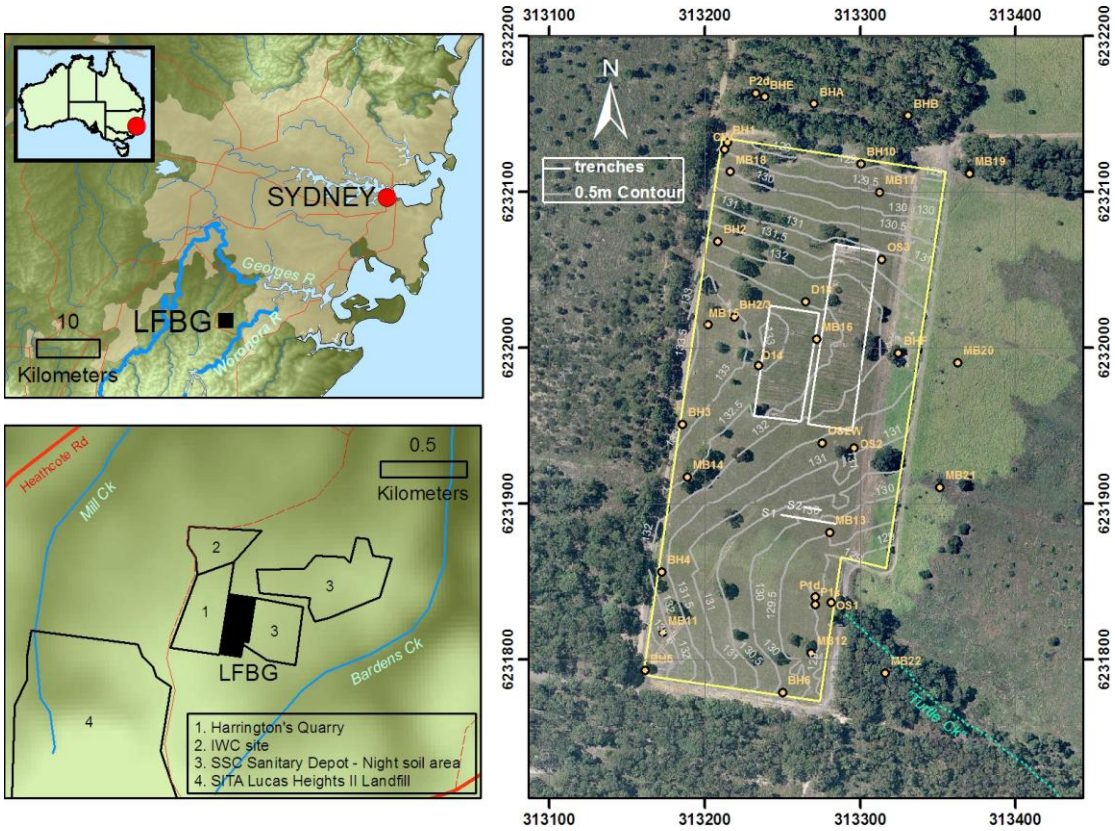

Figure 1. Location of LFBG showing aerial photograph 2007 and the existing bore network prior to this campaign.

Table 1. The burial history for the Little Forest Disposal Site (AAEC, 1985).

Year	Trenches filled	Estimated activity (mCi)[a]			Fissile content (g)			Fertile content (kg)		Be/BeO content	Liquid volume
		I	II	III	Pu	U^3	U^5	U	Th	(kg)	(m^3)
1960	1-5	0	0.1	0	0	0	0	0	0	0	0
1961	6-18	1	3.9	3.8	0	0	5.3	0.3	2.3	89.8	1.54
1962	19-26	0	4.2	6.2	0	0	23.6	0	0	105.4	2.25
1963	27-36	0	4.0	5.6	0	0	0	0	0	139.2	0.34
1964	37-46	0	77.6	74.6	0	0	18.2	3.8	0	237.1	0.09
1965	47-53	0	14.7	26.2	1.98	2.31	8.9	4.3	18.6	151.4	0.59
1966	54-61	0	39.4	20.8	4.44	0.4	17.6	0.3	5.6	157.6	2.88
1967	62-70 +S1	0	310	429	0.46	2.5	15.0	47.1	13.4	185.1	0.89
1968	71-76 +S2	19.3	603	2447	0	0	3.41	3.45	8.17	3.8	0

(a) The groups I, II, III are in descending order of radiotoxicity, based on drinking water standards[9]. U^3 and U^5 refer to uranium-233 and -235 respectively.

The waste at LFBG was emplaced in 79 parallel trenches, averaging 25 m long, 0.6 m wide and 3 metres deep and spaced 2.7 metres apart (AAEC, 1985). The trenches were machine excavated in clay and weathered shale (see **Figure 2**). After emplacement of waste, the trenches were back-filled with the excavated clay and weathered shale to create around a metre of overburden above waste materials.

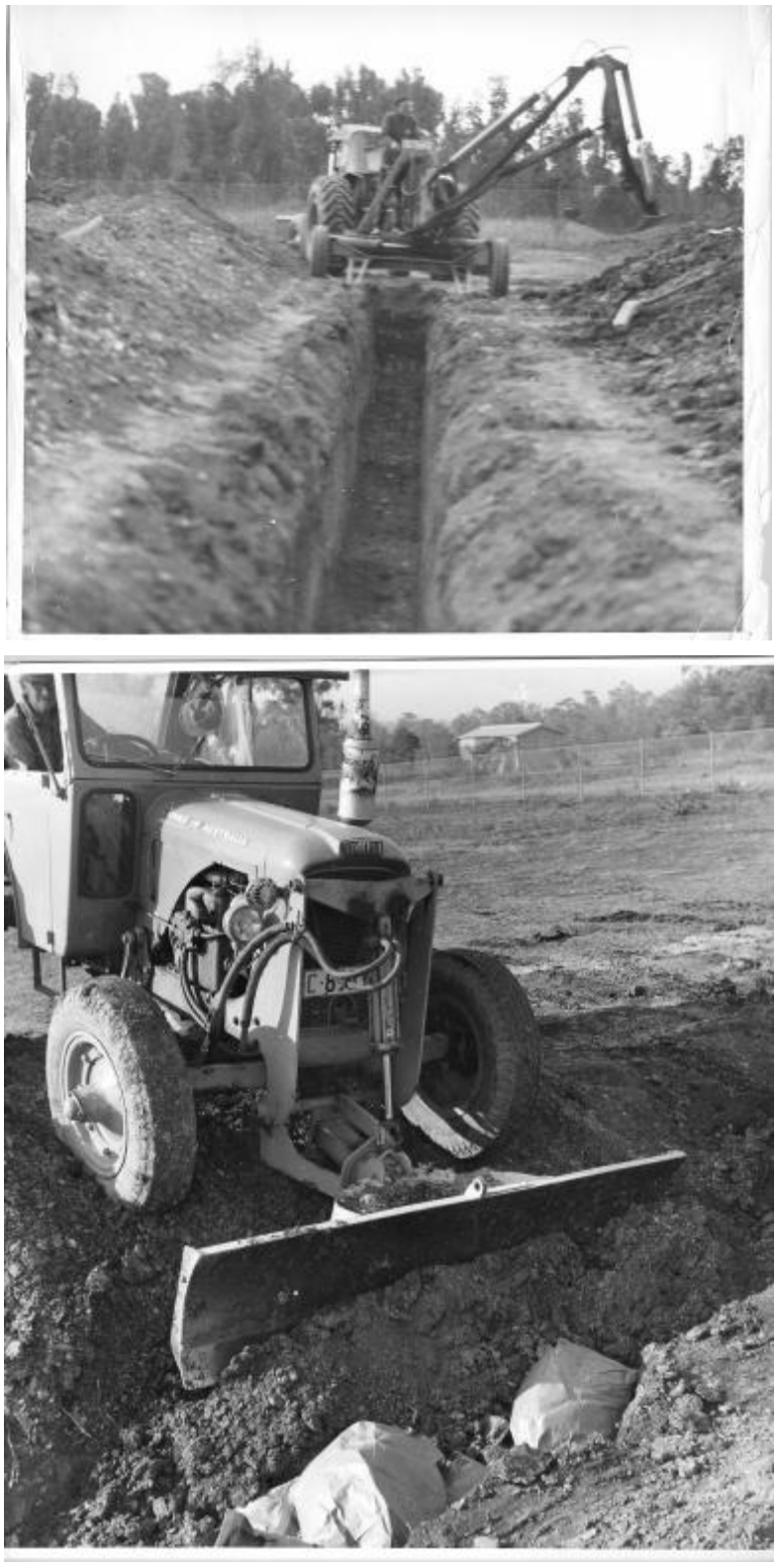

Figure 2. Original a) excavation and b) filling of trenches.

Some compaction and subsidence over various trenches has occurred since this time (see **Figure 3**), and some additional fill cover has been 'top-dressed' over areas of subsidence at various times as a remedial measure (AAEC, 1985).

Figure 3. Subsidence over trenches in March 1969.

The position of the start and end of each trench was marked with a labelled timber post (**Figure 4**). These were subsequently replaced in 1982 with 141 'Monier' wedge-shaped concrete marker posts pile-driven into the ground, and capped with an aluminium marker plate (AAEC, 1984).

Figure 4. Old trench marker posts.

The concrete marker posts were cut to ground level in 1984 and the aluminium capping retained. Marker posts are no longer visible at the site.

Today, the position and extent of the trenches is visible in many places from the ground surface on site, but visibility is greatly enhanced by aerial photography (**Figure 5**), now also available publicly online. This visibility appears to be due to a small amount of subsidence/compaction over each trench compared with the undisturbed material either side, and also a vegetation change where longer grass generally grows in the presumably more permeable trench fill material. A small step in the topography at the edge of the trench area (see **Figure 4**) was created by the back-filling or the top-dressing process, although the step is only visible at the northern, western and south-western edges of the trenches. At some locations however, particularly near trench ends, the exact extent of the trench boundary is not possible to distinguish by eye in the field.

Figure 5. Aerial photography over LFBG trenches, SKM, 2007 (see Figure 51 for trench numbering).

The only known survey data of the trench locations is contained in a drawing showing measurements of the position of each trench relative to a reference line 'XY' (see **Figure 6)** undertaken by contractor P.W. Rygate and West in 1970. The position of a reference line approximately normal to magnetic north was marked in the field with a nail in a concrete block at each end, labelled X and Y. The perpendicular distance in feet from the reference line XY to the ends of each trench, including trenches S1 and S2, was then measured. In addition, the distance from the eastern boundary fence-line was also measured for the ends of trenches 1, 37, 51, 52, 76, 77, S1 and S2. The eastern boundary fence has since been relocated 25 m further east, although the sawn-off ends of the old steel fence posts can still be relocated. Both X and Y concrete blocks are still visible on site today, and were surveyed as part of the 2010 well installation campaign (see Appendix D).

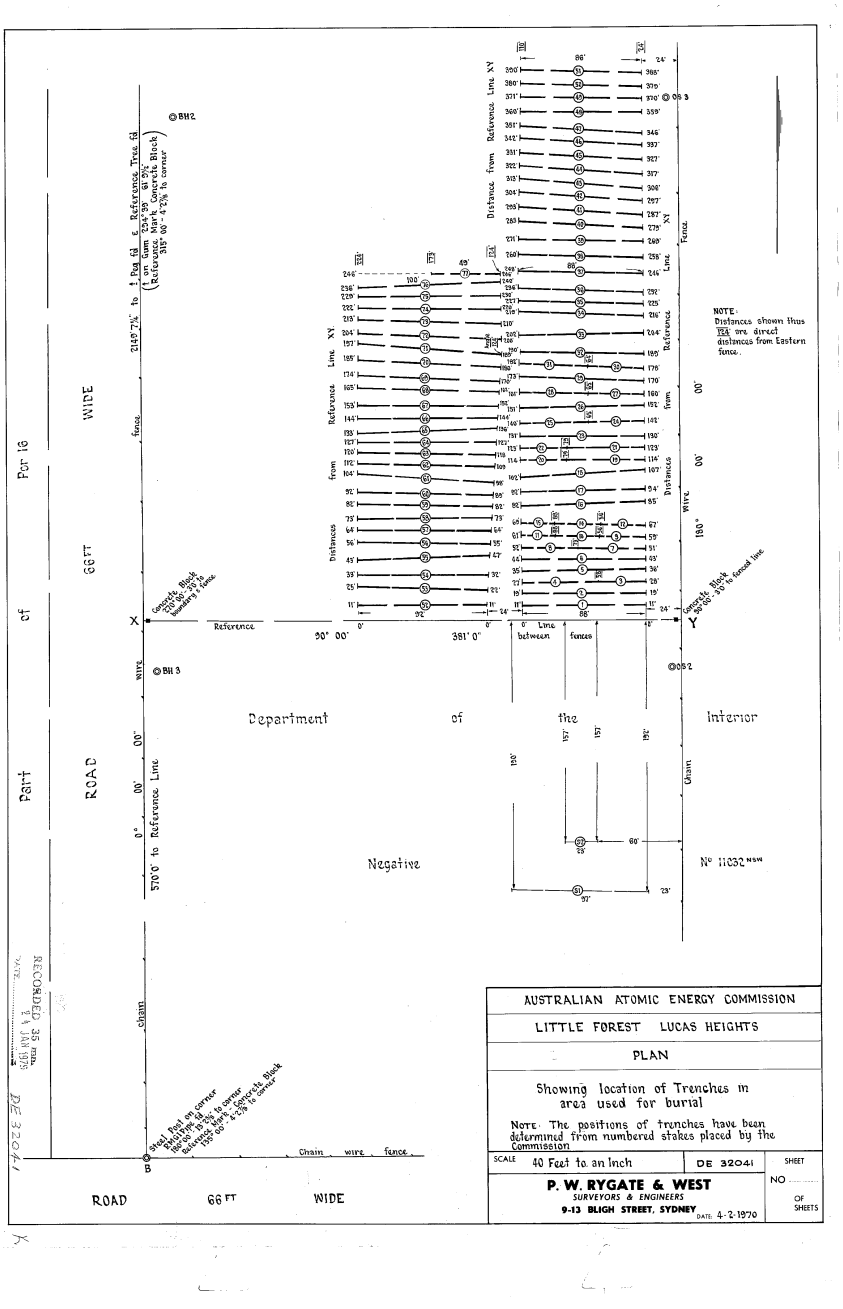

Figure 6. AAEC drawing number DE32041 – 'Plan – Showing location of trenches in area used for burial'. Note position of reference line XY.

The information contained in drawing DE32041 was also incorporated a survey plan **(**see **Figure 7)** showing the boundary and topographic contours of Harringtons Quarry in 1983, also by Rygate & West. The plan is presented with a grid of planar coordinates relative to the Integrated Survey Grid of NSW. In this plan, the position of X and Y concrete blocks are marked, but survey coordinates are not provided. Trenches S1 and S2 were omitted. Topographic information within LFBG was not included, although this was later surveyed by contractor Sinclair Knight Merz in 2003 to provide 0.5 m topographic contours (See Figure 1).

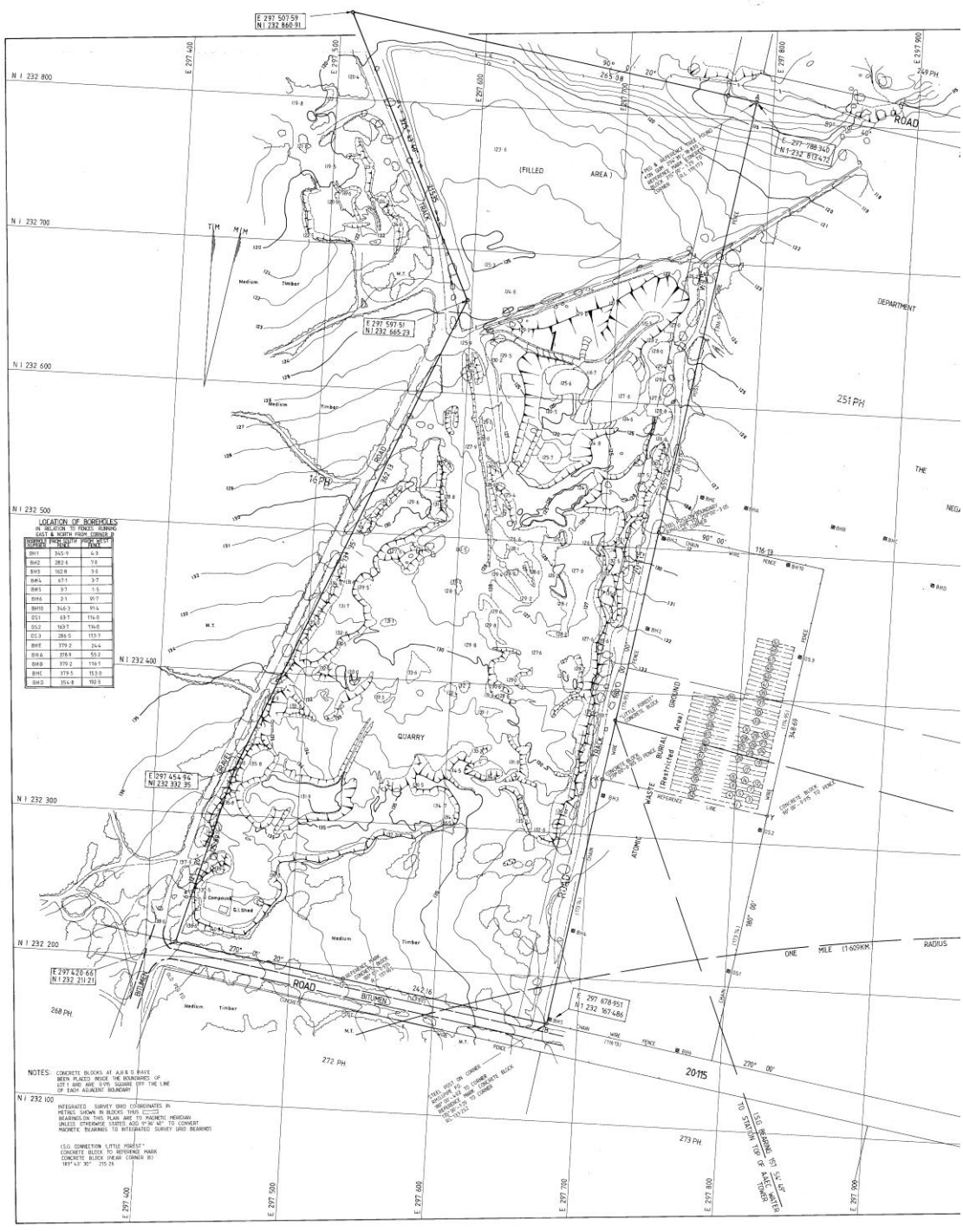

Figure 7. Part of drawing 100053D Plan of Harringtons Quarry 1983, also showing the position of trenches (excluding S1 and S2) at LFBG and reference line XY.

Environmental monitoring at LFBG of ground water, surface water, soil, vegetation and dust has been reported by the AAEC and ANSTO since 1959 (Hoffmann et al., 2008 and 38 prior reports). In addition to the environmental monitoring reports, the following documents also describe studies undertaken at LFBG since 1958 and contain references to drilling investigations:

- Mumme, 1974, Results of an early feasibility study of the Little Forest Burial Ground, AAEC ER/UN 51.
- Ellis, 1977, Possible methods of disposal of the AAEC's low and medium level solid radioactive waste and an environmental impact assessment of the reopening of an existing burial ground, AAEC/E421.
- Isaacs and Mears, 1977, A study of the burial ground used for radioactive waste at Little Forest area near Lucas Heights NSW, AAEC/E427.
- AAEC, 1985, The Little Forest Burial Ground – an information paper, AAEC, DR19.
- PPK, 2002, Geophysics and drilling program – Little Forest Burial Ground, Report 2114073A PR_2553 Rev B.
- Bradd, 2003, A report on the hydrogeology of the Little Forest Burial Ground, ANSTO/EM TN-01/2003.

In the course of these investigations, many prior episodes of drilling and well installation have been undertaken within the LFBG:

- 1957, eight auger bores, post hole drilling during site selection, AAEC and Geological Survey of NSW (Mumme, 1974), now abandoned.
- 1958, BH1-BH24, shale thickness investigation prior to trenching, also used for water sampling, (AAEC drawing E22479, 1966; Mumme, 1974), BH7-BH9 and BH11-BH24 now abandoned.
- 1961, BH1-BH6 and BH8-BH10 first used as monitoring wells (Mumme, 1974). A well "BH2/3" has also been rediscovered.
- 1969, OS1-OS3 installation (first reported in Cook and Dudaitis, 1970). A well "OS2/W" has also been rediscovered.
- 1970, BHA-BHE installation outside fence along northern boundary (first reported in Conway and Dudaitis, 1972), BHD destroyed.
- 1975, D1-D23 installed for tritium monitoring purposes (Isaacs and Mears, 1977), two have been rediscovered for sampling in 2009 (Hughes et al., 2011).
- 1984, BHF installation outside original eastern boundary fence (first reported in Giles and Dudaitis, 1986).
- 1987, MB11-MB22 installation (first reported in Giles et al., 1990).
- 2000, CW installation (DASCEM, 2000).
- 2002, P1s, P1d, P2d installation (PPK, 2002; Bradd 2003).

Available details of the above wells predating this campaign are summarised in Appendix A and their positions marked in Figure 1.

For the earlier BH, OS and D series of 33 boreholes, very little geological information was recorded apart from the initial interpretation of depth to the base of the shale in BH1-BH24 in 1958 (see **Figure 16**), and three intersections with sandstone in D1-D3 in 1975 (Isaacs and Mears, 1977). The monitoring wells installed during this period were not constructed to any known standard, and most have now been invaded by silt to varying degrees and are no longer used.

The MB series wells are still used today for environmental monitoring and reporting in conjunction with the newer generation P/CW series. All of these wells with the exception of MB16 were constructed around the fenced perimeter of the site to establish the groundwater condition leaving the site boundary. Geological logs for these wells were collated in Bradd, 2003.

In addition, a geophysical resistivity survey was conducted in 2002 prior to the siting of the P series boreholes, in an attempt to identify fracture sites and possible preferential flow pathways for groundwater. A higher resolution and deeper ranging geophysical resistivity survey was conducted by ANSTO in 2011 and these results are also presented in this report.

The new drilling and well installation described in this report is targeted around the immediate vicinity of the trenched area. The contractor reports for these works are:

- Alpha Geoscience, 2009, Geophysical survey – Resistivity and GPR detection of extents of buried trenches, Little Forest Burial Ground off New Illawarra Road, Lucas Heights NSW 2234, Project No AG-290.
- Consulting Earth Scientists, 2009, Drilling investigation report: Little Forest Burial Ground, Lucas Heights, NSW, Report ID: CES090517-ANS-01-F.
- Coffey Environments, 2010, Groundwater monitoring well installation: Little Forest Burial Ground, Lucas Heights, NSW, Project Ref: ENAURHOD04037AA.

1.2 Neighbouring Sites

To the immediate south and north of LFBG lies native open dry sclerophyll forest. From inspection of aerial photography (see Appendix C), this appears to have never been cleared.

To the east of LFBG is lower lying open grassland previously used for human excrement ("night soil") disposal by Sutherland Shire Council. Historical aerial photographs suggest this activity was well advanced by 1961 and ceased by 1978. In this area, night soil was mixed into the native topsoil in rows creating a disturbed surface soil layer to a maximum depth of 60 cm (EES, 2001).

The LFBG is bounded on the west by Harrington's Quarry, a former clay, shale and sandstone quarry excavated to a depth of 8-9 metres in places (see Figure 8). Harringtons Quarry was operational from 1959 to 1984 and subsequently filled in 1987 with putrescible waste interbedded with around 45% clay capping (Douglas and Partners, 2007). The present day remediated surface over Harrington's Quarry is slightly elevated above the level of the trenched area of the LFBG, although the majority of the site drains toward the north and north-west.

Figure 8. View across Harringtons Quarry prior to remediation, looking east toward LFBG, circa 1984.

Four hundred metres north of LFBG and 10 m lower in elevation lies the former Industrial Waste Collection Pty Ltd (IWC) liquid waste depot, the primary repository for Sydney's liquid industrial wastes between 1969 and 1980. This site occupies the headwaters of a tributary to Mill Creek, and prior to being used for industrial waste it was also a clay and shale quarry site operated by Harrington between 1959 and 1969. Filling and capping of the IWC site was completed in 1980, four years prior to cessation of the quarry activities to the south in Harrington's Quarry.

Historical aerial photography (Appendix C – 1970) and plan drawings reveal that the quarry floors of both the Harrington's Quarry and the IWC site were originally linked to lower lying natural drainage lines by long man-made ditches (see **Figure 9**). Presumably the ditches were constructed to allow accumulated rainwater, surface run-off and groundwater seeping from the quarry faces to drain away from quarry works.

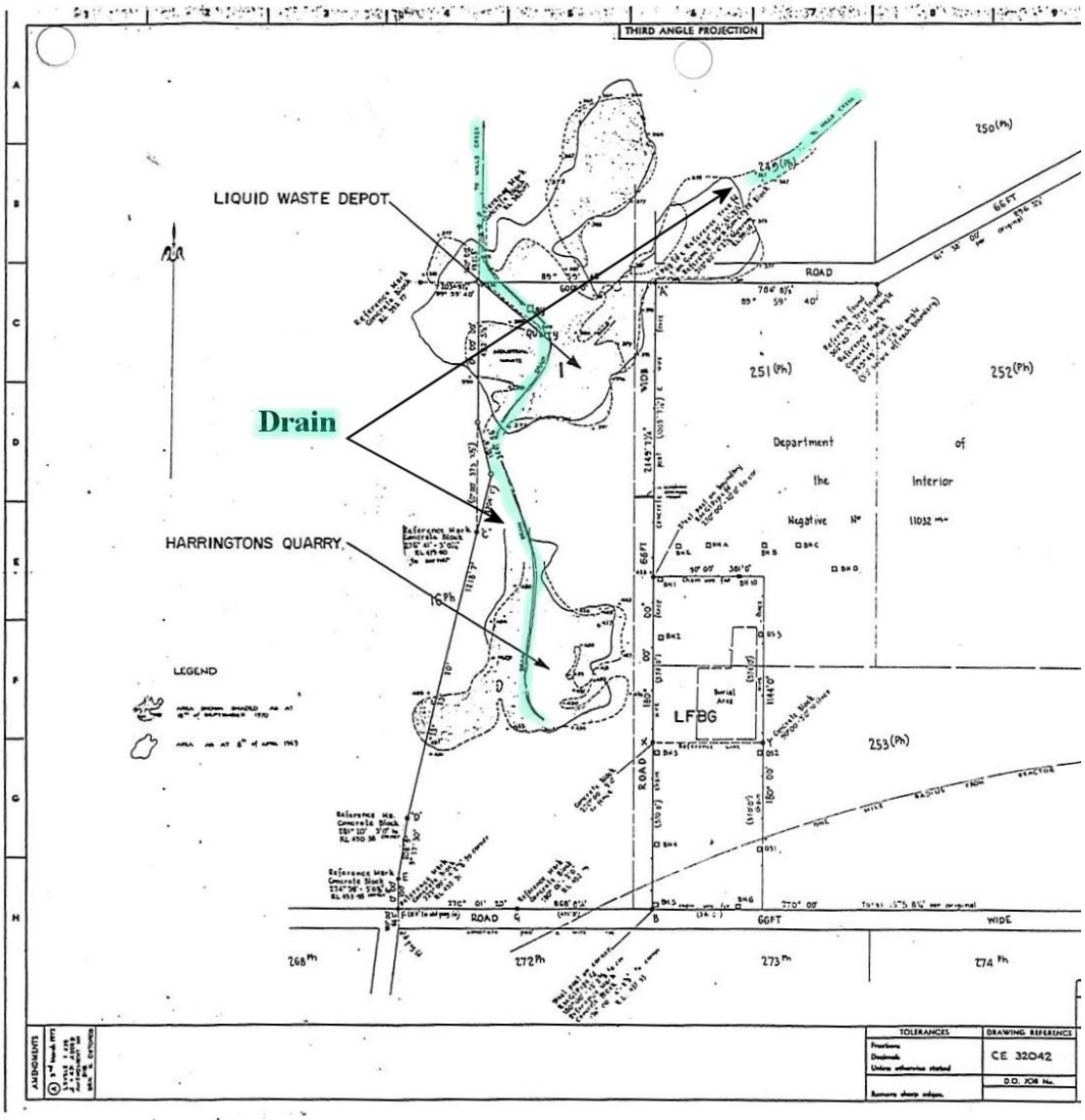

Figure 9. From AAEC drawing CE32042, plan of Harrington's Quarry and IWC site circa 1970 showing position of man-made drains.

Following cessation of quarrying and waste disposal, leachate collection systems were later installed which include interception of these drainage ditches. A leachate collection sump was installed at the lower lying eastern end of the IWC site in 1986. (CPI, 1991). Two leachate collection systems have been installed in Harrington's Quarry. The first system was completed in 1988 and consisted of a perimeter network of sand-filled trenches leading to a leachate pit in the north-west corner of the filled area (CPI, 1991). The second system installed in 2006 consisted of a 7.1 metre deep groundwater abstraction well located toward the north-east corner of the site intercepting the deepest of the former quarry pits (see Figure 7, Plan 100053D) where

the former excavated surface reaches 115 m elevation (Douglas and Partners, 2006). Chemicals related to the IWC site have been detected in Harrington's Quarry monitoring wells (GHD, 2003; GHD 2003b). The presence of the quarry/drain systems in the sixties and seventies and landfill/leachate extraction systems operated since the mid-eighties raise the possibility of an artificial shallow groundwater sink relative to the LFBG occurring to the W and NW for the last fifty years. Tritium above background levels has also been detected in Harrington's Quarry, and possible sources are evaluated in Hughes et al. (2011).

A cross-section diagram (CPI, 1991) shows the conceptual relationship between the geology, fill areas and groundwater of LFBG, Harrington's Quarry and the IWC site (see **Figure 10**). For illustrative purposes, this diagram shows only the downhill northern portion of the Harrington's Quarry fill area where the leachate extraction systems are installed, but the southward extension of this fill area lies immediately adjacent to the LFBG and at an equivalent elevation as per Figure 9 above (also see position of quarry in 1970 aerial photograph, Appendix C).

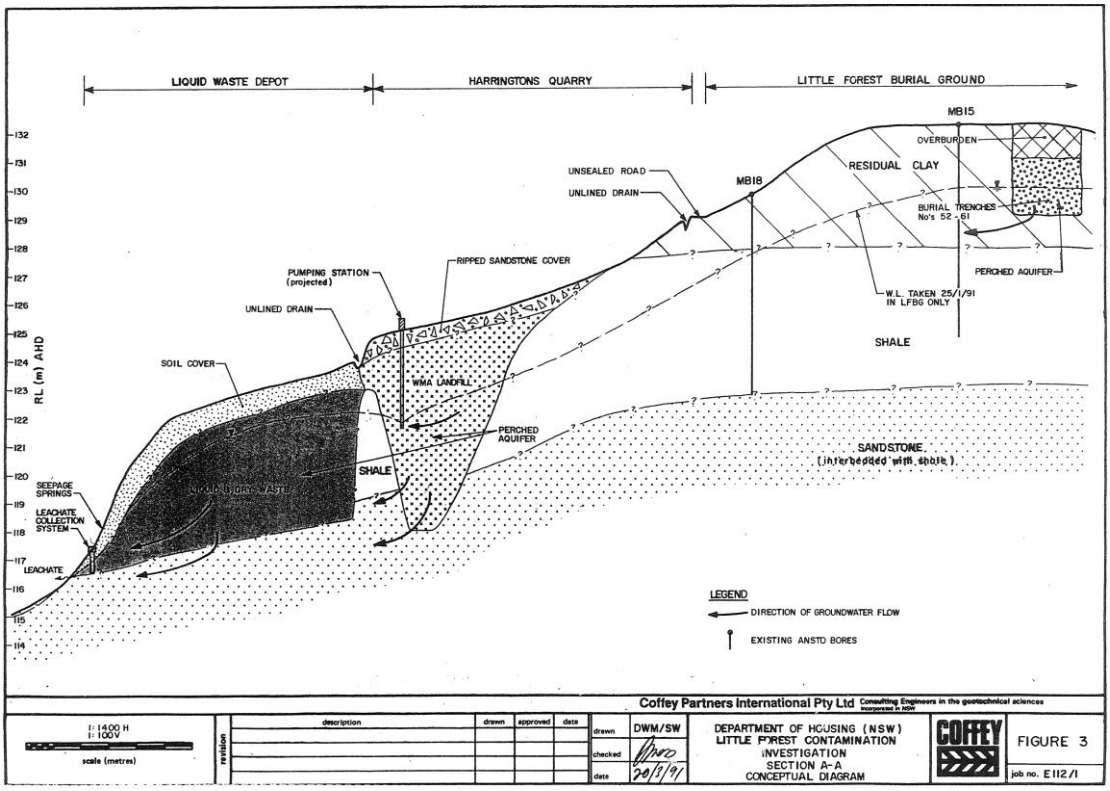

Figure 10. Conceptual model relating LFBG, Harrington's Quarry and the IWC site (CPI, 1991).

To the south-west of LFBG lies the present day open-cut excavation of the ~90 ha Lucas Heights II Landfill operated by SITA for disposal of municipal waste. The current north-western boundary of this excavation is an estimated 25-30 m deep face (see **Figure 11**) bench cut into sandstone lying approximately 380 m from the boundary of the LFBG. The base of this face lies at approximately 112-117 m elevation, or 17-22 m below the elevation of the LFBG trenches. The distance towards LFBG over which groundwater flow in the sandstone is affected by this void

could perhaps be estimated through collaboration with SITA and use of their existing groundwater monitoring network.

Figure 11. 25-30 m deep face cut in sandstone at Lucas Heights II landfill, 380 m from LFBG, 2012.

The surrounding waste sites have been subject to various investigations by external organisations. The following reports include many records of drilling and well installation in the near vicinity of LFBG:

- Coffey Partners International, 1991, Little Forest, Potential Contaminated Lands Investigation, West Menai, Stage 1, Report E112/1-AC
- Douglas and Partners and Coffey Partners International, 1992, (Joint) Report on hydrogeological investigation proposed extension regional waste depot Lucas Heights, Report CPI E156/1-CJ; DP 14780.
- Coffey Partners International and Douglas and Partners Pty Ltd, 1994, Report on hydrogeology and groundwater monitoring, Waste Depot, Lucas Heights
- DASCEM, 2000, Environmental assessment, former IWC landfill: Lucas Heights, NSW, Report CL426.
- GHD, 2003a, Groundwater contamination assessment report for: Northern boundary – Harrington's quarry, Lucas Heights NSW, Report 2111350
- GHD, 2003b, Additional groundwater contamination assessment report for: Northern boundary – Harrington's quarry, Lucas Heights NSW, Report 2112062
- Consulting Earth Scientists, 2004, Report on installation and sampling of wells MB301, MB302, MB303, MB304, MB305 and MB306 at Lucas Heights Waste Recycling and processing centre, Lucas Heights, Report ID: CES020510-WS-39-F
- Douglas Partners Pty Ltd, 2006, Report on groundwater bore installation – Harrington's Quarry – Lucas Heights Waste Management Facility, Report 43626.

Information from these reports, combined with LFBG drilling and geophysical data has been used here to map the shape of the shale lens, and hence predict the subterranean surface of the underlying Hawkesbury Sandstone at the base of the shale.

1.3 Physiography and drainage

On a regional scale, the LFBG site is located on the Woronora Plateau (see **Figure 12**), a ramp-like topographic feature that slopes upwards from the Georges River at sea level 10 km north, to the Southern Highlands region at 600 m in elevation some 60 km south. Locally, the sandstone plateau is incised by streams that generally flow northwards towards the Georges River. The parallel north-south orientation of streams appears well correlated with the dominant orientation of jointing in the sandstone.

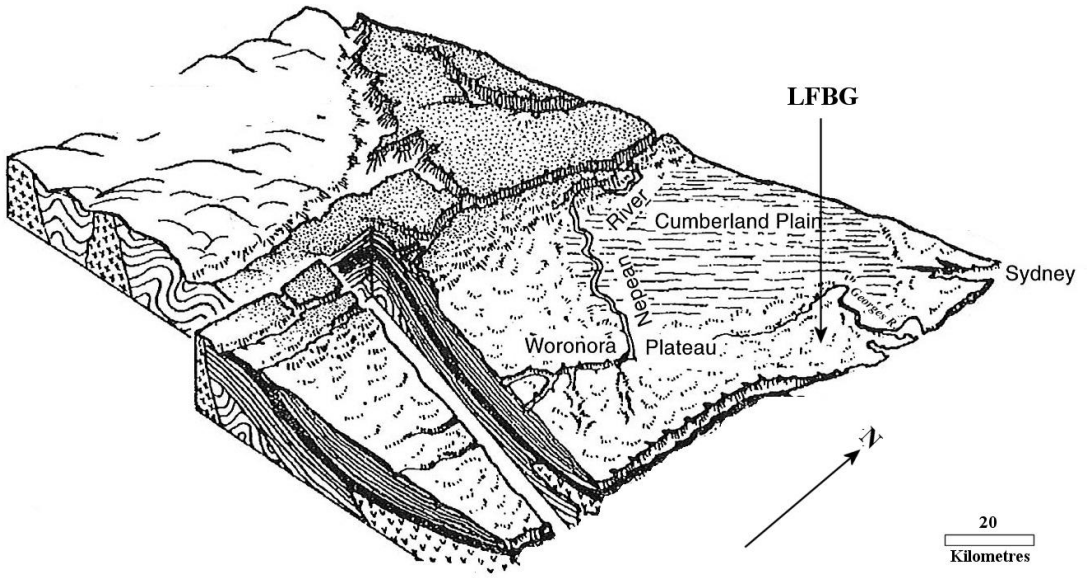

Figure 12. Regional physiography (after Branagan and Packham, 2000)

On a local scale, the LFBG trenches are emplaced in a SW-NE trending ridge-top that passes through the northern half of the site with a maximum elevation of 133 m AHD. The southern portion of the site is a shallow valley draining toward the south-east with a minimum elevation on-site of 129 m AHD, and hence there is approximately 4 m of topographic relief between the shallow valley and the ridge-top trench area. The ridge-top represents the hydrological divide between Barden's and Mill Creeks (see **Figure 1**).

On the southern side of the ridge, drainage is shed toward the shallow valley, which flows south-east off the site and becomes a tributary of Barden's Creek. This tributary, also referred to as "Turtle Ck", also captures some drainage from the night soil disposal area located to the east of the burial ground, and from the dry sclerophyll forested area to the south. Surface water originating from the south-eastern corner of the Harrington's Quarry site may also enter the shallow valley via a drain under the LFBG western boundary fence. From inspection of historical aerial photographs (see Appendix C) it appears this portion of the Harrington's Quarry lease was never excavated or cleared.

On the northern side of the ridge, drainage from the LFBG trench area is shed some 400 m north over a gentle grade toward the eastern end of the IWC site, where surface

water is captured by a tributary of Mill Creek. This tributary also captures drainage from the night soil disposal area, and from the IWC site itself. A surface drain has been constructed on the boundary between Harringtons Quarry and the IWC site.

At times of elevated rainfall, surface water may be observed seeping along contours in the lower lying areas of LFBG both north and south of the trenches. Creek gullying does not appear to develop over the well vegetated and cohesive clay-rich shale soils of the LFBG, and with sufficient rainfall, surface water flows over unbroken ground. To the south-east of the site, gully formation begins in "Turtle Creek" where the first sandstone outcrop is observed 170 m from the site boundary and 8 m lower in elevation than the trench area. Some small pools are present at this location for prolonged periods after rainfall. Elevated TDS levels in the water, observed base-flow into the pools during dry conditions and the change in surface lithology suggest this may be a site of groundwater discharge at an interface between the shale and the sandstone. A similar morphology may be found in the shallow creek beyond the eastern end of the night soil disposal area, which also has surface water pools forming where the sandstone is revealed.

1.4 Geology

1.4.1 REGIONAL GEOLOGY

In the sub-surface, the perimeter of the Woronora Plateau forms a structural sub-division of the same name within the Permo-Triassic Sydney Basin sedimentary sequence (Bembrick et al., 1980). The boundaries of the structural Woronora Plateau are defined by a perimeter of faults and folds, inside which the relatively flat-lying stratigraphic sequence has been offset relative to the surrounding areas. Nearest to Little Forest, the sequence has been uplifted some 100 m from west to east across a monoclinal structure known as the South Coast Warp (see **Figure 13**), with the result that the uppermost units of the Sydney Basin, found widespread elsewhere in the lower lying Sydney area and known as the Wianamatta Group, have been completely eroded away.

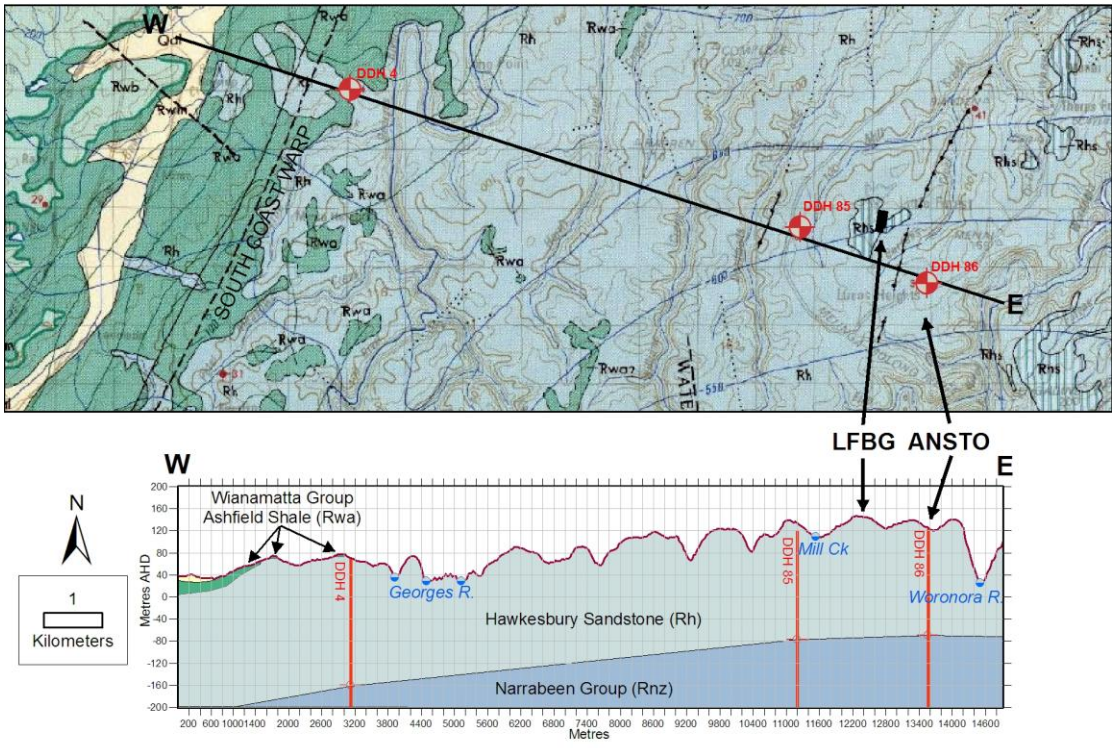

Figure 13. West-East cross section through the Woronora Plateau (map excerpt and data from Stroud, 1985; GS-NSW 1967; GS-NSW 1967b; GS-NSW 1972).

Hence, in the Little Forest area, the Woronora Plateau consists almost entirely of the early to mid-Triassic Hawkesbury Sandstone to depth of 70 m below sea level. The Hawkesbury Sandstone is composed mainly of medium-coarse size quartz grains with a silica-siderite cement and a variable proportion of clay and rock fragment matrix. Estimates of the average proportion of clay matrix range from 20-40% (Standard, 1969; Bowman, 1974).

The Hawkesbury Sandstone is generally considered to have been deposited by a vast braided river system, which has been compared to the modern day Brahmaputra

(Conaghan and Jones, 1975), with cyclical flooding events responsible for its bedding pattern and sedimentary structures. Individual sandstone beds representing preserved river channel deposits usually occur as elongate lenses typically up to 2 m thick and 300 m long, but in places up to 10 m thick and 1 km long (Standard, 1969). The regional dip of the beds is to the north at an angle of 1.5-2 degrees. Beds in the Hawkesbury Sandstone have been classified into 3 facies related to differing current conditions responsible for their deposition (Conaghan, 1980):

- *Massive* facies, deposited during peak flood conditions, largely devoid of sedimentary structure, typically with an erosional base, containing very poorly sorted fine to medium sand, commonly containing dispersed granules and small pebbles, abundant dispersed claystone fragments, relatively higher amounts of clay, lower amounts of cement and lower primary macro-porosity compared to *Sheet* facies;
- *Sheet* facies, deposited during the receding limb of flood events, characterised by ubiquitous large scale foreset cross-bedding occurring in sets and inclined at ~20 degrees, typically with a conforming base, containing medium to very coarse sand grains bound by a silica-siderite cement, common granules and small rounded quartz pebbles occurring as pebble trains on planar surfaces which separate sets of cross-strata;
- *Mudstone* facies (shales), deposited under low flow conditions during intra-flood periods or occurring as channel fill following avulsion, accounts for ~5% of the Hawkesbury Sandstone, characterised by laterally uniform planar black laminated mudstone with thin interbedded grey siltstone, typically 0.5 to 3 m thick, often terminated laterally by erosion surfaces and overlain by *Massive* facies.

Mudstone facies bodies, also commonly referred to as shales, have been observed with a thickness of 10 m and a lateral extent of several kilometres (Standard, 1964), and a rare example described on the Hornsby Plateau at 35 m thickness (Herbert & Uren, 1972). Mudstone facies or shales are proposed to form localised aquitards.

The high degree of clay matrix in *Massive* facies and high degree of cement in *Sheet* facies units reduces both units primary porosity, and hence limits their capacity to transmit water. Water flow is instead dominated by the secondary porosity created by weathering, jointing, fractures, cross-bedding and separations between beds. Joints are the most common rock defect. Joints are thought to be formed by shrinkage during lithification or stress from tectonic forces, and are later ‘opened’ by stress relief (unloading) due to erosion overhead or in adjacent valleys. Conversely joints are generally considered to become increasingly watertight with depth. Joints represent planes of weakness, and may also become subject to faulting under conditions of tectonic compression, tension or shear, and the Hawkesbury Sandstone has been subjected to all three modes of crustal stress during its 230 Ma history (Branagan, 2000). The uplift across the Woronora Plateau is likely to have been accommodated by many small offset normal faults, occurring on average every 140 m (ANSTO, 2002), forming localised fracture zones in the sandstone aligned with the dominant direction of jointing. In places, these planes of weakness have been invaded by dykes. One such feature passes through ANSTO and has been mapped continuing by the SE side of the Little Forest shale (Stroud et al., 1985; ANSTO, 2002).

In the Hawkesbury Sandstone, spacing between joints in the sandstone units is variable, but commonly is between 1 - 3 m and ranging up to 10 m. Individual joints commonly extend 100 m horizontally, but vertically are usually limited to a single bed (McKibbin and Smith, 2000). Enhanced water access is provided by zones of closely spaced, well developed jointing linked together by bedding planes, leading to deeper weathering. In the Little Forest area, sandstone weathering effects vary greatly, ranging from siderite oxidation of intact surficial sandstone, to complete disaggregation into a friable sand. Joints to 20 m depth and weathering 'troughs' of depths up to 30 m have been described (Douglas and Partners, 1992).

1.4.2 SHALE NOMENCLATURE

The shales at Little Forest and also in the wider Sutherland – Menai – Heathcote area are now considered to be shale lenses occurring in the Hawkesbury Sandstone (Sherwin and Holmes, 1986). The most recent geological map '9029-9129' of Wollongong-Port Hacking produced by the NSW Geological Survey in 1985 shows the shale pocket at Little Forest and surrounding areas have been classified as "Rhs - Claystone, siltstone, and laminate shale lenses" in the Hawkesbury Sandstone (Stroud et al., 1985). The supporting evidence provided in the accompanying explanatory notes is that other large shale bodies at nearby Loftus (see **Figure 14**) and Waterfall are surrounded by Hawkesbury Sandstone of higher elevation than the base of the shale, and therefore the shale must be a lens member of the sandstone, although the shale at Little Forest is not mentioned specifically. This 1:100 000 scale map series is the most recent and hence is the most likely to be referenced today for general geology in the area.

Figure 14. Interbedded sandstone and shale within the Hawkesbury Sandstone, exhibiting low-angle crossbedding. Exposure in rail cutting between Loftus and Engadine (Sherwin and Holmes, 1986).

Prior to this recent change in shale nomenclature, most AAEC and ANSTO reports refer to the shale at Little Forest as a remnant outlier of the Ashfield Shale member of the mid-Triassic Wianamatta Group. This interpretation appears to have been initially adopted by the AAEC during joint mapping exercises with the Geological Survey of NSW in 1958 in the initial phases of identifying a suitable site for waste burial (Mumme, 1974). At the time of production of most AAEC reports, the contemporary geological map for the area was the Wollongong 1:250 000 Geological Series Sheet SI 56-9 (Rose, 1966), which marked the shale at Little Forest as Ashfield Shale. This map was consistent with a widely published view that these large shale bodies surrounded by the Hawkesbury Sandstone were outliers of the Wianamatta Group isolated laterally by erosion (Clarke, 1878; Pittman, 1903; Harper, 1915; Willan,

1925; Joplin et al., 1952; Adamson and Lloyd, 1962; Stuntz, 1971; Bowman, 1974; Van Heeswyck, 1978; Herbert, 1979; Herbert and Helby, 1980).

In more local work, several authors have referred to both Ashfield Shale and "Hawkesbury type" shales in the Menai area as separate rock types with different ramifications for use as a raw material in making ceramics (Fergusson and Hosking, 1955; Loughnan, 1962; Dickson, 1967). Although in other work of the same period, concessions were already being made that some Ashfield shale pockets may have been mis-mapped due to a lithologic similarity with shale in the Hawkesbury Sandstone (Lovering, 1954). Cases are described (Loughnan, 1962) where there is considerable difficulty in distinguishing the boundary between large Hawkesbury type shales and overlying Ashfield Shale units.

Reference is also made to the increasing occurrence of thicker shales in the upper quarter of the Hawkesbury Sandstone in the Woronora Plateau (Standard, 1964), which was later corroborated by the NSW Department of Mines DM exploratory drill-hole series (Bowman, 1974; Stroud 1974). Little Forest is underlain by almost 200 m thickness of Hawkesbury Sandstone, based on its location 1.5 km east of exploration drill-hole DM Camden DDH85 with an eroded 199 m thickness of Hawkesbury Sandstone, and 1.5 km north-west of DM Camden DDH86 with an eroded thickness of 194 m of Hawkesbury Sandstone. A full thickness of 230 m of Hawkesbury Sandstone was intersected in DM Campbelltown DDH4, located in the edge of the Ashfield Shale 12 km west. This suggests that Little Forest is located very near the top of the Hawkesbury sandstone, with some thickness (perhaps only 30m) of the unit eroded away (Geological Survey of NSW 1967; 1967b; 1972).

X-ray diffraction analyses of Ashfield Shale and shale in Hawkesbury Sandstone, including samples specifically from the Little Forest shale body, suggest there is little difference in mineralogy between the two shales, with both rock types consisting dominantly of quartz, kaolinite and varying proportions of mixed layer illite-smectite (Slansky, 1974a; Slansky, 1974b; Slansky, 1975). The presence of frequent sideritic mudstone bands has been described as a characteristic feature of the lower reaches of the Ashfield Shale (Fergusson and Hosking, 1955), but other authors also describe sideritic mudstone bands in section samples identified as Hawkesbury type shale (Loughnan, 1962) and a siderite proportion of up to 7% (Sherwin and Holmes, 1986).

The boundary between the Hawkesbury Sandstone and Ashfield Shale is described as the Mittagong Formation, absent in places, consisting of fine grained sandstone interbedded with dark-grey siltstone and laminite in beds up to 6 m thick and having a disconformable upper surface (Lovering and McElroy, 1969; Herbert and Helby, 1980). The shale lenses in the Hawkesbury Sandstone are described as interbedded sandstone and shale, with interbeds of laminite, siltstone and claystone mid to dark grey in colour (Sherwin and Holmes, 1986). These two descriptions are markedly similar, and Sherwin and Holmes concede that some areas now mapped as 'Rhs - shale in Hawkesbury Sandstone' or as 'Rwa - Ashfield Shale' may in fact be outcrops of Mittagong Formation. Figure 15 demonstrates four different possible stratigraphic relationships between these three units. The geology at Little Forest is an example of one of these relationships revealed by erosion, but given the elevated, surficial and isolated nature of the shale deposit it would be difficult to prove which one unequivocally.

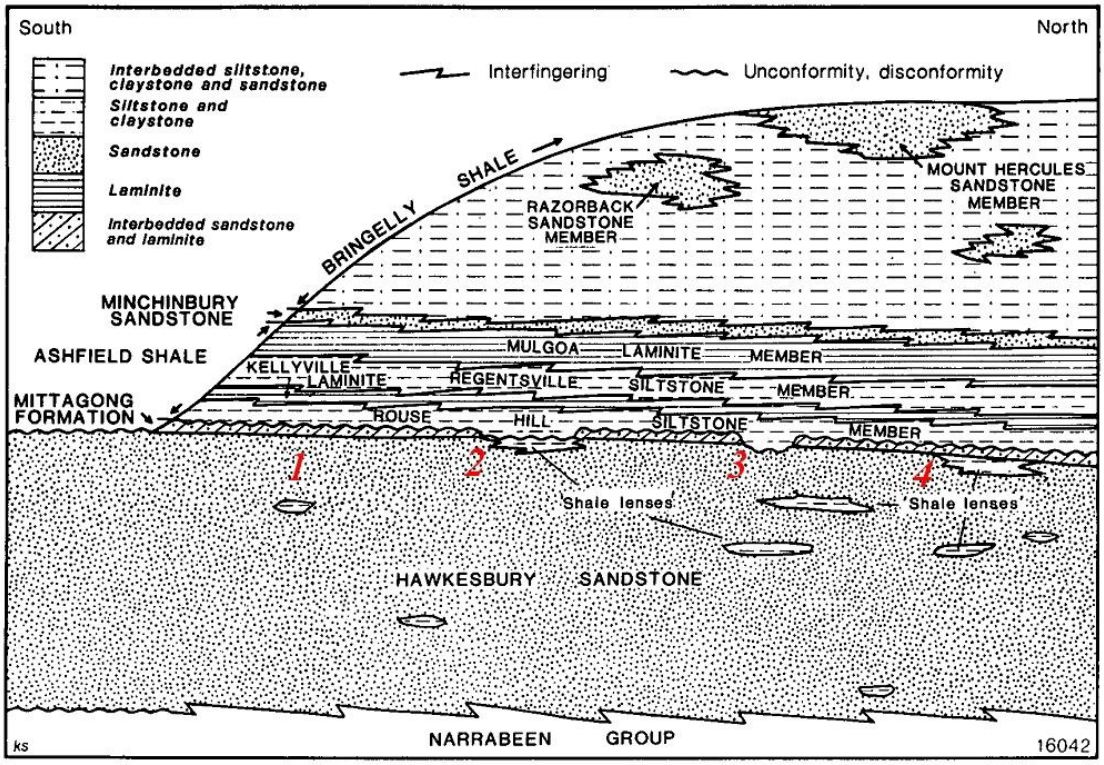

Figure 15. Stratigraphy of Wollongong–Port Hacking Sheet, from Sherwin and Holmes, 1986.

Lithologically and mineralogically, it appears the vertical progression from upper Hawkesbury Sandstone up into a shale lens member could look very similar to the progression from Hawkesbury Sandstone up into the lower Ashfield Shale via the Mittagong Formation, with the possible exception of sideritic bands. This perhaps could be expected considering that the source material and gradual transition in depositional environments from high energy braided river to low energy freshwater body was likely to be similar for both sequences. Hence, the map reclassification of the shale at Little Forest from Ashfield Shale to shale lens in Hawkesbury Sandstone is expected to have little or no consequence on the findings of the previous AAEC reports. Perhaps the only impact is that the new classification suggests a more complex and laterally heterogeneous conceptual model given the small scale of the freshwater body in which the Hawkesbury type shale lens would have formed, which may raise the likelihood of finding preferential flow pathways and localised hydraulic interactions between shale and sandstone aquifers.

1.4.3 SITE GEOLOGY

In cross section through LFBG, the general geology consists of a 10-15 m thick shale lens, underlain by sandstone. A review of the geological logs predating the 2009-2010 campaign, show that only two wells, P1d and P2d, penetrate the full shale sequence into the Hawkesbury Sandstone, and hence knowledge of the lower parts of the shale lens and it's lateral variability is very limited. A third well W2d, also penetrating into the Hawkesbury Sandstone, was installed during this 2009-2010 campaign. The majority of stratigraphic descriptions are obtained from boreholes which were terminated at some depth within the shale.

The thickness of the shale at Little Forest was tested in 1958 by drilling 24 auger holes during early investigations into the site for radioactive waste burial. From this work, a contour plan of base of shale elevation was produced (see **Figure 16**). In general, the lenticular morphology defined by the base of shale contours over the night soil area is supportive of the abandoned channel fill model of shale deposition. The map suggests the LFBG trenches have been sited close to the thickest part of the shale (15 m thick) aligned with the centre of the lens.

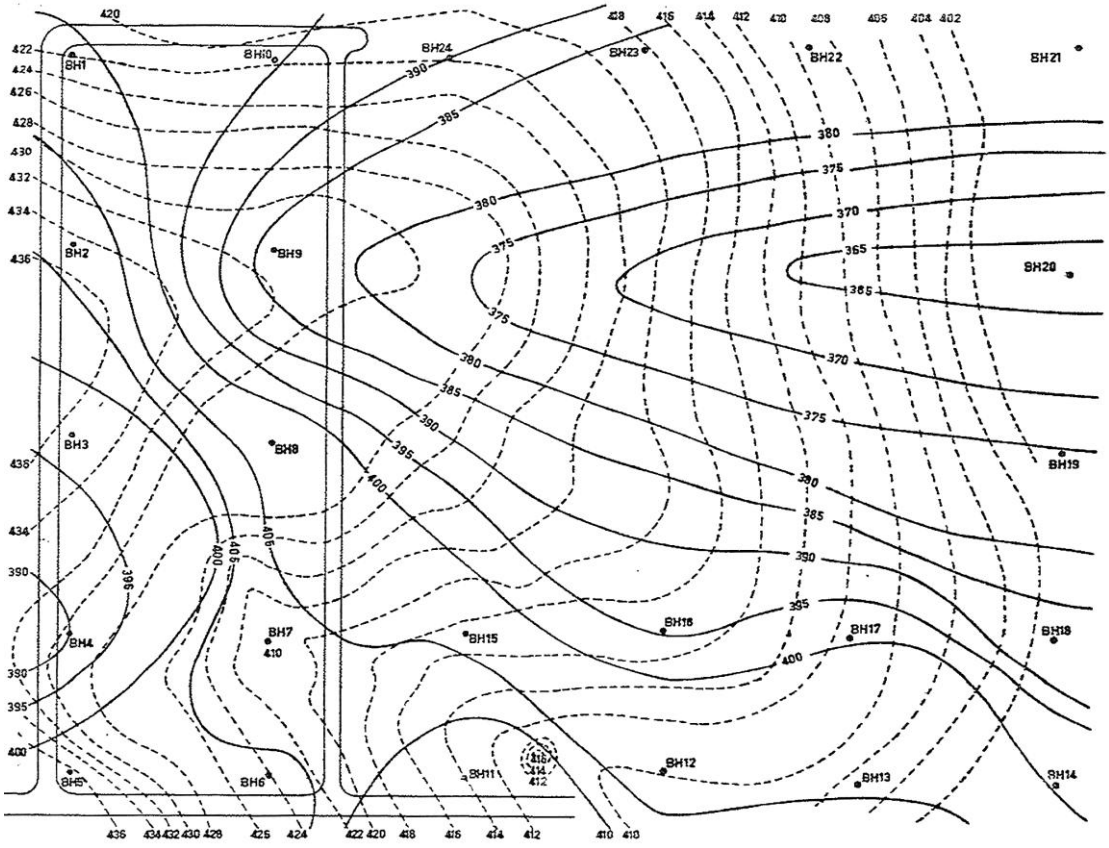

Figure 16. Elevation of base of shale (solid lines) versus topography (dashed lines), excerpt from AAEC drawing E22479, 1966 (Mumme, 1974).

The accuracy of the majority of this map, however, remains unproven. There appears to be a large gap in data density over the night soil area where the lens shaped

contours are drawn. No supporting evidence was found in the form of 'BH' drilling records corresponding to the map, and only a brief reference is made that the boreholes 'probably reached the underlying sandstone, as it was reported that boring was carried down to a very hard layer' (Mumme, 1974). Comparison between logs from recent drilling of the P series and W series and the depth to base of shale inferred from the BH contour map show discrepancies ranging from 1.5 to 8 m. This discrepancy may have arisen due to drilling limitations in 1958, with possible auger refusal at some hard layer in the shale. The discrepancy may also have stemmed from a difference in interpretation of what is the base of the shale and what is the top of the sandstone given that there is an interbedded transitional zone of both materials up to 8 m thick in some locations.

The surface extent of the shale body has been estimated by several workers and represented differently in various maps and publications (Rose, 1966; Dickson, 1967; Stuntz, 1971; Mumme, 1974; Stroud et al. 1985). The most recent version was produced in 1991 as a result of field mapping for an investigation into potential contaminated land resulting from the waste sites of the area (CPI, 1991). This map shows the shale body extending beyond the boundary of the LFBG in all directions (see **Figure 17**). The position of the shale/sandstone contact shown in the south-eastern corner of this map has been verified by ANSTO in 2012. The characteristics of the soil and weathered zone could be expected to change towards the margins of this area given this is where the interbedded shale/sandstone transitional zone is likely to outcrop at the edges of the lens.

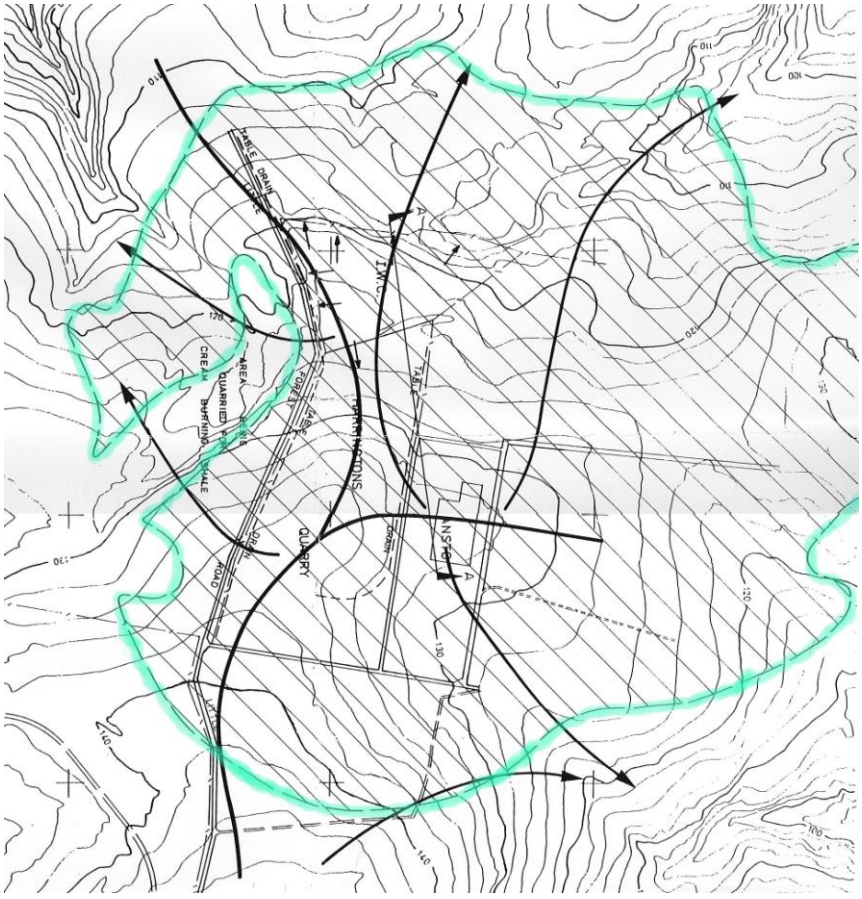

Figure 17. Highlighted area shows shale outcrop, solid lines show topographic surface water divide, arrows show inferred groundwater flow (CPI, 1991).

In vertical profile, the shale can be broadly sub-divided into three groups, although the boundaries between groups are gradational:

- a weathered shale zone of variable thickness, consisting of topsoil, clay, and a 'leached' unconsolidated shale (Mumme, 1974);
- 'parent shale' (i.e. the cohesive parent of the weathered material) in which the carbonaceous darker colouring originating from organic matter is retained;
- interbedded shale and sandstone basal transitional zone.

Mumme (1974) included a brief summary of the weathered shale zone from the eight preliminary bore-holes sunk in 1957, and considered it comparable to the shale weathering profile of a quarry at Barden Ridge described in Loughnan (1962). Mumme also conveys the findings of Loughnan regarding Triassic shale weathering processes in general. Mumme presented characterisation of LFBG groundwater levels, dissolved solids, run-off, groundwater response to rainfall, results of in-situ borehole tracer and laboratory exchange column experiments. Mumme concluded a two layer model for radionuclide dispersion based on geology, separating an upper weathered shale zone of enhanced permeability ('leached zone' of Loughnan, 1962) and a lower unweathered shale formation ('parent shale') where jointing and fracturing only allows groundwater flow and radionuclide transport at a subdued rate. Mumme assumed limited mixing between the two layers.

Isaacs and Mears (1977) described the drilling of the 23 'D-series' cores, with all holes converted to 40 mm wells. A profile for cores D4 to D23 was not included. Cores D1-D3, located between the eastern fringe of the LFBG and ~50 m east into the night-soil area, were completed to at least 9 m, but suffered core loss for the first 6 m, and hence no description of this interval is put forward. It is reported that D1-D3 intersected the 'sandstone profile' at 8.8 m. In terms of elevation, this is the same as the top of the interbedded shale/sandstone interval reported in P1d and P2d drilling logs (PPK, 2002; Appendix B). The composition presented for a sample 'F5' of this material is 50% kaolinite, 50% mixed-layer mica-smectite, presumably the percentages refer to clay fraction only and are exclusive of quartz content (see **Table 2**). Table 2 presents the findings of Slansky (1975) XRD analysis, in which four shallower samples are also described from a 2.5 m deep sampling trench in the NW of LFBG. A geological profile from the trench is also presented in the table, which would appear to validate the weathering profile of Mumme (1974).

Table 2. Soil trench profile from Isaacs & Mears, 1977.

Fraction	Sampling Depth (m)	Description	Composition	Cation Exchange Capacity meq/100 g
F1	0.0-0.5	Top soil	Kaolinite (> 50%) Mica, smectite (< 50%) Quartz	7.3
F2	0.5-1.0	Red-brown clay	Kaolinite (80%) Mixed-layer mica-smectite (20%) Quartz	9.0
F3	1.0-1.5	Greyish clay	Kaolinite (80%) Mixed-layer mica-smectite (20%) Quartz	7.1
F4	1.5-2.5	Weathered shale	Kaolinite (65%) Micaceous clay mineral (35%)	8.3
F5	9.0	Sandstone	Kaolinite (50%) Mixed-layer mica-smectite (50%)	4.5

The Bradd (2003) description of the weathered shale and parent shale zones concurs with the findings of Mumme (1974). Geological logs recorded from the 1987 drilling of the 'MB series' wells are presented in Bradd (2003) (see Appendix B), and a description is provided per 1.8 m interval of hole. Presumably the interval is the result of using 6 foot length auger stems. The MB series boreholes range from 5.4 to 8.4 m depth, and in general the logs describe the weathering profile grading into parent shale as per Mumme (1974), with the weathering front varying in thickness between 3.2 and 7 m and most holes terminated in black parent shale. The logs frequently refer to hard reddish or iron-stained shale fragments within the weathered grey leached shale zone. At the south end of the site, the black parent shale appears to become very thin (MB11) or absent (MB12), and below the weathered grey leached shale these holes feature a fine sandstone lens and what is possibly the top of the interbedded shale/sandstone interval at depths of around 5 m. These units were not intersected in the rest of the MB series located in the middle and north end of the site.

DASCEM Pty Ltd drilled an 11.9 m deep DDH corehole 'CW' in the NW corner of LFBG and completed it as a control site well to complement their environmental assessment of the former IWC landfill site in 2000. The geological log (DASCEM, 2000; Appendix B) describes the typical site weathered shale profile, including some ironstone layers, to a depth of 5.4 m. Below this depth a thin interbedded shale/sandstone layer was encountered followed by at least 6 m of a thinly bedded to laminated fine grained sandstone, containing numerous bedding plane partings (see **Figure 18**). The screen interval of the CW well is restricted to this laminated fine sandstone layer between 5.9 and 11.9 m depth. CW is located adjacent to the 6 metre deep MB18, and while the logs appear to be a good match, MB18 was terminated at the top of this laminated fine sandstone layer. CW is also located within 40 m of P2d which was completed to a much deeper 35 m. In P2d, the equivalent layer to the laminated fine sandstone of CW occurs from 7.5 to 14 m depth and is described as the interbedded sandstone/shale with fine silt size grains dominating.

Figure 18. Core from DDH CW (DASCEM, 2000) showing detail of the laminated fine sandstone lens.

PPK Pty Ltd were commissioned by ANSTO in 2002 to drill (by air hammer) and install monitoring wells in predicted groundwater flow pathways (CPI, 1991; PPK, 2002; Bradd, 2003) toward the SE and NW of LFBG (see **Figure 17**). Possible zones of vertical fracturing interpreted from a surface resistivity survey (GCDS, 2002) were also taken into account when siting the wells on the premise that these might represent preferential pathways for groundwater, but no evidence of a pervasive fracture zone was encountered during drilling (PPK, 2002). The two deeper wells P1d and P2d (PPK, 2002; Appendix B) are located at opposite ends of the site and are the first to penetrate into the Hawkesbury Sandstone, although the 2009-2010 campaign has now added a third well to this depth at W2d. As per P2d, the geological log for P1d describes an interbedded shale/sandstone interval below the typical weathered shale profile, here extending between 7 and 13 m depth. Below this layer, P1d and P2d were drilled a further 7 m and 21 m respectively into the underlying continuous sandstone unit, in which these holes are terminated and screened as wells. This sandstone layer below 13 m in P1d and below 14 m in P2d, is interpreted as the Hawkesbury Sandstone. Drill chip samples from the lower sandstone unit are described in the logs as sand grains, silty sand and rock fragments. A high clay content was observed in P1d drill chips, and slug testing of this well yielded a low hydraulic conductivity of 2.8 cm/day (Bradd, 2003). Both wells encountered water bearing fracture zones containing coarser sand and large rock fragments up to 9 mm, which are likely to represent bedding plane partings in between massive and sheet facies units. Two 30 cm thick shale bands are described in P2d at 21 m and 24 m depth, which are likely to represent thin mudstone facies units and may impede vertical groundwater movement at this location.

A site stratigraphic column is presented in Table 3 to summarise the above geological data, largely corroborated by field observations of the 2009-2010 campaign. Boundaries between layers in the shale weathering profile should be considered gradational, whereas boundaries above sandstone units were abrupt where these were encountered in the field. This stratigraphy is extended to a site conceptual geological model presented in **Figure** 56, Section 5.

Table 3 LFBG stratigraphy.

Unit	Appearance
Top Soil	Loose dark brown soil underlain by clayey red soil; 20-50cm thick
Mottled Zone	Red and white marbled clay without structure; numerous iron-stained segregations or nodules; ~1m thick
Leached Zone	White grading down to into pale grey weathered shale; soft and unconsolidated; increasing fabric preservation and rock strength with depth; contains occasional hard thin mudstone bands <5 cm thick
Parent Shale	Dark grey to black hard shale; displays shale fabric - thinly bedded to laminated and tight, high frequency jointing; contains fine sandstone/siltstone lenses up to 3m thick in some locations
Interbedded Shale/Sandstone	Alternating bands of fine sandstone and shale; ranges laterally from shale dominated laminite to being dominantly grey to white fine grained sandstone/siltstone with thin cross-bedding; unit is up to 6m thick
Hawkesbury Sandstone	Light grey to orange, medium to coarse size sand grains, rock fragments, clay rich in places; contains occasional thin shale bands ~30cm thick

1.5 Groundwater

The LFBG is considered to support perched unconfined water bodies in the weathered shale zone underlain by the relatively impermeable parent shale. The underlying Hawkesbury Sandstone is considered to contain a separate aquifer, vertically confined by the main shale lens.

The piezometric surface of the shale aquifer has been studied at intervals using different generations of boreholes (Mumme, 1974; Ellis, 1977; Isaacs and Mears, 1977 and CPI, 1991). The resulting surface resembles a subdued version of the topography and suggests the recharge area is at the crest of the hill where the trenches are located, and that the natural direction of groundwater flow would be away from this divide toward the north and south east, following the topographic slope. Isaacs and Mears (1977) attempted to directly measure groundwater flow direction using three different methods, but failing to obtain consistent results, concluded a highly complex flow path exists within the shale aquifer on a local scale. Studies conducted during the seventies also show the localised effect of the void of Harringtons Quarry with the predicted flow direction diverted toward the west and north-west on this side of LFBG. These studies also showed a rapid groundwater level response to rainfall events. The horizontal hydraulic conductivity of the shale aquifer varies from 0.5 to 9 cm/day according to slug test data depending on the stratigraphic unit measured, with the highest values found in weathered shale (Bradd, 2003).

The piezometric head of the sandstone aquifer, measured in two wells only (P1d and P2d), is lower than the shale aquifer, and shows subdued and delayed response to rainfall, suggesting a downward hydraulic gradient and probably a separate recharge area lateral to the shale deposit. The hydraulic conductivity of the sandstone aquifer has only been measured at one well (P1d) at 2.8 cm/day, suggestive of a low porosity lithology with low incidence of rock defects such as jointing and permeable fractures at this location. The Hawkesbury Sandstone is known however to have much higher hydraulic conductivities along such rock defects which tend to form localised preferred flow pathways for groundwater, and hence the figure of 2.8 cm/day is possibly not representative of the whole aquifer beneath LFBG. Regionally, groundwater in the sandstone aquifer would be expected to also flow downhill toward major drainage lines in accordance with the topography, although local flow directions may be affected by the morphology of the base of the main shale lens and the presence of the nearby void of SITA, and also by leachate extraction in Harrington's Quarry.

Virtually all previous LFBG studies make an assessment of groundwater chemistry and contaminant migration, with the most recent and detailed studies being:

- Hughes, C.E., et al., 2011. Movement of a tritium plume in shallow groundwater at a legacy low-level radioactive waste disposal site in eastern Australia, Journal of Environmental Radioactivity 102, pp 943-952
- Bradd, 2003, A report on the hydrogeology of the Little Forest Burial Ground, ANSTO/EM TN-01/2003.

2 Drilling Objectives

The core sample locations and design, location and quantity of wells installed as part of this 2009-2010 project were determined by the research objectives in Table 4.

Table 4. Research objectives supported by samples from this campaign.

Objective	Key Activities
Targeted characterisation of soils and lithofacies relevant to contaminant transport pathways. This will include mineralogy, petrology, geochemical and adsorption characteristics of shallow (within and above shale) materials and deep (within sandstone) materials at the LFBG. Focus question – "what are key site characteristics governing contaminant release and transport?"	Shallow and deep core (solid phase and porewater) retrieval from near the trench areas. Locations selected to ensure all important potential contaminant pathways are sampled.
Determine downward contaminant flux from the trench bottoms to, within and through the shale layer below the LFBG. Focus question -"what is the rate of contaminant flux from the trenches downward through the shale into the Hawkesbury Sandstone?" If necessary, follow with activities to determine lateral extent of contamination in the Hawkesbury Sandstone.	A set of nested coreholes completed to wells with depths targeting above, within, and below the shale layer into the sandstone. The W6d well (just outside the trench area) will be constructed first to demonstrate feasibility of proper construction of a deep well in the trench area. Phase II work will include a deep well (W11d) within the centre of the trench area near MB 16.
Better determine lateral (horizontal) migration rates of contaminants above the shale near the LFBG. Focus question- "what is rate of movement of contaminants above the shale, particularly the long-lived radionuclides?"	Series of shallow coreholes with depths to the top of shale. Locations are sequential beginning near the south boundary of the western block of trenches and progressing away from the trenches along the southward dominant flowpath. Sequentially spaced data will allow determination of lateral contaminant migration rates.

Better understanding of contaminant transport in seepage/infiltration areas Obtain groundwater data relative to transpirate and other key exposure or study locations Better understanding of mixing of contaminants between LFBG and the adjacent Harrington's Quarry.	Shallow core from two seepage/infiltration areas. Make use of data from two shallow core locations and one well location near existing transpirate areas. Shallow core and one well from near the boundary between LFBG and Harringtons Quarry

The objectives of the 2009-2010 campaign required drilling close to the trenches, and in the case of the one angle hole, drilling underneath the trenches. At many locations, the boundary of the trenches is not readily visible on the ground surface. As an extra precaution prior to commencement of drilling, a geophysical surveyor was engaged to attempt confirmation of the outside edge of the trench area.

In support of the above stated objectives, the program of drilling and well installation works was undertaken in two phases. In the first phase initiated in 2009, NMES project contracted Consulting Earth Scientists Pty Ltd (CES) to:

- undertake a geophysical survey to define the trench area (subcontracted to Alpha Geoscience Pty Ltd);
- obtain continuous core soil/rock samples (by direct-push drilling) or crushed rock samples at 0.5 m intervals (by auger drilling) adjacent to the trench area at 30 locations;
- obtain one continuous core rock sample angled underneath the trench area by diamond core drilling;
- install and develop a 45 degree angle observation well;
- assist ANSTO to install and develop four observation wells;
- provide surveyed MGA94 coordinates and AHD (Australian Height Datum) levels of new wells and trench boundary marks established in the geophysical survey.

In the second phase conducted in 2010, NMES project contracted Coffey Environments Australia Pty Ltd to:

- obtain crushed rock samples at 0.5 m intervals by auger drilling at ten locations;
- install and develop 15 observation wells;
- provide surveyed MGA94 coordinates and AHD levels of new wells.

3 Methods

3.1 Geophysical Surveys

In July 2009, electrical resistivity, time domain electromagnetic and ground penetrating radar methods were employed for detection of the edge of the trenched area by contractor Alpha Geophysics. In May, 2011 another resistivity survey aimed at detecting geological layers was conducted by ANSTO and Dr Ander Guinea visiting from the University of Barcelona.

3.1.1 RESISTIVITY

In DC electrical resistivity surveying, the subsurface resistivity distribution is determined by making a series of measurements on the ground surface, and from these measurements the true resistivity of the subsurface can be modelled. The resistivity measurements are made by injecting a known current into the ground through two electrodes, and measuring the resulting voltage at two other electrodes.

The resistivity of the subsurface can vary greatly with rock or soil type, degree of weathering or fracturing, clay content, water content and salinity. Horizontal and vertical changes in resistivity can be mapped along a survey line using a large number of electrodes connected to a multi-core cable, and a pre-programmed electronic switching unit to automatically select the relevant four electrodes for each measurement and record the results. The configuration or array of electrodes used can be selected to suit the geometry, depth, orientation and scale of the intended target.

Typically 100 to 1000 measurements are made in series to provide the data necessary to construct a two-dimensional contoured image of apparent resistivity or 'pseudo-section'. By convention, individual data points are plotted on the pseudo-section at the mid-point of the set of electrodes used to make the measurement and a vertical offset proportional to the separation between the electrodes. The depth of the plotted point is schematic only and does not represent the actual depth.

Software is then used to convert the data into a resistivity model section that can be used for geological interpretation. The most common method used is inverse modelling, where an initial cell-based model of the sub-surface is first proposed by the interpreter (or the software default), and an iterative least-squares inversion method is applied to find an optimised model in which the discrepancy between calculated model resistivity and measured apparent resistivity is minimised (Loke, 1999). Some interpreter bias may be inherent in the inversion process, as the operator makes some assumptions in choosing the cell structure to which the model is fitted, and also select constraints and parameters for the model algorithm. The purpose of this is to address the problem of non-uniqueness of mathematical solutions, where multiple models may give rise to the same measured dataset, hence a framework may be proposed for the inversion based on prior geological knowledge of the site.

At LFBG, the 2009 resistivity data was collected with an IRIS Instruments Syscal Kid Switch 24 instrument, and a 36 m long array of 24 electrodes spaced 1.5 m apart (Figure 19). The array style selected was dipole-dipole (Figure 20) with nine depth

levels and an approximate depth of investigation of 3.8 m. The reported horizontal resolution of the method used is +/- 0.25 m. The dipole-dipole array has a shallow depth of investigation and is very sensitive to horizontal changes in resistivity, but relatively insensitive to changes in vertical resistivity, and hence good in mapping vertical structures, but poor in mapping horizontal layers. The raw apparent resistivity data was inverse modelled using software Res2Dinv (Loke et al., 1996). Thirteen separate resistivity arrays were set out perpendicular to the trench area across the proposed drilling locations, such that the array was approximately half covering the trench area and half over undisturbed ground (**Figure 21**). Where it was possible to identify a trench by vegetation change, east-west trending dipole-dipole transects were aligned along the centre of that particular trench.

Transect positions were recorded using a Trimble AG-114 DGPS with Omnistar differential corrections to a reported accuracy of +/- 0.25 m.

Figure 19. Mr. George Brabec from Alpha Geophysics collecting resistivity data at proposed corehole site CH11.

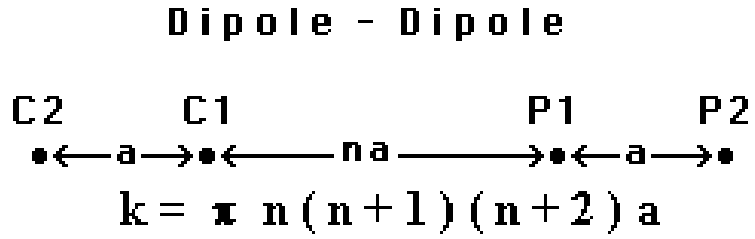

Figure 20. Diagram of the dipole-dipole array, where C1 and C2 are the injecting current (I) electrodes, P1 and P2 are the measurement potential (V) electrodes, and k is the geometric factor used in determining the apparent resistivity P_a = k V/I (Loke, 1999).

Figure 21. Location of dipole-dipole resistivity transects, July 2009.

The second resistivity survey performed in May 2011 crossed the full north-south length of the LFBG along three sub-parallel arrays (Figure 22). Resistivity data was collected using an ABEM Lund 64 with 64 electrodes at 5 m spacing. The electrode array selected was the Wenner-Schlumberger array (Figure 23), which is well suited to detection of layers and is moderately sensitive to both horizontal and vertical features.

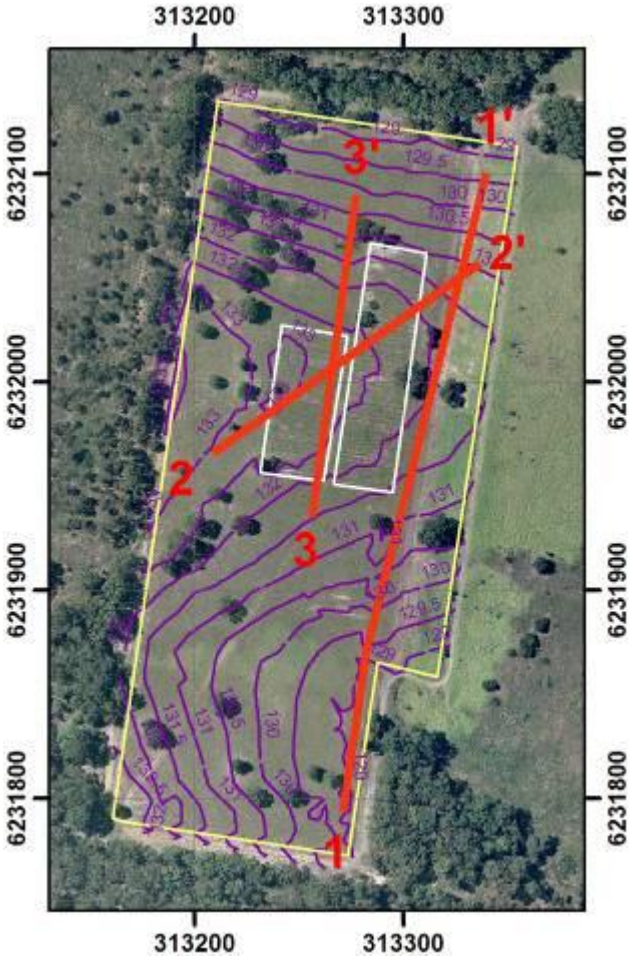

Figure 22. Location of Wenner-Schlumberger resistivity transects May, 2011.

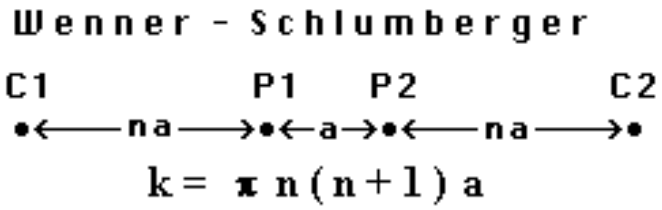

Figure 23. Diagram of the Wenner-Sclumberger array, apparent resistivity P_a = k V/I (Loke, 1999).

3.1.2 GROUND PENETRATING RADAR

Ground penetrating radar (GPR) is a high resolution electromagnetic technique designed to investigate the shallow subsurface, and uses the principle of scattering electromagnetic waves to locate buried objects. In GPR, an electromagnetic wave pulse is radiated from a transmitting antenna on the ground surface and travels through the ground at a velocity determined by the permittivity of the ground material. When the wave encounters an object that has different electrical properties to the surrounding medium, part of the energy is reflected (stored briefly and re-emitted) back to the surface, where it is captured by a receiving antenna and the arrival time and amplitude is recorded. The returned energy from a single propagating pulse is recorded over time at the receiving antenna as a *trace*, or a plot of amplitude versus two-way travel time. The two-way travel time is greater for deeper objects than for shallow objects, and if the permittivity of the medium is known, the time of arrival of the reflected wave can be used to determine the depth of the buried object (Jol, 2009).

GPR surveys are conducted by moving the antennas continuously over the ground to record a cross-section of traces. The radar frequency and antenna size may be selected to suit the size and depth of the target object. Lower radar frequency may improve signal penetration, but will also result in lower resolution of reflections. Due to the vertical orientation of radar wave propagation into the ground, the best reflections will be obtained from horizontally aligned objects or soil horizons. GPR is most useful in low electrical loss materials. Clay rich environments or areas of saline groundwater create conditions where radar signal penetration is very limited.

At LFBG, the GPR data was collected using a MALA Tamac xv11 monitor with 250 MHz antenna (Figure 24). The MALA system includes an on-board display of the raw GPR section which allows a crude assessment of the data in the field. Eighteen GPR transects were completed at locations perpendicular to the trench block boundary on all sides (Figure 25). Where it was possible to identify a trench by vegetation change, east-west trending GPR transects were aligned along the centre of that particular trench.

Figure 24. Mr. George Brabec from Alpha Geophysics collecting GPR data at proposed corehole site CH24.

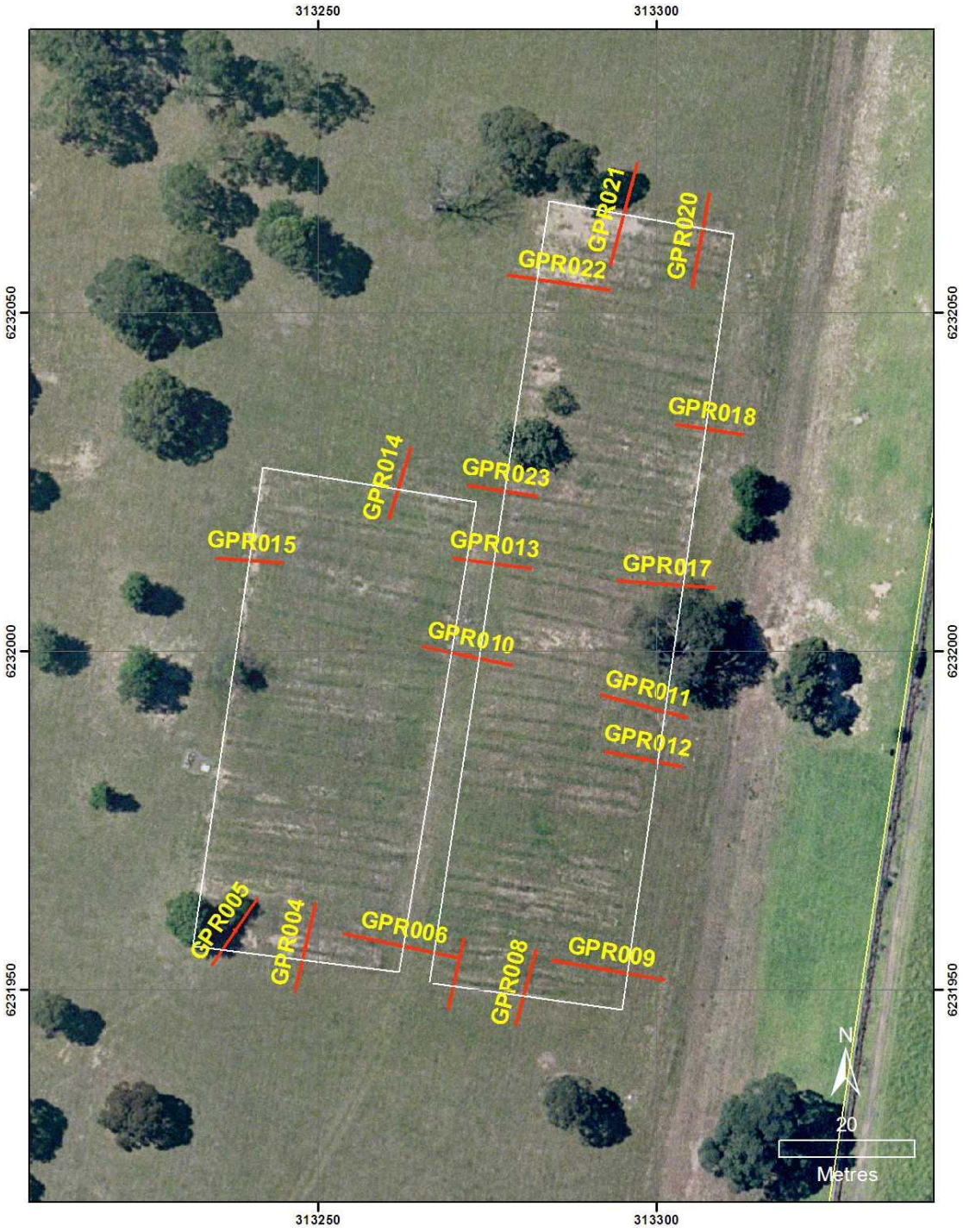

Figure 25. Location of GPR transects.

3.1.3 TIME DOMAIN ELECTROMAGNETIC METHOD

Time domain electromagnetic (TDEM) techniques are used in mineral exploration and have also been adapted for environmental and engineering applications requiring the mapping of buried metal objects, for example buried drums, underground storage tanks or unexploded ordnance. At LFBG, TDEM was used to map the remnant trench marker posts.

TDEM techniques operate by switching current on and off in a transmitter coil over the ground surface to generate a primary electromagnetic field pulse. When the current is switched off, the current flow in the coil stops over a brief period of time known as the ramp time, during which the primary electromagnetic field also varies with time. The change in the primary electromagnetic field inducts a momentary secondary electromagnetic field in the ground beneath the coil, which immediately begins to decay, and in doing so generates eddy currents that propagate into the subsurface. The eddy currents in the ground vary in strength and longevity with the conductivity of the ground and with the conductivity of objects buried in the ground. The eddy currents are sensed by electromagnetic induction at the ground surface using a receiver coil. Measurement of the receiver coil only takes place while the transmitter coil is switched off, and multiple measurements can be time gated to detect eddy currents at progressively greater depths. Transmit-receive duty cycle, current and transmitter loop size can be varied to suit the size and depth of the intended target. TDEM can suffer from unwanted fields generated in nearby surface metallic objects such as fences or overhead power lines, and hence is typically not well suited to urban areas (McNeill, 1990).

At LFBG, TDEM data was collected using a Geonics EM-61 with a duty cycle of 150 Hz (150 measurements per second). The EM-61 TDEM device is especially adapted for buried metal detection. After each EM pulse, the secondary fields induced in the ground decay faster than the fields in metallic objects, and the EM-61 measurement cycle is timed after the earth response dissipates, and hence is optimised for detection of the prolonged response from conductive metal objects, both ferrous and non-ferrous. The EM-61 small loop size is also optimised for detection of small shallow targets such as buried drums, and the system is reported capable of detecting drums at depths of over 3 m (McNeill, 1996). The EM61 contains two receiver coils, and the differential response can be used to reject response from surface objects or overhead interference, and to determine the approximate depth to detected targets. Due to the horizontal orientation of the receiver coil, metallic objects which are buried flat lying will induct a greater signal in the receiver coil than if the same object were buried vertically aligned.

The EM-61 data was collected in a grid pattern over the eastern and western ends of the trenches with the aim of detecting the remains of buried trench marker posts. The EM-61 was interfaced with a sub-meter accuracy DGPS for positioning information, and wheeled along parallel survey lines separated by one meter, with a GPS triggered data station interval of 20 cm. The stored data was later contoured and the resulting false colour image was plotted over an air photo image of the trench area. This final map of EM response was used to interpret and mark-up possible trench marker post targets, and a list of possible target coordinates was produced.

3.2 Drilling and Sampling

A 'dial-before-you-dig' check for buried services was performed for the general LFBG site area (search address submitted "Little Forest, north of New Illawarra Road") prior to the commencement of drilling, with no services reported in the area. In addition, all proposed drill sites were checked with a hand-held electromagnetic pipe and cable locating detector to a radius of 5 m.

3.2.1 DIRECT-PUSH CORING

Direct-push coring is a rapid percussion drilling technique used for sampling unconsolidated soil materials and very soft rock. A steel push-tube containing a polyethylene liner is forced into the ground in 1 m lengths by an overhead hydraulic hammer. After each metre of drilling, the steel push tube is retrieved and an intact core sample is obtained inside the polyethylene liner. Each core is variably compacted by the percussion process depending on the compressive strength of the intersected lithology, for example a 1 m core of clay material may be compacted to a final length of 90 cm.

At LFBG, a Geoprobe 7720DT track-mounted direct-push rig (**Figure 26a**) operated by Macquarie Drilling Pty Ltd was used in August 2009 to obtain shallow soil and weathered shale cores at 33 locations specified in **Figure 52** (see page 74). The Geoprobe has a specified hammer frequency of 32 Hz and a down force of 160 kN per blow. A narrow core sample diameter of 38 mm was selected to maximise chances of penetration into material of greater rock strength, although the operator considered the system incapable of penetrating Class IV shale (Pells et al., 1988).

Direct-push cores were retained in aluminium core trays for later sub-sampling in the laboratory and long term storage. A window was cut in the polyethylene tubing to allow inspection, photography and sampling of core. Samples 3 cm in length were cut from selected cores at 0.5 m intervals for the measurement of soil moisture.

The steel push tubes were cleaned between coring locations with a high pressure water cleaner and Decon-90 inside a decontamination trailer (**Figure 26b**). Rinsate was captured for later disposal offsite. All direct-push coreholes were subsequently abandoned with bentonite grout to the surface.

Figure 26. a) Geoprobe 7720DT Direct-push coring rig and **b)** decontamination trailer.

3.2.2 SOLID FLIGHT AUGER DRILLING

In solid flight auger (SFA) drilling, a helical screw is driven into the ground with rotation. A drill bit (auger head) at the tip of the auger cuts into or crushes the rock/soil material, and the cuttings are mechanically lifted to the surface on the blades of the screw. Auger drilling is generally restricted to shallow holes in soft unconsolidated material or weak weathered rock. Penetration is superior to direct-push, as auger heads with tungsten carbide cutting teeth can chip through harder materials by abrasion. Samples obtained by SFA drilling are disturbed and considered to be a mixed representative of a certain length or interval down-hole. Auger drilling eliminates the need for a drilling fluid (liquid or air), although there is a high potential for smearing cuttings or contaminants along the hole.

SFA drilling to obtain rock chip samples and prepare holes for well installation was performed at LFBG in two different rounds of drilling by separate companies in 2009 and 2010.

In August 2009, the Geoprobe 7720DT was used with a 125 mm solid flight auger (**Figure 27**) in selected coreholes where the direct-push technique failed to achieve the target depth. Four holes were extended to a depth of 5 m, and the drill string was retrieved every 0.5 m to obtain a cuttings sample. Samples were bagged in plastic and later transferred to 20 L buckets. The auger holes were then used for TYPE I shallow groundwater monitoring well (see page 49) construction performed by Consulting Earth Scientists Pty Ltd.

Figure 27. Sampling at CH21 from SFA using the Geoprobe 7720DT.

In September 2010, a utility mounted Edson MRA260 rotary drill rig operated by EPOCA Environmental was used with 100 mm solid flight augers (**Figure 28**) to obtain a cuttings sample every 0.5 m and allow geological logging. Samples were retained in 500 ml LDPE jars. These holes were subsequently over-drilled with 150 mm SFA in preparation for TYPE II shallow monitoring well installation.

Figure 28. SFA drilling at W12 with the Edson MRA260.

3.2.3 ROTARY AIR HAMMER DRILLING

In air hammer drilling, a pneumatic piston-driven percussion head is used to drive a tungsten drill bit to hammer away cuttings from the rock. Compressed air is used to power the percussion and is also forced through the drill string to lift the cuttings to the surface. Rotary air hammer methods are suitable for drilling into harder consolidated rocks and for identifying groundwater bearing formations. Samples obtained by rotary air drilling are highly disturbed and drill cuttings are ejected continuously and forcibly from around the drill string. The introduction of high pressure air may affect the hydrochemistry of some aquifers.

In September 2010, the Edson MRA260 rotary drill rig was used with 95 mm air hammer (**Figure 29**) for second stage drilling following augering in preparation for TYPE III deep groundwater well installation. Sampling was not undertaken for holes drilled by air hammer due to the highly disturbed nature of the cuttings, although colour and texture changes in cuttings were noted for geological logging purposes.

Figure 29. Air hammer drilling at W2D using the Edson MRA260.

3.2.4 DIAMOND CORE DRILLING

In diamond core drilling, a rotary drill rig with a steel ring-shaped diamond-impregnated drill bit (**Figure 30**) attached to a hollow drill string is used to cut a cylindrical core of intact rock. Water, often combined with other additives, must be circulated through the drill string during drilling to lubricate and cool the drill bit and to remove drill cuttings from the hole. Core samples are forced inside a hollow core tube, which fits inside the end of the core barrel at the cutting face. As drilling progresses, rock core is pushed into the core tube, which may be extracted from the drill string at intervals by winching to the surface. Diamond core drilling is capable of penetrating very hard rock at depths exceeding a kilometre, although it is not well suited to surficial weathered rock or unconsolidated material which tends not to cut well and the core falls out of the core barrel. Typically, some metres of hole will be augered out first until more cohesive material is encountered.

In August 2009, a Hydrapower Scout VI coring rig operated by Macquarie Drilling Pty Ltd was used to obtain NQ size diamond drill core in hole CH31 angled at 45 degrees from the vertical, underneath trench 52. A solid flight auger was first used to clear the unconsolidated material to a depth of 2.23 m, and coring then commenced to a total hole-length of 10 m (7 m below ground). The core was retrieved using a 'split spoon' type core tube, considered by the driller to have the best chance of retrieving core in unconsolidated materials. The core was assembled in 1 m lengths in aluminium core trays for inspection, sampling and storage.

Figure 30. Diamond drill bit used with Hydrapower Scout VI coring rig at CH31.

3.3 Well construction

Two rounds of well construction were undertaken by separate companies in August 2009 and September 2010. The companies were selected following assessment of tenders for each campaign. All wells are compliant with minimum construction requirements for water bores in Australia (ARMCANZ, 2003).

Four different types of well design were used (see **Figures 31** and **32**):

- TYPE I, CH series shallow wells,
- TYPE II, W series shallow wells
- TYPE III, W series deep well
- TYPE IV, CH series angle well

3.3.1 TYPE I, CH SERIES SHALLOW WELLS

In August 2009, four type I design shallow wells were installed by Consulting Earth Scientists at direct-push core-hole locations CH17, CH18, CH21 and CH30 (see **Figure 52,** page 74). Following direct-push coring, the holes were subsequently over-drilled with 125 mm solid flight auger to a depth of 5 m. A variable amount of cavings or wash-out from water bearing zones in the loose formation fell into the open holes in between drilling and well installation, effectively reducing the available depth for wells CH17 and CH30. The monitoring wells were constructed using 50 mm internal diameter Class 18 UPVC with threaded couplings and o-ring seals. Ninety cm long slotted casing screen sections were installed above a 25-30 cm sump, and a plastic centraliser was included at the threaded join at the top of the screen. A 2 mm sand filter pack installed from the hole base to a height of 0.5 m above the top of the screened interval. The remainder of the annulus surrounding the casing was completed to the surface with bentonite pellets. All hole filling materials were poured by hand from the surface without use of a 'tremie pipe' down-hole guide tube. CH18 and CH21 were capped with a 1.1 m tall 'monument' style well cover set in a concrete pad. CH17 and CH30 were completed with a ground level 'road box' style well cover set in a concrete pad. Well specifications and construction diagrams and are listed in **Appendix A** and **B** respectively.

3.3.2 TYPE II, W SERIES SHALLOW WELLS

In September 2010, twelve Type II design shallow groundwater wells were installed by EPOCA Environmental under the supervision of Coffey Environments at locations W2s, W2m, W3, W4, W5, W6, W7, W9, W10, W12, W13 and W15 (see **Figure 55**). Following sampling of auger cuttings, these holes were widened to 150 mm by solid flight auger and a 100 mm internal diameter temporary PVC casing was inserted. The monitoring wells were constructed inside the temporary casing using 50 mm internal diameter Class 18 UPVC casing, with a slotted screen interval generally 2 m in length and a sump at the base generally 1 m in length. A threaded coupling was used to connect the casing to the top of the slotted screen interval, and a push-in connector was used to connect the sump to the base of the screen. A plastic centraliser was included at the threaded join at the top of the screen. With the exception of W5, the

base of each hole was sealed with bentonite pellets to a minimum of 0.5 m below the level of the slotted casing. A filter pack consisting of 2 mm sand was then emplaced to minimum of 0.5 m above and below the slotted casing. The sand filter packs range from 2.7 to 4 m in length. With the exception of W9, the top of each filter pack was sealed with a minimum of 1 m length of bentonite pellets. All seal and filter pack materials were placed during gradual removal of the temporary casing. Any remaining annulus above the top seal was completed to ground surface with bentonite/cement grout. All wells were capped with a 1 m tall 'monument' style well cover set in a reinforced concrete pad with a steel bollard. Inside the monument, the PVC casing extends approximately 0.7 m above ground surface.

Exceptions with bentonite seal designs were made at holes W5 and W9. Hole collapse during installation of W5 left collapsed fill material at the base of the hole and insufficient room remaining for a standard 0.5 m bentonite bottom seal. As an alternative, bentonite pellets were mixed into the collapsed fill material. In W9, the filter pack extended to 0.3 m below ground surface and as a consequence only a 0.3 m bentonite top seal was installed.

3.3.3 TYPE III, W SERIES DEEP WELL

One type III design deep groundwater well was installed at W2d (**See Figure 55**) by EPOCA Environmental under the supervision of Coffey Environments. Following sampling and widening of the top 5.5 m of the hole to 150 mm diameter by solid flight auger, a 5.5 m length of 100 mm internal diameter (125 mm external diameter) Class 18 UPVC was installed as a permanent outer casing. A 1.5 m thick bentonite/cement grout seal was then emplaced at the base of the permanent casing. The annulus outside the permanent outer casing was then filled with bentonite/cement grout to ground surface. Following a 2 day period during which the grout was left to cure, the seal was then drilled through using a 95 mm rotary air blade tool, and then the hole was continued to total depth of 20.5 m using 95 mm rotary air hammer drilling. During air hammer drilling, the driller added a small quantity (~ 50 ml) of organic lubricant 'hammer oil' to the drill string. The inner well was then constructed using 50 mm internal diameter UPVC casing with a slotted screen interval 2 m in length, and a 1 m long sump at the base. Threaded couplings with hole centralisers were used to join sections of casing except for the join between the base of the slotted interval and the sump, where a push-in connector was used. A 4 m long filter pack consisting of 2 mm sand was then emplaced from the hole base to 1 m above the slotted interval. A 1.5 m thick bentonite top seal was placed above the filter pack, then the remaining annulus above the seal filled to ground surface with bentonite/cement grout. As per the Type II wells, W2d was capped with a 1 m tall 'monument' style well cover set in a reinforced concrete pad with a steel bollard. Inside the monument, the PVC casing extends approximately 0.7 m above ground surface.

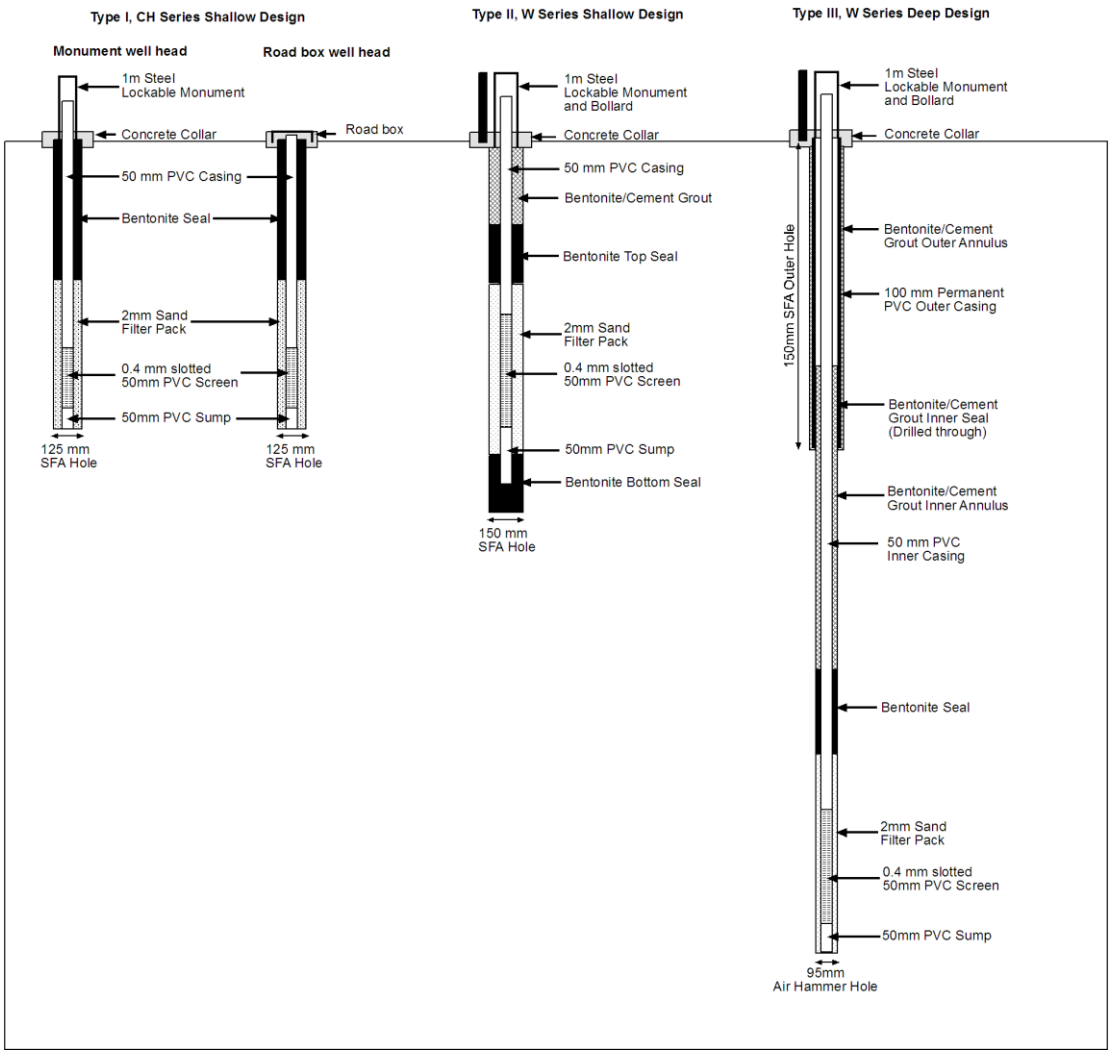

Figure 31. Type I, II and III well designs.

3.3.4 TYPE IV, CH SERIES ANGLE WELL

In August 2009, well CH-31 was installed by Macquarie Drilling under the guidance of Consulting Earth Scientists in the 45 degree angled diamond drill hole adjacent to trench 52 (see **Figure 51**). After diamond drill coring, the hole was widened to 150 mm by reaming and wash boring to allow insertion of a temporary steel casing. Significant problems with hole collapse were encountered during widening of the hole, and approximately 1 kg of the guar gum based organic drilling compound 'Tuff Loss' (essentially a fluid thickening agent) was added to hold the hole open until the temporary casing could be installed. Approximately 1500 L of water was used during this process, although it is not reported what proportion of water was lost to the formation and how much was recirculated to the surface during the wash boring process.

Well construction took place inside the temporary steel casing. The groundwater monitoring well was constructed using 50 mm internal diameter Class 18 UPVC with threaded couplings and o-ring seals, with a 1.5 m slotted screen section and a 0.5 m

sump at the base. Three PVC spacer guides were used to hold the well assembly in the centre of the hole. A 3 m long filter pack consisting of 2 mm sand and was extended from the hole base to 1 m above the slotted screen. The filter pack was sealed with a 1 m bentonite seal, and the remainder of the annulus was filled to ground level with bentonite/cement grout. Bentonite, sand and grout materials were emplaced during gradual removal of the temporary casing. The well head was completed with a ground level 'road box' style well cover set in a concrete pad.

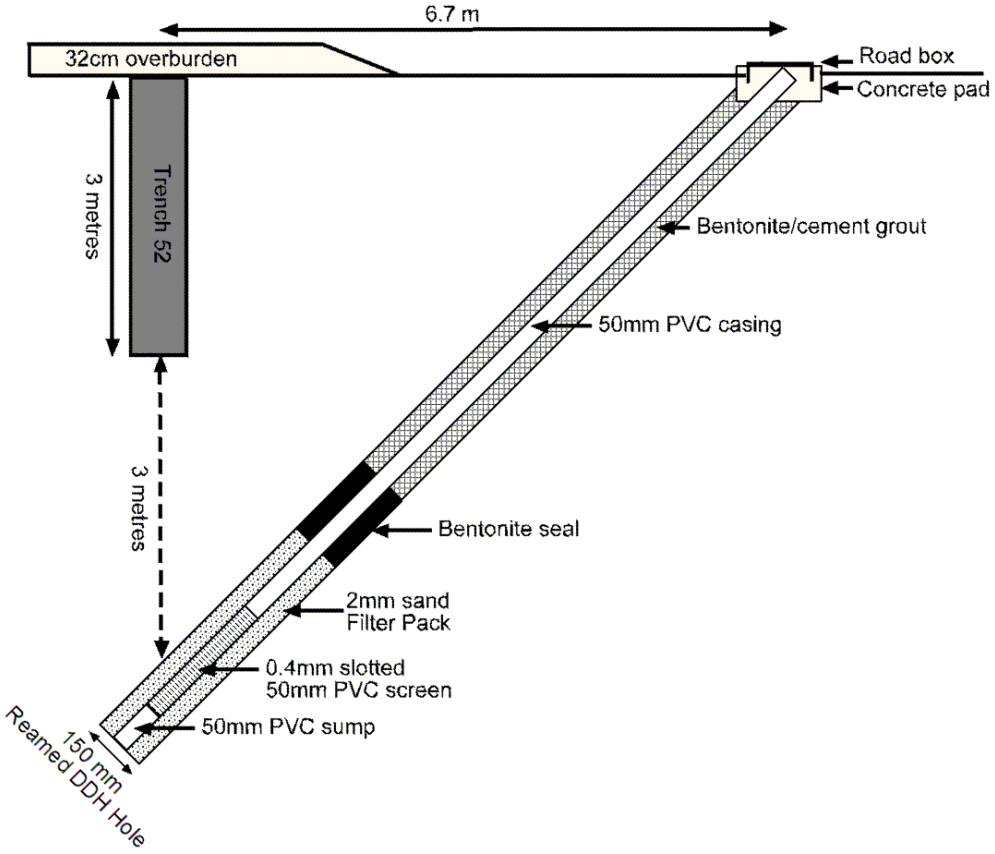

Figure 32. Type IV well design.

3.4 Well development

The process of well development involves extraction of water from the newly constructed well in order to remove fines from the well and filter pack, to remove water added during the drilling process and to allow the flow of representative aquifer groundwater into the well. Well development is usually commenced with a surging action to agitate water into and out of the filter pack in order to mobilise fines (or residual drilling mud) into suspension so that they can be drawn into the well and removed. Following this, the well may be purged by airlift or pumping and water quality parameters measured until the water produced is free of turbidity, sand or silt. The Australian guidelines suggest development should continue until a minimum of ten bore volumes is removed, or until three consecutive water quality parameter measurements produce similar results (ARMCANZ, 2003).

At LFBG, the Type I CH series shallow wells were developed in August, 2009 by ANSTO. Initial surging was undertaken using a 'Waterra' footvalve and subsequent purging by 12v submersible pump.

The Type II and III W series wells were developed in September, 2010 by Coffey Environments. Development was deliberately performed using low turbulence methods due to the fine clay-silt size and unconsolidated nature of the formation in which the wells are emplaced. Initial surging was performed using a stainless steel bailer (see **Figure 33**). All wells were purged by hand bailing, and W2m and W7 were further purged using submersible electric pumps due to the higher yield. Water quality parameters were measured at 5 wells during development.

The Type IV CH series angle well was developed in August, 2009 by Consulting Earth Scientists. Initial surging was performed using a 'Waterra' footvalve and subsequent purging by nitrogen gas airlift (sparging). The well was then purged three times till dry using a submersible electric pump.

Figure 33. Well development of W6 using the stainless steel bailer.

3.5 Well and core-hole abandonment

The proper decommissioning and sealing of core-holes or undesired monitoring wells is especially important at contaminated sites due to the potential for cross-contamination between aquifers and to prevent contaminants at the surface entering the hole. In cases where hydraulic head can exceed topographic elevation, well abandonment may be required to prevent outflow of contaminated water.

With the exception of coreholes CH17, CH18, CH21, CH30 and CH31 which became operational groundwater wells, all remaining 29 core-holes drilled in the CH series were filled to ground surface with bentonite pellets. During the drilling of CH1, one steel direct-push tube became dislodged from the drill string and was unable to be retrieved by the driller. This push tube remains buried at 2-3 m depth and CH1 was backfilled to ground surface with bentonite pellets.

Four holes: W1, W7a, W11d and W14d; were abandoned during the installation of the W series wells.

Well W1 was compromised due to over-filling of bentonite during construction of the bottom seal, and the borehole was subsequently abandoned to ground surface with bentonite/cement grout.

During drilling of W7a, one solid flight auger drill rod became dislodged from the drill string and was unable to be retrieved by the driller. The drill rod remains buried at 4.5 – 6 m, and W7a was back-filled to ground surface using bentonite pellets.

Type III wells W11d and W14d were partially completed to first stage emplacement of permanent outer casing, but were compromised due to failure of the bentonite/cement grout inner seals, which did not cure properly and allowed water/slurry to be pushed up into the hole. The permanent casing was subsequently removed and the holes were backfilled to ground surface using bentonite pellets to 1 m depth, then completed to ground surface with bentonite/cement grout.

4 Results/Discussion

4.1 Geophysics

4.1.1 DIPOLE-DIPOLE RESISTIVITY FOR TRENCH DETECTION

Alpha Geophysics reported raw and calculated apparent resistivity pseudo-sections together with an inverse model resistivity section for each of the thirteen traverses. The inverse modelled resistivity sections are here evaluated for interpretation (see **Figure 34 and 35).** With the exception of Traverses 009 and 013, all inverse modelled sections exhibit between 2% and 6% RMS error compared with the measured data. The resistivity colour scale presented is not consistent from section to section.

In general, despite the poor ability of dipole-dipole method to model horizontal layers, all sections display a clear two horizontal layer model. Laterally, the sections can be separated into two zones, with a distinct change in the resistivity distribution and intensity over the trench area (trench zone) compared with outside the trench area (undisturbed zone).

Over the trench zone, the contrast between horizontal layers is more pronounced, with a relatively high resistivity layer near surface (up to 250 ohm.m in the top 1-1.5 m), and low resistivity layer at depth (80-90 ohm.m). The boundary between these two layers is sharp. The low resistivity of the bottom layer suggests high water content. The high resistivity of the top layer and sharp boundary between layers suggests it may be above the local water table at the time of the measurements, and hence also that this layer is not holding moisture and is more susceptible to evaporation and/or is more permeable than soils in the undisturbed zone.

In the undisturbed zone, the contrast between the two horizontal layers is much less pronounced, and often the pattern is reversed with a lower resistivity top layer (~100 ohm.m) and higher resistivity bottom layer (150-200 ohm.m). This pattern is interpreted in conjunction with the direct-push drill cores to represent a variably moist topsoil and clay layer, underlain by the dry weathered shale zone. In some sections (Traverses 004 and 010), the presence of a third lower layer is suggested below 3.75 m depth with low resistivities down to 50 ohm.m. This may represent the top of the deeper water bearing zone encountered during drilling of the W series wells, and/or a transition to less weathered shale which may be more conductive than its weathered counterpart.

The lateral boundary between these two zones is taken to represent the edge of the trench block area. Often the lateral boundary between zones is sharp with highly contrasting resistivity, although in some sections the boundary cannot reliably be distinguished without comparison to the air photo due to low contrast between zones (Traverse 004). It is reasonable to expect variation in water content or fill material in different parts of the trench area, and hence that lower contrast in resistivity across the trench boundary in some areas may be real.

In some sections, a distinct boundary between zones appears misaligned with the edge of the trench area, and the low resistivity layer, elsewhere associated with high water content, can be seen to extend into the undisturbed zone by up to 4 m (Traverses 002 and 008). This would not seem to be caused by systematic GPS error, as the boundary in most traverses appears well matched to the air photo.

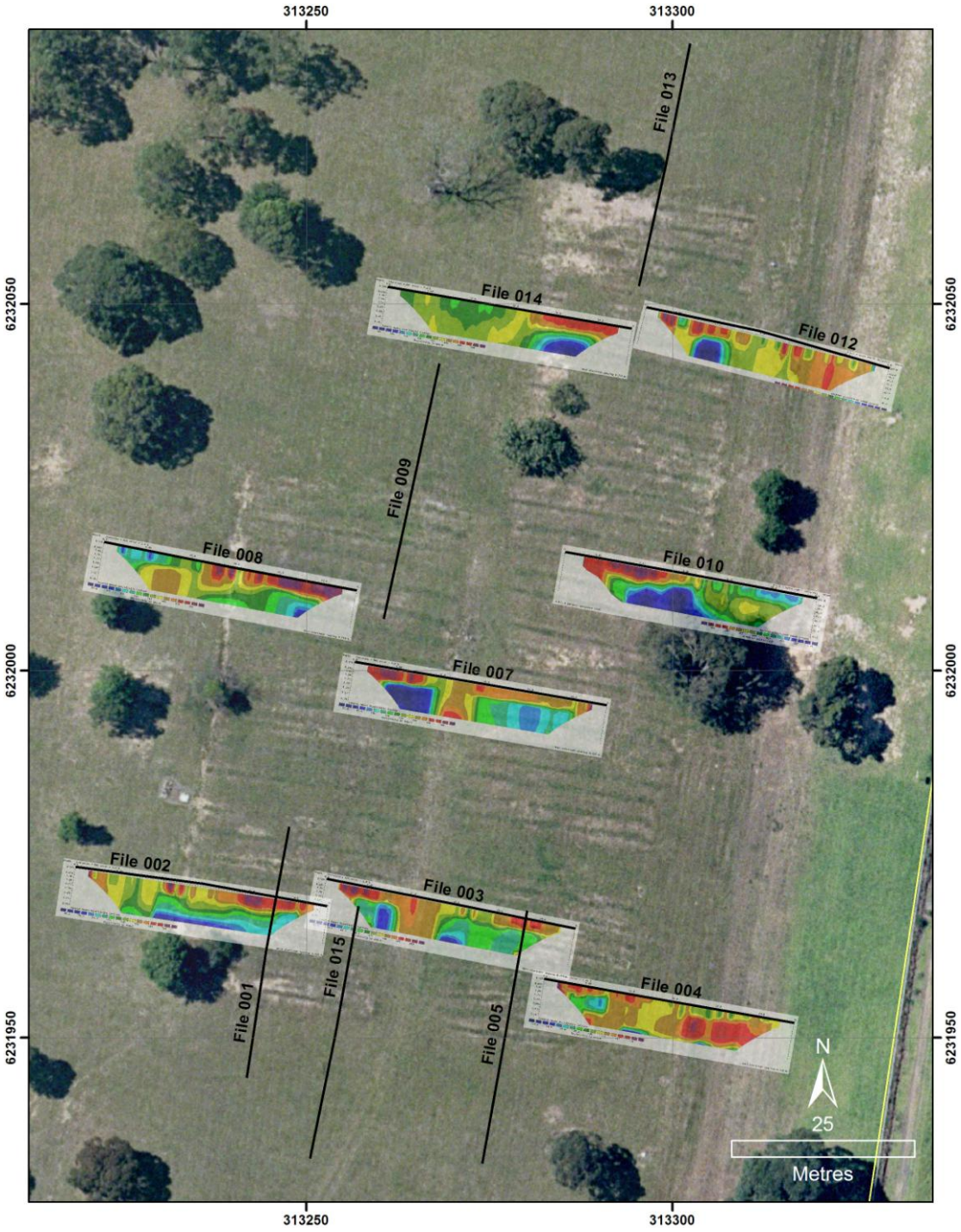

Figure 34. Eight east-west oriented inverse model resistivity sections plotted over aerial photographs. Traverse location measured by GPS is marked by the black line. The orientation of the depth axis of each section should be considered into the page.

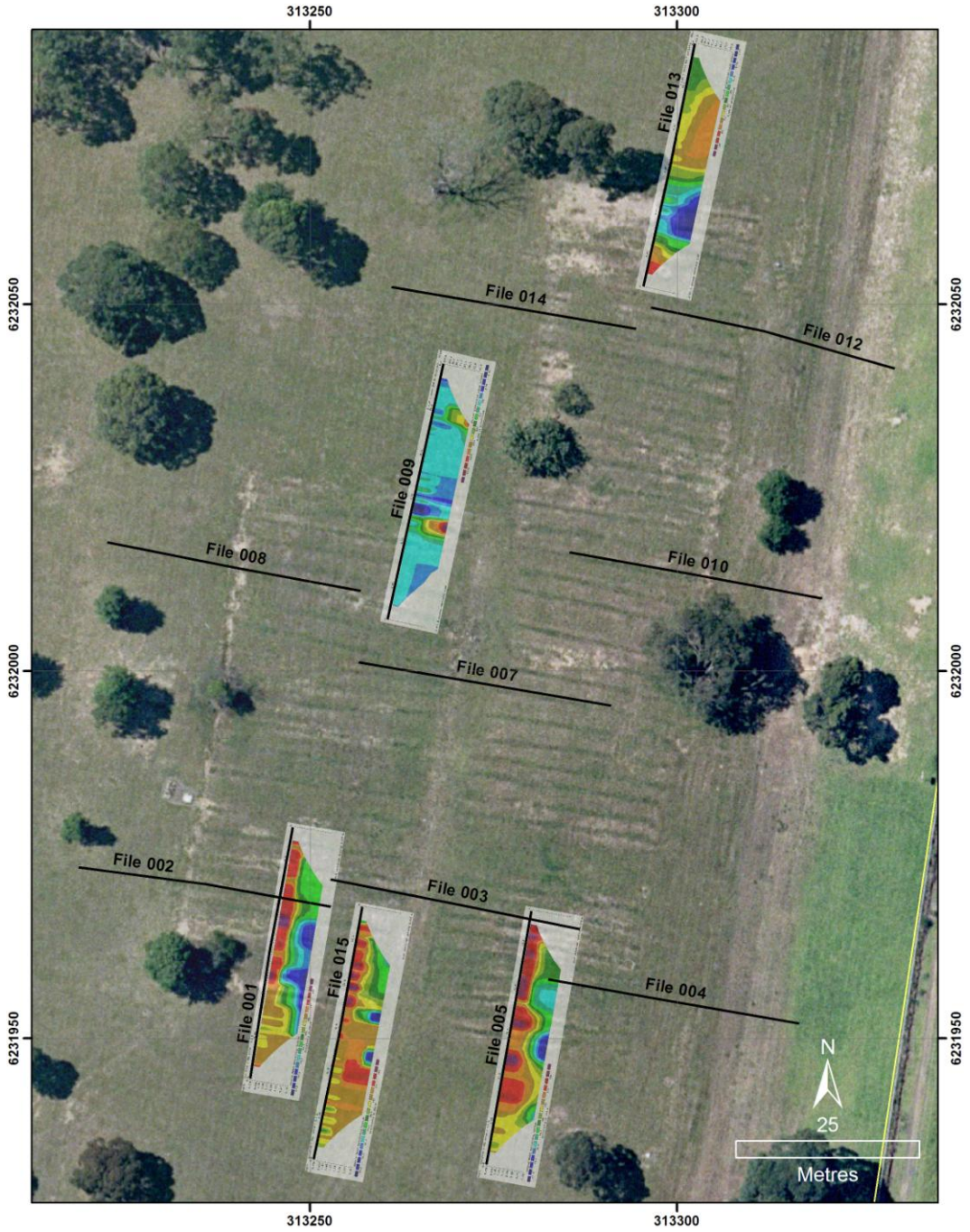

Figure 35. Five north-south oriented inverse model resistivity sections plotted over aerial photographs. Traverse location measured by GPS is marked by the black line. The orientation of the depth axis of each section should be considered into the page.

Traverse 9 has significantly worse convergence with measured data compared to the other sections, with a residual 18.5% RMS error. The maximum resistivity modelled in Traverse 9 exceeds all other sections by a factor of 20. This anomalously high value appears to be represented by 3 data points in the measured section (Alpha Geophysics, 2010), and possibly these values have been overlooked during filtering for unrealistic data. Otherwise, if real, they may be interpreted as a discrete high resistivity object towards the eastern end of the base of trench 75, such as an impermeable boulder or void (air-space).

4.1.2 WENNER-SCHLUMBERGER RESISTIVITY FOR GEOLOGICAL LAYERS

The data of these sections (see **Figure 36**) is reported to be of high quality in general, the measurements had a low standard deviation and low RMS error values ranging from 0.67 to 1.3% (Guinea, 2011). Damp weather conditions at the time of the survey ensured good electrical coupling of the electrodes with the ground. Due to the 320 m length of section A, large electrode separations were possible and resistivity was modelled to over 50 m depth. Sections B and C were 160 m long and the maximum depth modelled was around 25 m. The sections have not been corrected for ground surface elevation, which in the trench area may account for a 3 m over-estimation of depth.

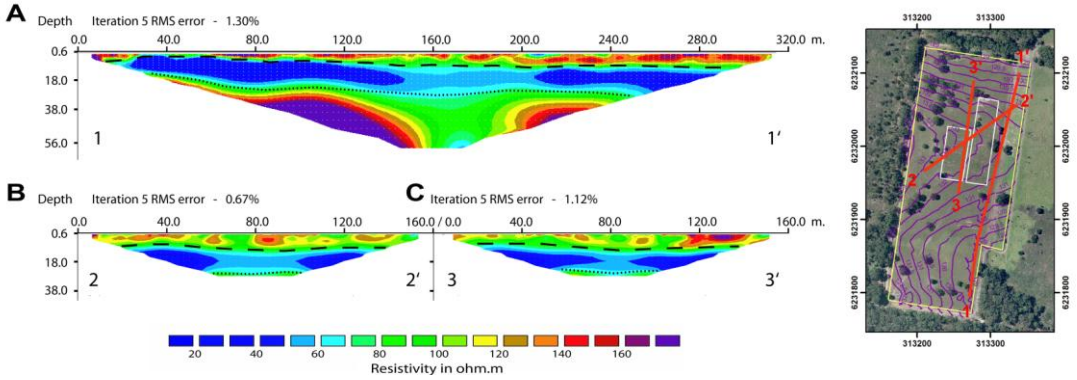

Figure 36. Three Wenner-Schlumberger resistivity inverse model sections with Layer 2 outlined.

The sections can be separated into three resistivity layers:

- Layer 1, a moderately resistive thin upper layer ranging from 130 to 160 ohm.m, shown thickening toward the north in Section A. This layer appears very thin or absent towards the southern end of Section A coincident with the shallow valley occupying the lowest topography on site. This layer thickens to around 7 m deep at the northern boundary.
- Layer 2, a low resistivity layer ranging from 20-60 ohm.m, shown dipping to the north at around 2 degrees, up to 15 m in thickness. A band of relatively higher resistivity (60 ohm.m) is present between 150 and 200 m along Section A, and this position is also confirmed in Sections B and C.
- Layer 3, bottom layer with high resistivity grading from 70 to 200 ohm.m, shallowing in the south and much less resistive in the centre of the section (90 ohm.m). The top of the lower layer ranges from 17 m deep in the south to 30 m deep in the north.

The best geological control available for this survey is the geological log for the drilling of piezometer P1d (PPK, 2002; Appendix B). P1d is located adjacent to Section A at 45 m, and the log shows the start of the Hawkesbury Sandstone at 13 m depth. This depth is corroborated by the log of W2d which encountered the Hawkesbury Sandstone at a similar elevation.

Geologically, the resistivity layers may be interpreted as:

- Layer 1, 'weathered zone' consisting of around a metre of topsoil and clay above several metres of dry leached weathered shale. From drilling, this layer is known to also contain thin bands of hard siltstone. At the north end of site, a high resistivity feature appears to be present at the same northing on both Section A and Section C. The connection between these two parallel sections may indicate the position of a near surface sedimentary structure or channel, possibly a larger body of the siltstone.
- Layer 2, 'shale', consisting of bands of black shale and siltstone. The low resistivity of this layer (20 ohm.m) suggests water saturation, and that it corresponds to the shale aquifer of Bradd, 2003. At the south end of site where Section A passes through the topographic low, Layer 2 appears to come closer to the ground surface. This may represent a thinning of the weathered zone in this area. It is probable that the water represented by the low resistivity passes up into the weathered zone at this location, and hence it does not appear possible to distinguish the boundary between Layer 1 and Layer 2 where both layers are saturated. The higher resistivity (60 ohm.m) in the centre of all Sections A,B,C in this layer may not be significant and may just represent natural variation of resistivity in the shale layer. It is also possible this band may indicate the presence of relatively fresh water at the centre of the LFBG site.
- Layer 3, 'sandstone'. This resistive layer (200 ohm.m) is interpreted as representing the coarse grained Hawkesbury Sandstone. The gradient of resistivity over the top 10 m of Layer 3 may represent a gradual change in lithology with depth, such as a transitional zone between the sandstone and shale consisting of alternating bands or interbedded sandstone and shale, described as laminite in the drilling of P1d and P2d. This gradient may also represent a gradual transition from relatively saline groundwaters in the shale to fresh groundwaters deeper in the sandstone. The lower resistivity (90 ohm.m) band centred at 170 m on Section A may be due to a lithological change at the level of the sandstone such as increased clay content, or alternatively it may represent increased or changed water content at this location. If due to water content, this feature could represent water moving downward from the upper layers within LFBG, or water moving horizontally beneath LFBG from a neighbouring site, and the water would be relatively more saline compared to the remainder of Layer 3. The feature is almost perfectly aligned with the resistivity anomaly observed in the centre of Layer 2.

In **Figure 37**, the base of shale contours presented in AAEC drawing CE22479 (AAEC, 1966) are compared with the resistivity Section A. The elevation of the base of the shale contours, shown as the yellow line overprinted on Section A, does not match well with the base of the resistivity Layer 2 'shale', suggesting that the BH auger holes did not reach this depth. Instead, the comparison shows the base of shale contours match better with the base of the resistivity Layer 1 'weathered zone'.

From **Figure 37**, it is also evident that the long axis of the lenticular feature defined by the contours does not align with the low resistivity anomaly in the Layer 3 'sandstone' of Section A. The lenticular feature occurs 50 m offset to the north. In addition, where the base of shale contours intersect with Section A, the lenticular

feature occurs at a much higher elevation than the Layer 3 ‘sandstone’ and its low resistivity anomaly. The lenticular feature occurs at 115.8 m at its lowest contour. The low resistivity feature in the sandstone Layer 3 extends some 40 m below this level. Hence, the feature described by the contours and the low resistivity in the sandstone do not appear related.

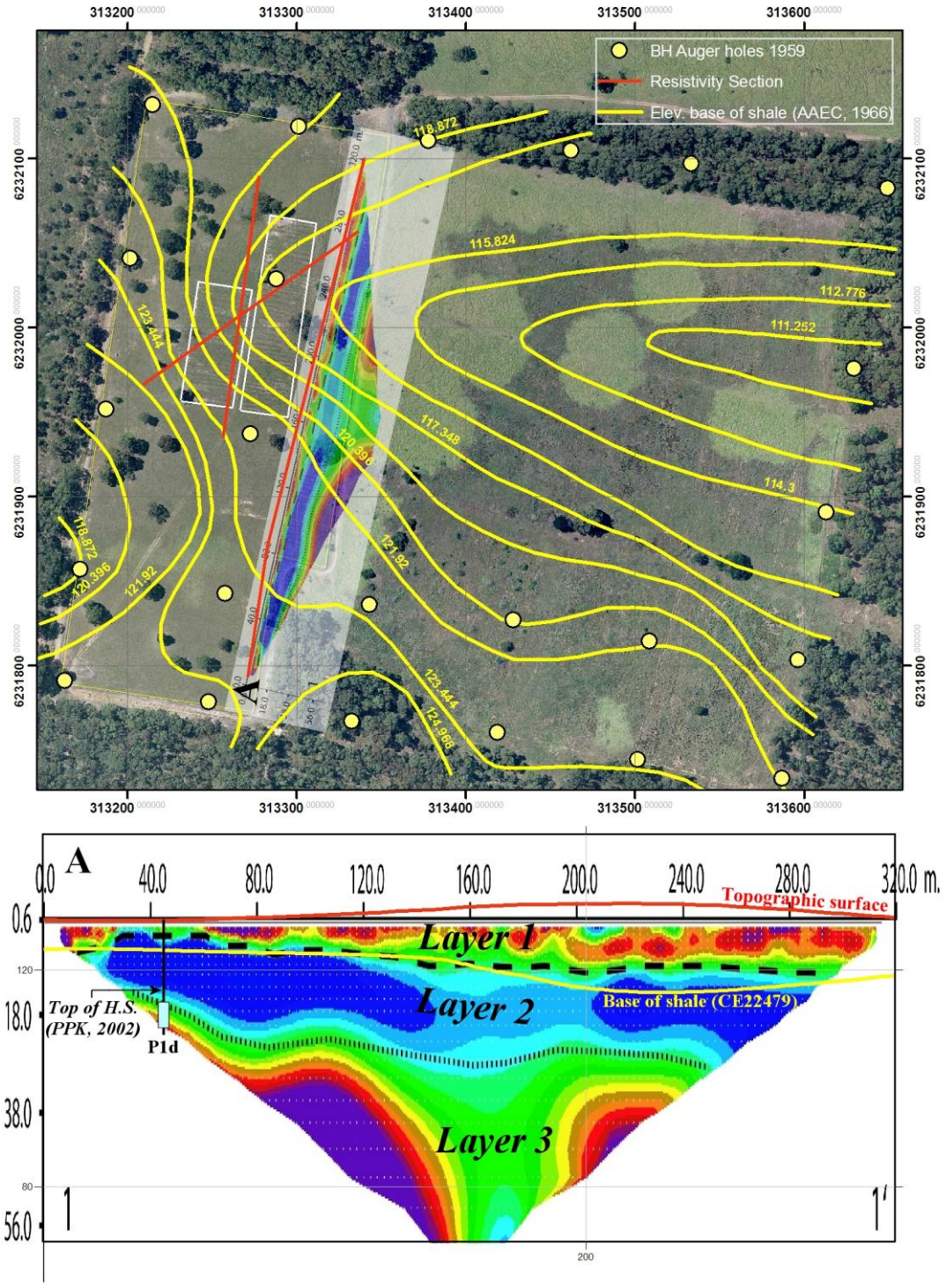

Figure 37. Comparison of Section A with base of shale contours after AAEC drawing CE22479 (AAEC, 1966).

A significant pattern in Section A is the 50 m wide central resistivity anomaly extending to the full depth of the section through both Layer 2 and Layer 3 adjacent to the southern half of the trenched area. At the Layer 2 level, the resistivity is slightly higher in the centre than laterally. At the Layer 3 level, the resistivity is much lower in the centre than laterally.

Four possibilities are considered below as causes for this pattern:

1. Lithology. In this possibility, the change in resistivity is entirely lithological in nature and likely relates to a lateral variation in clay content, although it is difficult to conceive why such a lithological change should occur in both the shale and the sandstone at the same location and extend to a depth of 50 m unless vertical fracturing and deep weathering were involved.

2. Fluid. Here, the resistivity pattern represents the presence of a different water content and/or salinity pervasive through both layers at the same location. Two different groundwater models can be conceived to explore this concept.
   a) Rainwater is recharging a relatively saline Layer 2, and after mixing is followed by vertical leakance to a relatively fresh Layer 3 (downward evolution of groundwater). Given the shale is proposed to be an aquitard, and that vertical hydraulic conductivity is usually considered an order of magnitude lower than horizontal hydraulic conductivity, the fluid scenario is unlikely unless a preferential flow pathway is present at this location, such as a vertical fracture network, or a lithological gap in the shale aquitard such as a sedimentary channel of more permeable material.
   b) A laterally moving groundwater plume of different resistivity passing beneath LFBG, without vertical leakage between layers. A plausible source/sink zone could be the fill area of Harringtons Quarry to the west, which has a possible hydraulic connection to both shale and sandstone aquifers. Alternatively, the trench area may be locally dominating recharge to the shale aquifer, while the water in the sandstone aquifer is being transported laterally underneath it.

3. Combination lithology/fluid causes. Here, freshwater recharge explains the pattern in Layer 2 and completely unrelated lithological changes explain the pattern in Layer 3; however the vertical alignment of the two patterns is just coincidence.

4. Combination lithology/artefact. It is possible the highly contrasting resistivity pattern of Layer 3 has some influence on how the resistivity of Layer 2 is measured, and that the apparent resistivity change seen in Layer 2 is an artefact of the method and is not real.

The existing groundwater well network does not capture samples of rock or water from the area of the central anomaly in either layer.

4.1.3 COMPARISON WITH PREVIOUS RESISTIVITY SURVEY

In **Figure 38**, Section A is compared to parallel Section C and excerpts of resistivity traverses "Line 1", "Line 2" and "Line 3" collected by GDCS in 2002 (PPK, 2002). Line 3 is located very close to the position of Section A. The GDCS sections, while only modelled to 20 m, also clearly define the shale layer, but insufficient coverage of the sandstone layer is provided to show whether the central anomaly pattern is present at depth. In the figure the aspect ratio of the GDCS sections has been changed to match the depth scale of Section A. Section A and Section C have also been truncated to 20 m to allow more direct comparison between all sections across the shale layer.

Note that from direct comparison of Section A with GDCS Line 3, the GDCS model appears to place the base of Layer 2 approximately 5 m shallower than the ANSTO model. While the GDCS lines were modelled using a different cell structure, different inversion parameters, different resolution and were visualised using a different (logarithmic) colour scheme, the comparison in **Figure 38** shows that in Layer 2 the central anomaly is repeatable in multiple adjacent sections (Section B not shown) collected in the two different surveys nine years apart. Also, the central anomaly is laterally traceable in Layer 2 across all six sections distributed across site in a line trending NWW-SEE. If a fluid cause is investigated for this pattern, then perhaps an evaluation of lateral transport along this line should also now be considered.

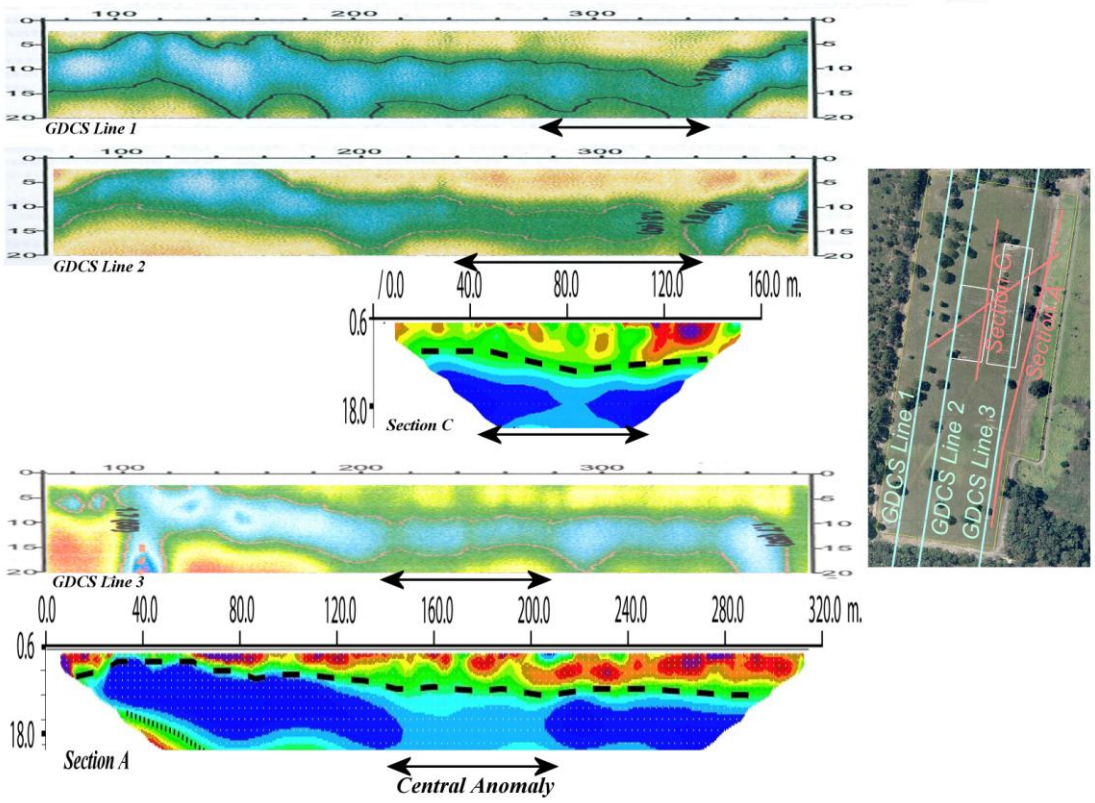

Figure 38. Comparison of ANSTO resistivity, 2011 vs GDCS resistivity 2002.

4.1.4 GROUND PENETRATING RADAR FOR TRENCH DETECTION

Seventeen out of the eighteen reported GPR transects are plotted (see **Figure 39**) over the aerial photograph for comparison with the trench locations. The location map and CAD drawing provided by Alpha Geophysics did not provide the location of GPR transect 019, and this has not been included in the figure. In addition, Alpha Geophysics provided the location of a GPR transect 023, but the data for this transect was not included in their report.

In general, it does not appear possible to use these transects to reliably distinguish between trench area and undisturbed ground, thus the technique would not appear suitable for delineating the edge of the trench block boundary. Contributing factors may include radar energy loss due to high clay content, and insignificant contrast in electrical permittivity between trench fill and undisturbed ground. Detail from the GPR transects compared with aerial photography are shown below at **Figures 40** to **48**.

Figure 39. Location of GPR transects.

Figure 40 shows GPR sections GPR004 and GPR005. GPR004 shows a weak reflector at 6 metres distance, aligned with trench 52. GPR005 shows two strong reflectors, the larger of which appears in line with trench 53. The smaller reflector appears originate in undisturbed ground in between trenches 52 and 53.

Figure 40. GPR sections 004 and 005.

Figure 41 shows GPR sections GPR006 and GPR009. GPR006 spans the access track between the two trench blocks, and it appears the most significant feature in the section is well aligned with the wheel tracks visible in the air photo. Both section GPR006 and GPR009 both show indistinct reflectors at the opposite ends of half-trench 3 and half-trench 4.

Figure 41. GPR sections 006 and 009.

Figure 42 shows sections GPR sections GPR007 and GPR008. GPR008 shows a buried object between 6.5 m. Both sections show some weak reflection hyperbolae which may be related to trenches 1,2 and 4 but comparison with the air photo shows they are not well aligned with trench positions.

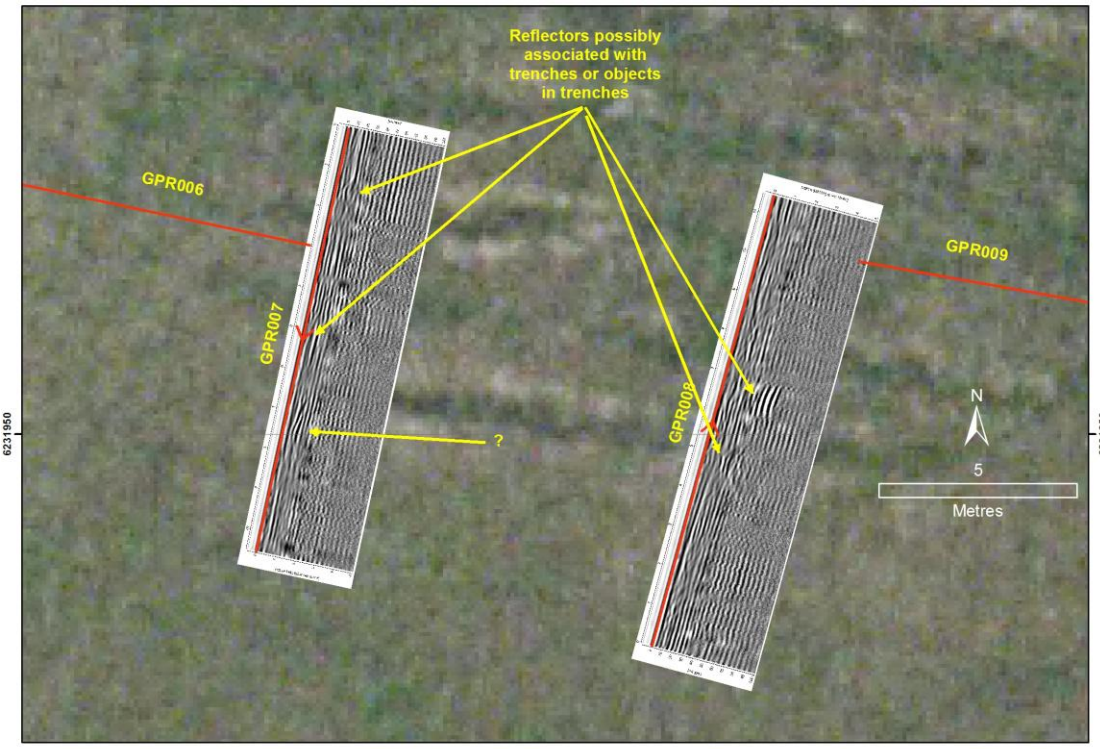

Figure 42. GPR sections 007 and 008.

Figure 43 shows sections GPR011 and GPR012, which were aligned with trenches 27 and 23 respectively in the field. GPR011 shows a horizontal reflector on the eastern side which disappears at approximately the start of trench 27, although this may also be noise reflected from the overhead tree canopy. Aside from two weak hyperbolae there is little in these sections to suggest the presence of a trench.

Figure 43. GPR sections 011 and 012.

Figure 44 shows section GPR015, in which a reflector is visible aligned with the edge of the trench block boundary. This feature could be associated with the small step in topographic elevation located on this side of the trenches, where perhaps the GPR unit lost even contact with the ground.

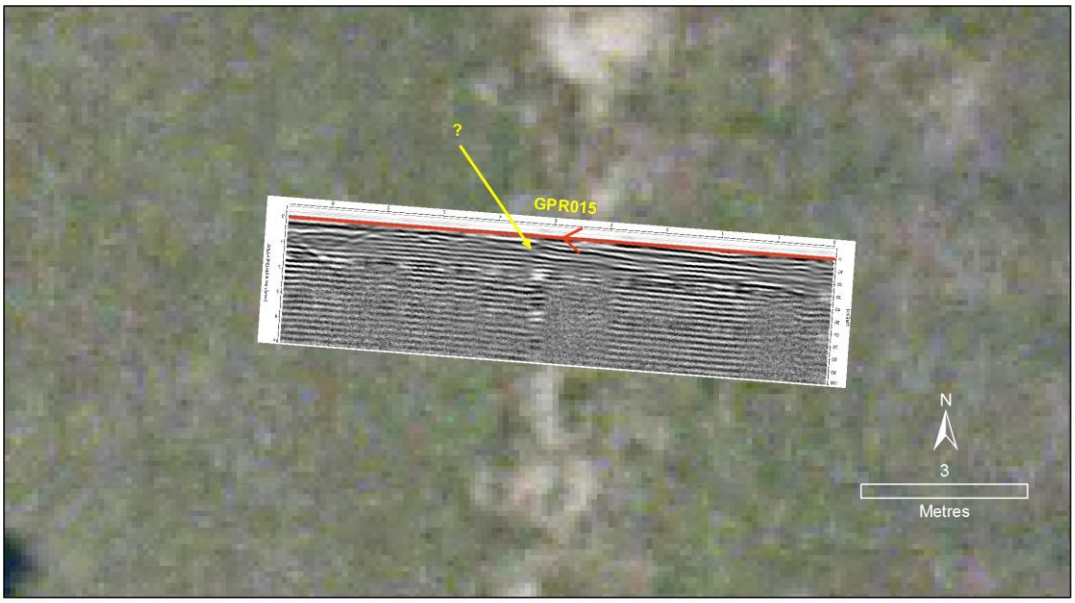

Figure 44. GPR section 015.

Figure 45 shows section GPR014. Weak reflection hyperbolae are visible at the location of trenches 75 and 76.

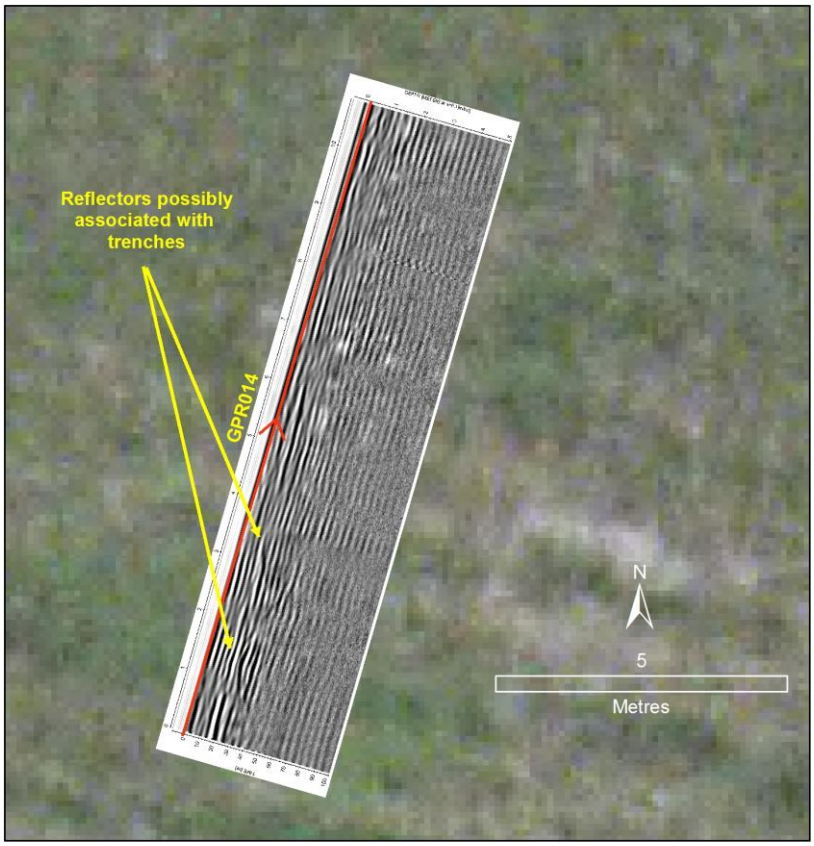

Figure 45. GPR section 014.

Figure 46 shows section GPR017. A very long curved, but weak reflector is seen covering the eastern two thirds of the section. This is interpreted as radar noise reflected down from the overhead tree canopy seen in the air photo. Another small reflector is visible at the approximate end of trench 34.

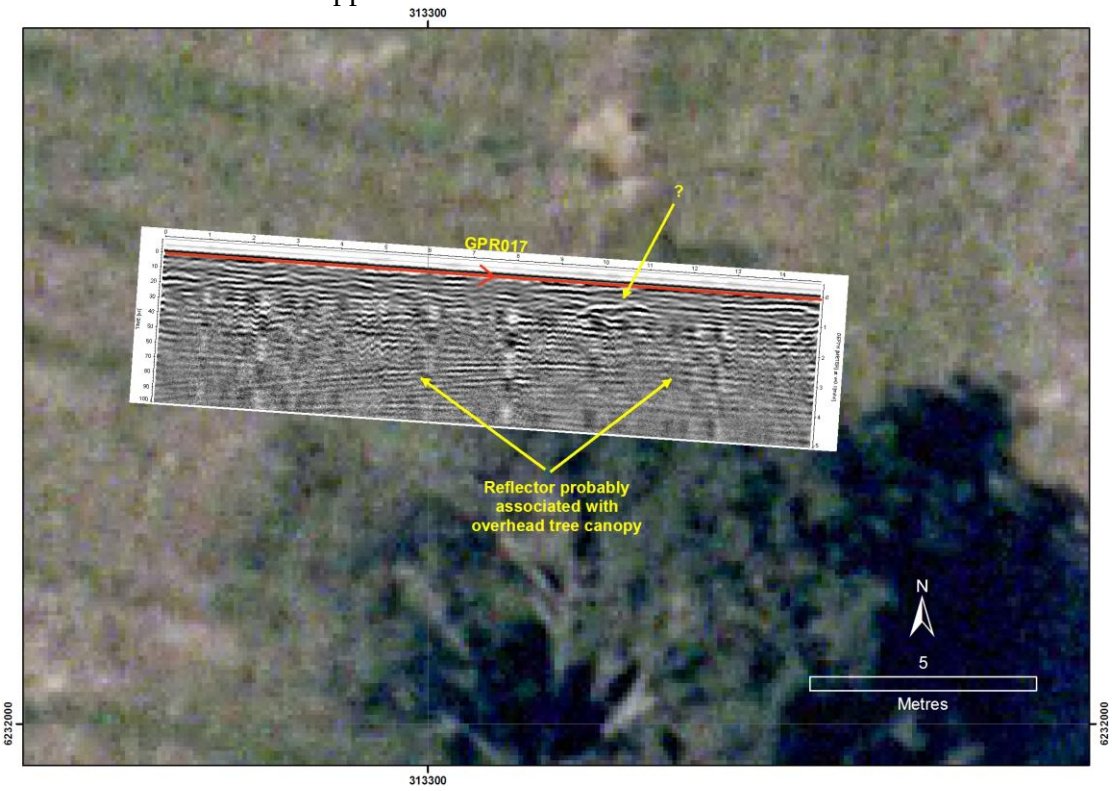

Figure 46. GPR section 017.

Figure 47 shows section GPR018 which was approximately aligned with the eastern end of trench 42. Strong reflection hyperbolae from a buried object are visible at 1 m depth, 2 m along trench 42.

Figure 47. GPR section 018.

Figure 48 shows GPR sections GPR020 and GPR021, which straddle the northern boundary of the eastern trench block, crossing trenches 50, 51 and 52. Section GPR020 has one string reflector which aligns wells with trench 51, although nothing significant can be seen at the location of trenches 50 or 52. Section GPR021 shows two weak reflections coinciding with trenches 50 and 51. Note, however that similar weak features are visible over undisturbed ground.

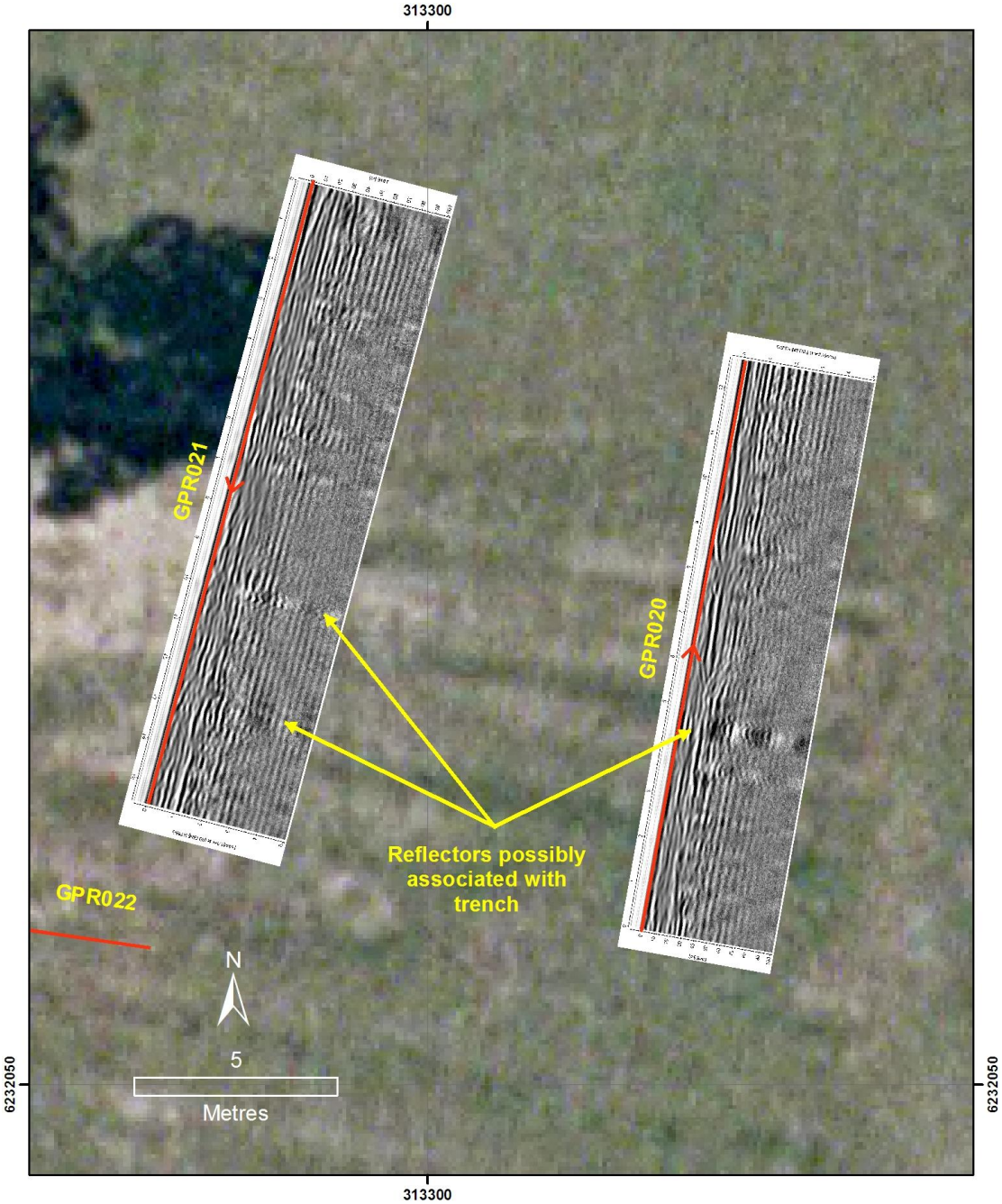

Figure 48. GPR sections 021 and 022.

In the above comparisons of the GPR data with the air photo, sections 10, 13, 19 and 20 are omitted due to a lack of features of any interest. While the included figures contain occasional GPR features which align in some cases with trenches shown on the air photo, in general these features are rare, inconsistent and vague. It is not considered possible to use the above data for the purpose of locating the trenches.

4.1.5 TDEM (EM61) FOR BURIED TRENCH MARKER DETECTION

Prior to commencement of this survey, an area check was conducted by ANSTO with a hand-held CSCOPE CS550 metal detector in an attempt to locate the aluminium capping of the old trench marker posts which were cut to ground level in 1984. Five buried marker posts were detected using this method and their position confirmed by digging (see **Figure 49**). The markers were buried under approximately 15-20 cm of soil, which may give an indication of how much thickness of 'top-dressing' cover has been added to the site since 1984. No markings or identification numbers were present on the exposed caps.

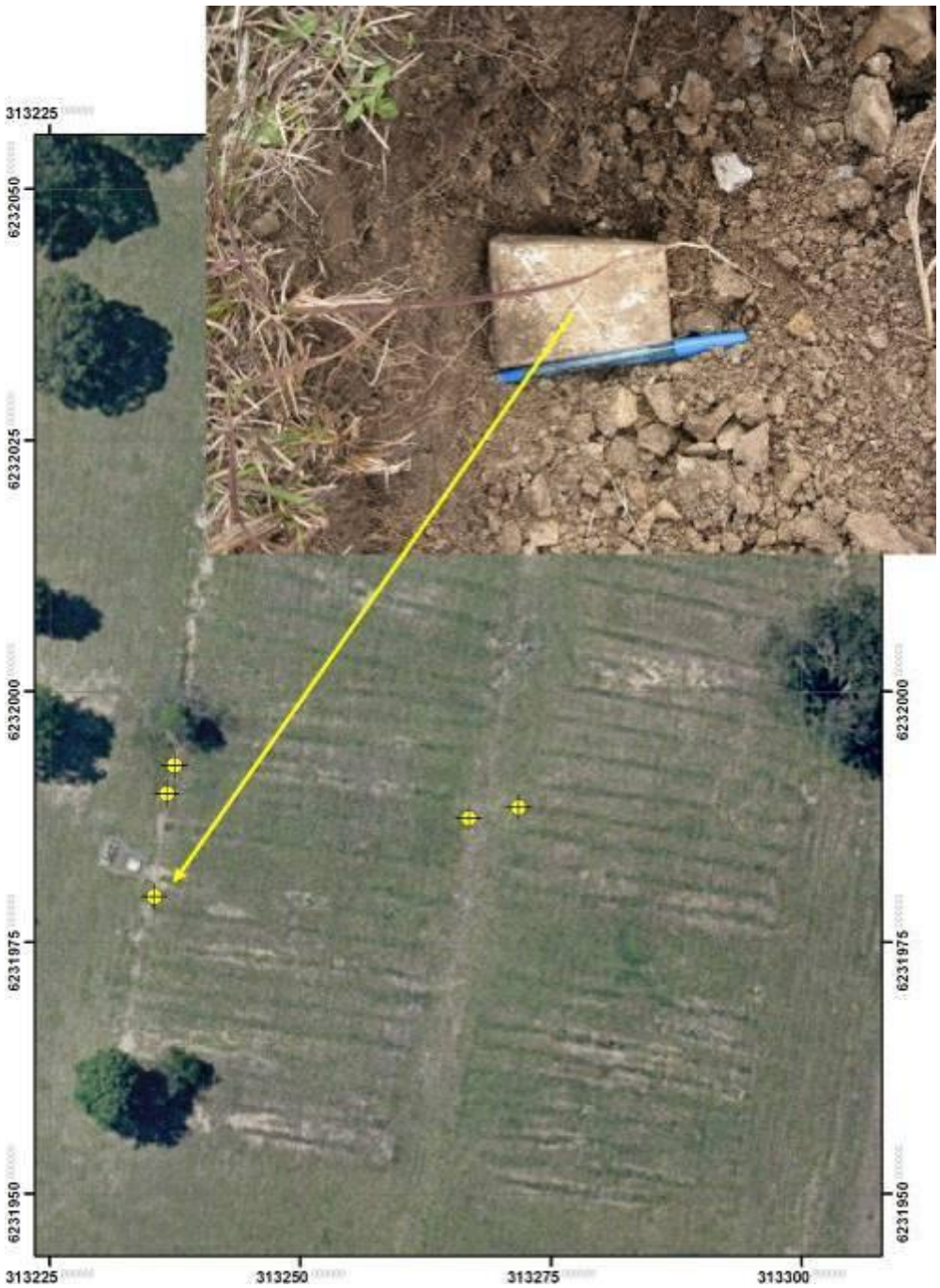

Figure 49. Buried trench marker posts located by metal detector, wedge shaped aluminium capping over sawn-off concrete post.

The TDEM data presented by Alpha Geophysics shows the likely position of 67 of the trench marker posts (indicated by cross and green arrow in **Figure 50**) and a list of MGA coordinates is provided (Table 5).

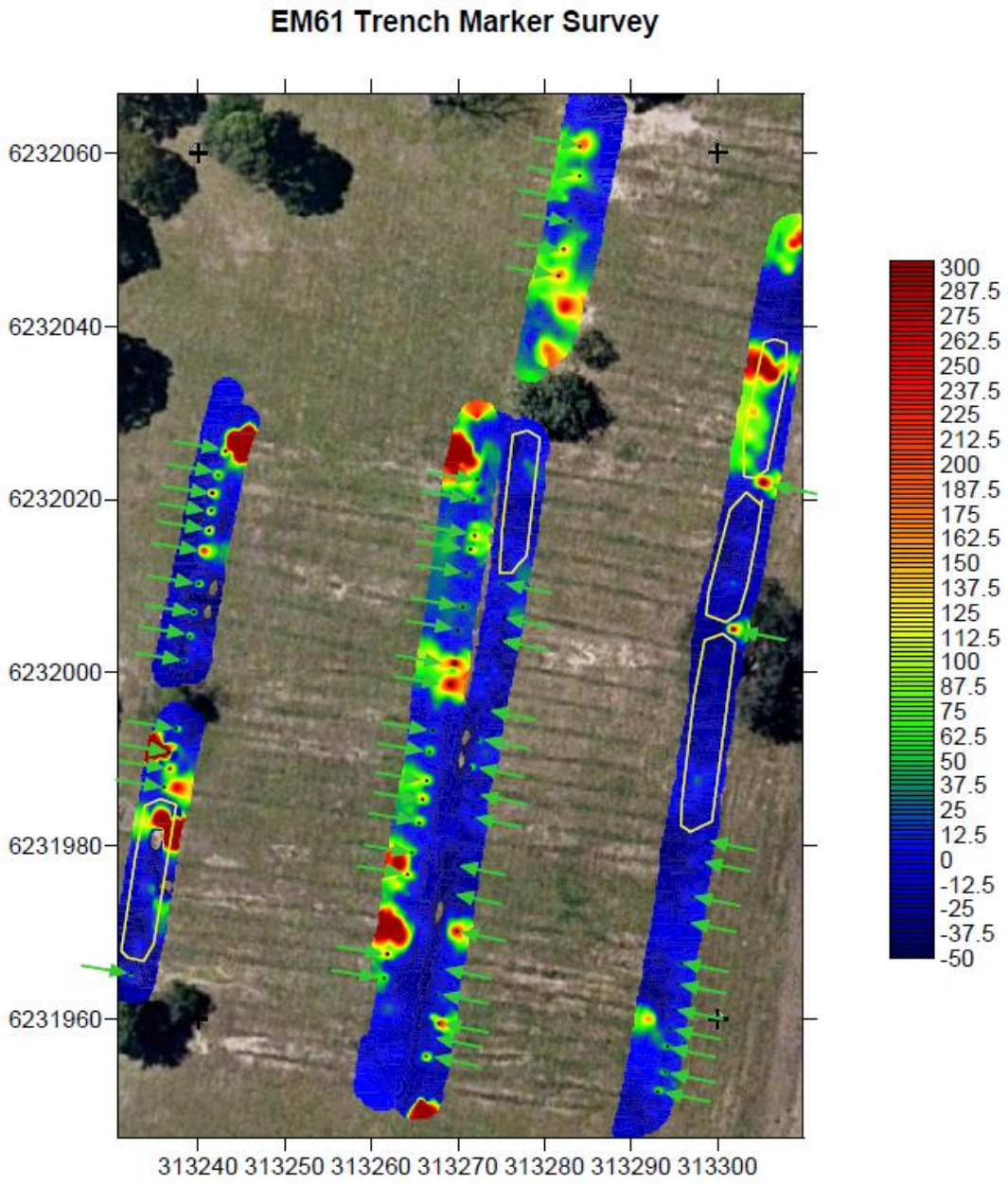

Figure 50. Results of EM61 trench marker survey.

Some variation can be seen in the intensity of EM response from various trench markers. The more intense responses are expected to be from locations where the flat topped aluminium cap is intact with the concrete post and under less cover of soil. More muted responses are expected from locations where the aluminium capping may be absent and only the vertical concrete post stub is remaining. Following from this observation, it is important to consider that the aluminium capping may have become separated from the concrete post during top-dressing exercises and moved to some

other position away from the concrete post, and that both items may be detectable separately by the EM-61.

By comparison with the air photo, it can be seen that not all marker post anomalies appear to align exactly with the end of a trench, and some appear offset by up to 50cm. Several of these locations were confirmed be digging to reveal an aluminium cap intact with concrete post. The reason for the offset is not known. In some parts of the survey area marked by the yellow circles in **Figure 50**, the marker post was not able to be detected by the EM61.

Given the uncertain history associated with the placement of the marker posts, and the lack of any identification marking on the recovered capping, no attempt has been to link a marker post with any specific trench. It is assumed, however, that the marker posts were placed at some distance beyond the end of the trench, and where the EM61 anomalies have defined a straight line, they can be used to infer the position of the trench block boundary in general.

There are also several larger and more intense EM features located over the trench area which cannot be explained by trench marker posts. These are expected to indicate the position of metal objects of various sizes, orientations and depths associated with waste buried within the trenches.

Table 5. MGA coordinates of marker posts interpreted in the EM61 survey.

Target Coordinates			
mE	mN	mE	mN
313243.18	6232025.59	313266.60	6231958.02
313242.30	6232022.78	313267.77	6231959.47
313241.63	6232020.75	313267.47	6231962.86
313241.53	6232018.72	313268.06	6231965.76
313241.24	6232016.40	313269.89	6231970.12
313240.59	6232014.10	313269.51	6231974.38
313240.08	6232010.30	313270.09	6231977.77
313239.50	6232007.00	313271.64	6231983.29
313239.01	6232004.20	313272.12	6231986.00
313238.34	6232001.39	313271.44	6231989.00
313237.46	6231993.55	313272.32	6231992.29
313236.69	6231990.74	313273.38	6231995.68
313236.69	6231988.90	313274.83	6232003.71
313236.11	6231986.77	313275.32	6232006.33
313232.24	6231965.28	313275.12	6232010.20
313272.22	6232022.30	313293.13	6231951.63
313271.83	6232019.98	313293.90	6231953.86
313271.93	6232015.81	313294.19	6231956.86
313271.44	6232014.27	313294.48	6231958.89
313270.96	6232011.55	313294.97	6231961.12
313270.57	6232007.59	313295.36	6231964.02
313269.99	6232004.87	313295.74	6231966.44
313269.60	6232001.10	313296.52	6231971.19
313269.12	6231998.68	313297.00	6231974.09
313267.09	6231993.35	313298.07	6231978.06
313266.70	6231990.84	313298.65	6231980.48
313266.41	6231987.55	313301.84	6232004.97
313265.93	6231985.32	313305.33	6232021.91
313265.54	6231982.61	313281.61	6232045.82
313264.67	6231979.22	313282.19	6232048.92
313264.18	6231976.70	313282.96	6232052.12
313261.86	6231967.51	313284.03	6232057.34
313261.47	6231964.70	313284.03	6232060.73
313266.31	6231955.70		

4.1.6 DRILLING BOUNDARY

The proposed core-hole and well sites were initially marked in the field by timber peg, taking care to avoid marking a site over the trenched area by allowing a 2 m safety margin taking into account the below factors:

- Visual sighting of subsidence or vegetation change over trenches in the field;
- Visual sighting of topographic step of backfill or top-dressing soil material in the field;
- Position of pre-existing wells.

In view of the ambiguity of the position of the edge of the trenches in some locations, the proposed sites were additionally checked that they fell outside a drilling boundary (see **Figure 51**) established by the consideration of each of the below factors:

- MGA (Map Grid of Australia) coordinates obtained from aerial photograph interpretation of trench position;
- MGA coordinates transformed from ISG drawing 100053D (AAEC, 1983);
- MGA coordinates from combined results of the dipole-dipole resistivity survey and EM61 marker post survey for trench detection.

MGA coordinates determined during the above exercise are presented in Table 6. In all cases the most conservative interpretation of the trench block corners was selected to establish the drilling boundary. In most cases the most conservative estimate originated from interpretation of the geophysics. Through this exercise, several proposed core-hole locations were moved to the drilling boundary.

Table 6. Interpreted MGA coordinates of the trench blocks extent used to define the drilling boundary.

Drawing 100053D		Air photo		Alpha Geophysics		Drilling boundary	
Easting	Northing	Easting	Northing	Easting	Northing	Easting	Northing
313243.20	6232028.28	313242.45	6232029.39	313241.41	6232028.17	313241.60	6232029.54
313274.02	6232023.54	313273.00	6232023.38	313273.81	6232022.28	313274.02	6232023.54
313231.68	6231957.52	313231.65	6231958.69	313230.52	6231957.89	313230.49	6231957.72
313259.28	6231953.29	313259.92	6231953.73	313260.77	6231952.47	313260.77	6231952.47
313284.34	6232066.38	313284.18	6232065.69	313284.37	6232068.54	313284.37	6232068.54
313309.80	6232062.00	313311.80	6232061.30	313313.35	6232063.58	313313.35	6232063.58
313266.27	6231952.23	313266.09	6231951.46	313264.68	6231951.03	313264.68	6231951.03
313292.59	6231948.35	313293.64	6231947.97	313293.83	6231946.22	313293.83	6231946.22

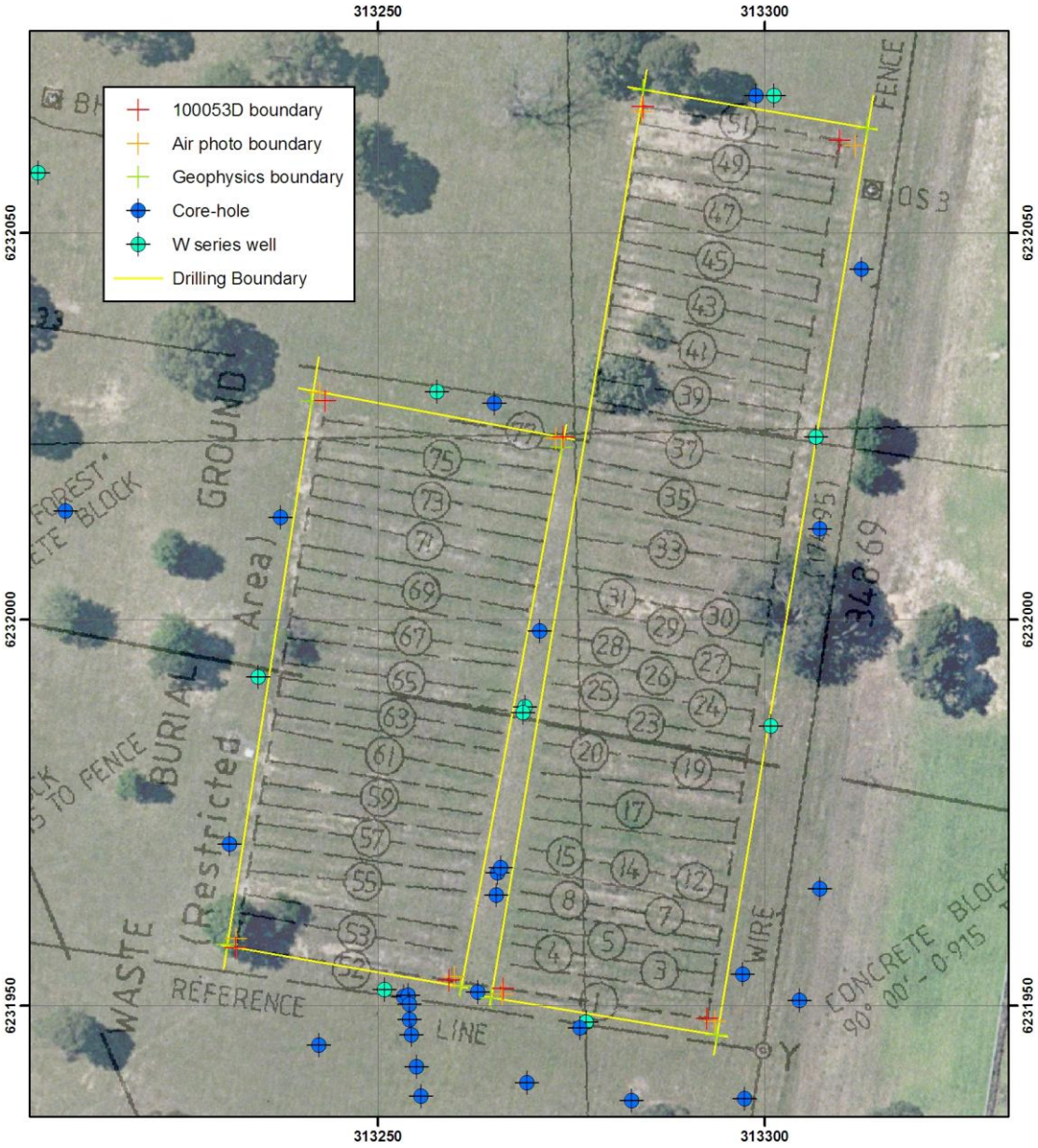

Figure 51. Location of drilling boundary and final location of drilling sites. The 100053D boundary refers to ISG coordinates of trench corners translated from Rygate & West plan, 1983 (See Figure 7).

4.2 Drilling Results

4.2.1 CH series

The CH direct-push core-holes were sited to meet one of the following criteria:

- in a ring around the perimeter of the trench blocks at a distance of 2 m;
- in an EW transect line parallel to the southern boundary and SE corner of the trench blocks at a distance of 10 m;
- along a potential groundwater flow pathway leading away from the trenches a total distance of 80 m toward the SE;
- along a potential groundwater flow pathway leading away from the trenches a total distance of 140 m toward the N;
- along potential groundwater flow pathways to the W and NW of the trenches at a distance of 30 m and 80 m respectively;
- at one control site established at the LFBG southern boundary fence 175 m from the trenches.

The location of the CH core-holes is shown in **Figure 52** and coordinates and depth of penetration listed in Table 7. A target depth of 5 m was set for all direct-push locations in order to obtain samples from below base of trench level (estimated at 3 m depth).

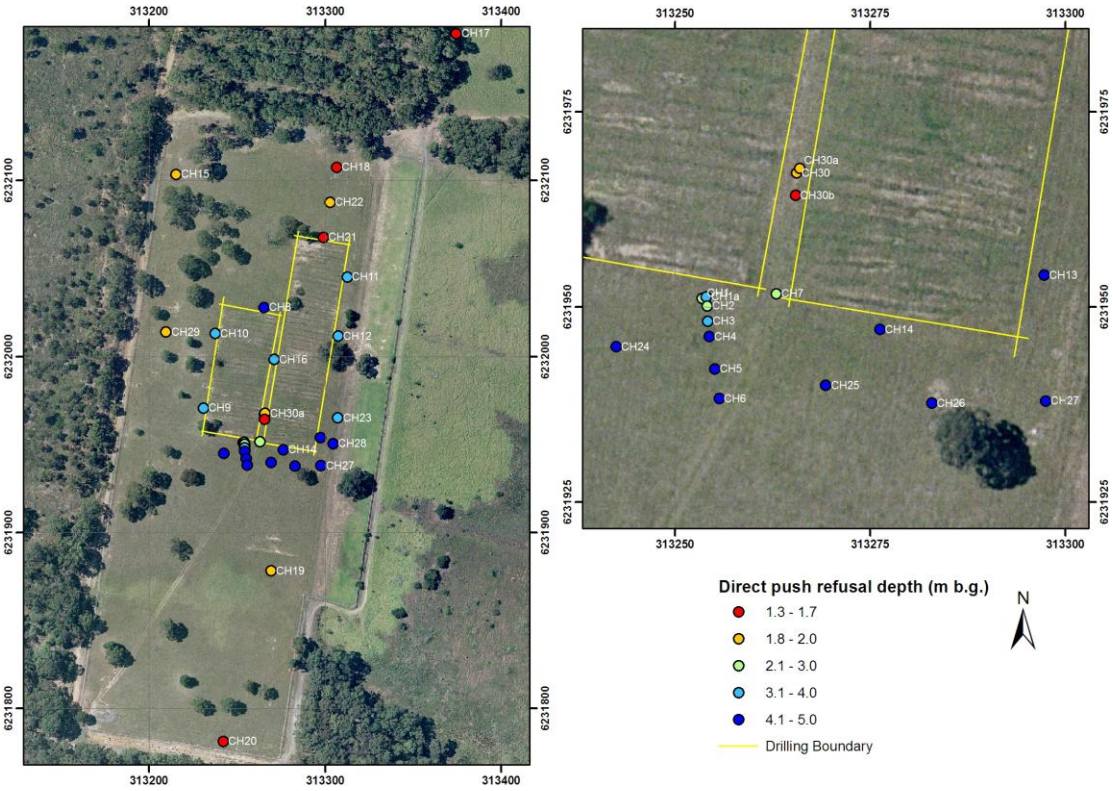

Figure 52. Location of direct-push CH series core-holes showing depth of push tube refusal.

Table 7. Table showing CH core-hole coordinates and depth of penetration.

Hole ID	Easting	Northing	Refusal Depth (m b.g.)
CH1	313253.42	6231951.14	3.0
CH1a	313253.96	6231951.31	4.0
CH2	313254.11	6231950.16	2.8
CH3	313254.12	6231948.22	4.0
CH4	313254.34	6231946.20	5.0
CH5	313255.06	6231942.06	5.0
CH6	313255.61	6231938.27	5.0
CH7	313262.96	6231951.71	2.5
CH8	313265.11	6232027.95	5.0
CH9	313230.83	6231970.87	3.4
CH10	313237.43	6232013.15	3.6
CH11	313312.59	6232045.27	4.0
CH12	313307.22	6232011.71	4.0
CH13	313297.26	6231954.09	5.0
CH14	313276.21	6231947.13	5.0
CH15	313215.12	6232103.62	2.0
CH16	313270.97	6231998.44	4.0
CH17	313374.49	6232183.62	1.3
CH18	313306.39	6232107.61	1.7
CH19	313269.32	6231878.27	1.9
CH20	313242.02	6231781.34	1.5
CH21	313298.96	6232067.80	1.7
CH22	313302.78	6232087.69	2.0
CH23	313307.20	6231965.14	3.6
CH24	313242.41	6231944.92	5.0
CH25	313269.28	6231939.97	4.8
CH26	313282.89	6231937.69	5.0
CH27	313297.47	6231937.97	5.0
CH28	313304.55	6231950.66	5.0
CH29	313209.60	6232014.02	2.0
CH30	313265.55	6231967.18	2.0
CH30a	313265.92	6231967.81	2.0
CH30b	313265.38	6231964.33	1.7

The target depth of 5 m was only achieved at 11 out of the 30 direct-push sites. Where penetration depth was not sufficient, the drill rig was moved ~1 m to drill again, and repeated to attempt improved penetration. Where the target depth was not achieved, push tube refusal occurred at an average of 3.6 m, and refusal depths ranging from 1.3 to 4.8 m (see **Figure 52**). Deeper cores were obtained in the vicinity

of the trench area, with the best penetration to target depth occurring in a clustered band immediately to the south of the trench area. This clustering may be indicative of a change in weathered lithology, and this should be considered when comparing their analytical data with other core-holes placed further from the trenches along potential flow pathways, where only shallow penetration was achieved.

Small pieces of hard siltstone recovered from the end of some refused push tubes suggest this material is the likely cause of refusal at many sites, although increasing general rock strength with depth of typical leached zone material may have also been a factor. Over-drilling by auger at four of these sites to target depth was accomplished with relative ease, although some difficulty was encountered penetrating occasional thin layers, with the drill stem lifting the rig off the ground at times. With persistence, the auger method abraded through these hard layers to achieve the full 5 m target depth. Small pieces of hard siltstone were also recovered at times during auger drilling. Successful penetration of the push tubes to target depth at some locations and not others suggests a non-uniform distribution of these hard layers. It is probable that these hard layers may locally restrict the downward flow of water through the unconsolidated leached shale material, supporting perched groundwater during recharge periods. Such water was not encountered direct-push drilling which took place under dry weather conditions in August 2009.

Most of the holes selected for auger over-drilling are located to the north end of the site (CH21, CH18, CH17). In each of these holes 'siltstone' material was recorded in the geological log up to 3 m thick as opposed to the weathered shale of the 'leached zone' found elsewhere at equivalent depth. This 'siltstone' recorded in the log does not refer to the hard thin bands mentioned above. Given the ease of augering, apart from the short-lived difficulty with the thin layers, this 'siltstone' is interpreted as a local increase in grainsize of the unconsolidated 'leached zone' material in which laminations were not detected. The auger cuttings lifted to the surface were generally dry and powder like in texture for both siltstone and weathered shale material. Comparison with the log of MB17 and MB19 in this area shows the same material has been previously interpreted as weathered shale.

Where penetration was successful, the direct-push cores provided an intact continuous sample through the weathered shale profile some distance into the leached zone (see **Figure 53**).

Figure 53. Five metres of direct-push core from CH13, showing topsoil, mottled clay zone and leached shale zone. Note increased compaction of the softer top layer.

A common feature observed through the CH cores, not readily identifiable in the more disturbed samples of other drilling methods, is the presence of narrow lenses of coarse size ironstone gravel identified in the leached shale zone, and identified as potential water bearing zones.

Bands of ironstone gravels were also logged in the diamond drill core retrieved from the angle hole CH31, at depths of 4 m immediately adjacent to trench 52. Deeper in CH31, a short intact sample of hard black parent shale material was recovered at 6 m, grading into the top of a 'siltstone' at 7 m directly beneath trench 52 (see **Figure 54**). On closer inspection, the 'siltstone' material at the base of the hole appears to have the same grain size and laminations as the more carbonaceous black parent shale material above it. Given there is no textural change, the material logged as 'siltstone' should here be considered a continuation of the shale unit rather than the beginning of a separate lens. In general, the first 7 m of hole (to 5 metres in depth) did not hold together well as a core and presents as highly fractured and unconsolidated pieces of rock material, albeit assembled in approximate order of depth in the core tray. The base of this loose material at 5 m is taken to represent the base of the leached zone at this location.

Figure 54. DDH core from CH31. Note diagonal laminations in parent shale material forming planes of core separation at 8 m are related to the 45 degree angle of coring, and these laminations would be flat-lying for the in-situ material.

4.2.2 Soil moisture profiles

Soil moisture profiles from ground surface to approximately 5 m depth are indicated by core samples taken at ~0.5 m intervals. Percentage soil moisture (mass of water / (mass of soil+ water)) was calculated from the ~30mm (length) x 38mm (diameter) samples, which were containerised immediately following drilling, then weighed wet, and after drying. Samples were taken from six cores: CH-8, CH-10, CH-12, CH-16, CH-23, and CH-25. Soil moisture percentages were typically about 20% at the 0.5 m depth which agrees with the observation of several precipitation events prior to drilling. Moisture percentages decrease to below 10% at lower depths, which agrees with the generally dry characteristic of the soils observed from 0.5-5.0 m. Note that the 0.5 sampling interval did not necessarily capture the most saturated layers. Often there were thin semi-saturated layers observed near ~3 m depth, but not right at the sampling depth, although increased saturation at this depth is apparent in CH-8 for example.

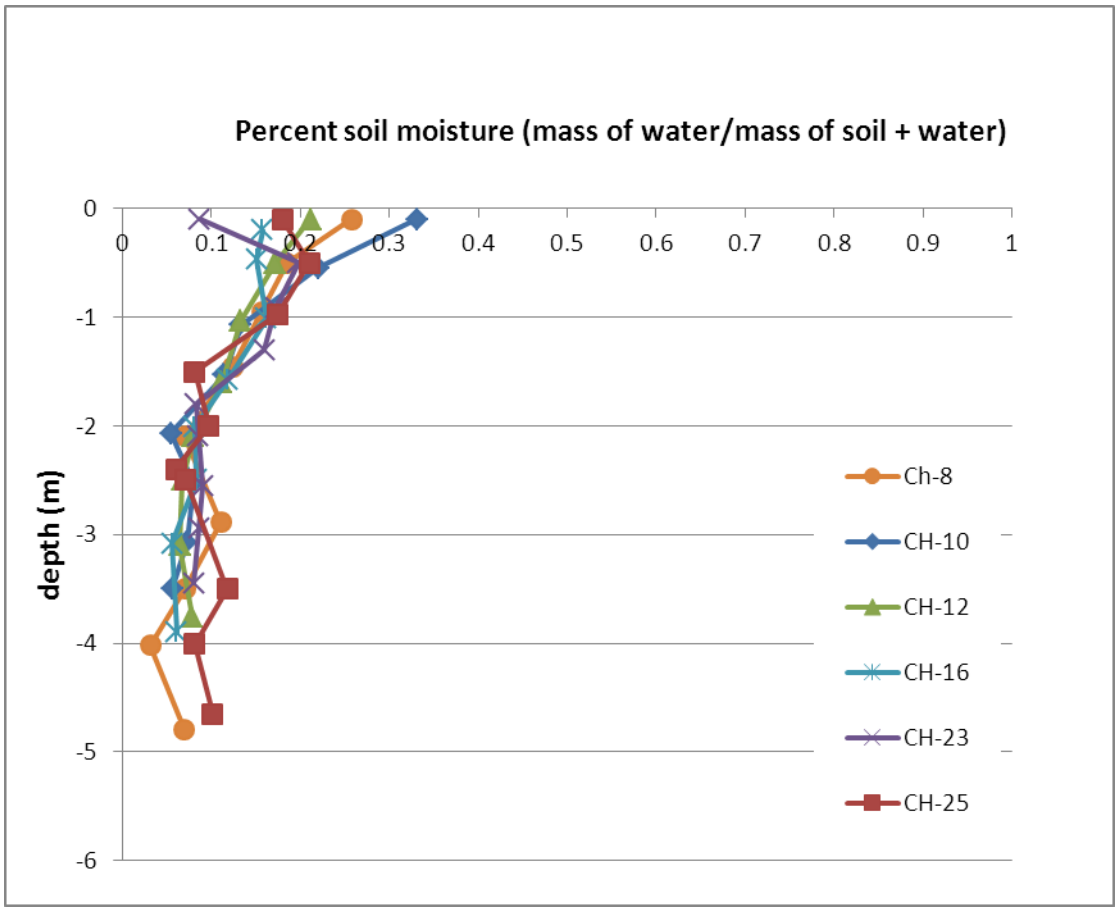

Figure 55. Percent soil moisture versus depth of selected CH direct-push cores.

4.2.3 W series

Following the basic rationale of the CH core-hole series distribution, holes for the W series wells were augered:

- in a ring around the trenches at a distance of 2 m;
- along a predicted groundwater flow pathway 45 m W of the trenches towards Harringtons Quarry;
- at a control site toward the SE corner of the LFBG site, 140 m from the trenches

The augering of the W series wells took place under wetter climatic conditions in September 2010, and a dramatic change in cohesion and adherence of auger cuttings was noted in some wet zones down-hole compared to the previous year. In general, where wet zones where encountered, W series auger cuttings remained intact on the auger stem (see **Figure 28**), resulting in increased confidence of the precision of sampling depth compared with the loose material encountered in the CH series (see **Figure 27**). The location of wet zones logged during drilling was used as the basis for deciding the level of screen placement during well construction, and these zones were also recorded on the W series geological logs (Coffey Environments, 2010; Appendix B). In the W series auger holes located close to the trenches, wet zones were detected consistently between 2 to 3 m, which is close to base of trench level at 3 m. Typically these wet zones were underlain by dry weathered shale material to the base of the hole. The deeper auger cuttings presented as dry crushed rock material beneath a wet outer skin, presumably the wet outer surface originating from water leaking down the hole from the shallower wet zone. These moisture observations indicate perched water at 2-3 m depth, and considering that each location prior to drilling was plugged from above with a metre of red mottled zone clay, it is likely this water has moved laterally from the trench area at this depth. A higher amount of water was encountered at this level during drilling of W5 and W15 resulting in hole collapse problems during drilling of these two wells and complications during well construction (see logs Appendix B). These two sites were areas noted on dipole-dipole resistivity transects 013 and 002 respectively (see **Figures 34** and **35**), showing an overlap of the bottom low resistivity layer with the trench boundary. Hence the resistivity data may also be indicating lateral water movement into the undisturbed zone at these locations. If so, these images would also suggest that the total resistivity measured (lithology plus water content) is being dominated by the electrical properties of the water content.

A 3 metre thick grey fine sandstone lens was encountered within the shale during the auger drilling of W1, W2m and the W2d air hammer holes located in the SE corner of LFBG. Rock material of this kind was not encountered at any other part of site during this campaign, although it is possible the grey fine sandstone may be similar to that encountered in CW drilled in 2000 (see **Figure 17**). Examination of previous logs shows fine sandstone was also encountered at this elevation in nearby MB11 and MB12. W1, MB11 and MB12 were all terminated in this layer, and notes in the MB geological logs suggest this layer was previously interpreted as the start of the interbedded shale/sandstone zone. The deeper W2m and W2d however show that the fine sandstone is underlain by a further 7 m of shale of moderate strength immediately overlying Hawkesbury Sandstone. A rapid inflow of water into the hole was observed

during drilling at approximately 11 m depth within this lower 7 m thick shale. A comparison of the lower 7 m of shale in W2d with the equivalent elevation in P1d and P2d shows interbedded shale/sandstone of similar thickness has been interpreted previously at these locations. This layer in W2d may be the lateral equivalent of the interbedded shale/sandstone zone with a local tendency towards shale, otherwise it may represent the edge of a separate lens of parent shale. The base of shale contours drawn in AAEC E22479 (see **Figure 15**) suggested a deepening of the shale begins at this edge of LFBG.

4.3 Well installation

The location of wells installed during this campaign are shown at **Figure 56**, and coordinates and other specifications are included in Appendix A. The location of abandoned wells is also included and marked with a white cross.

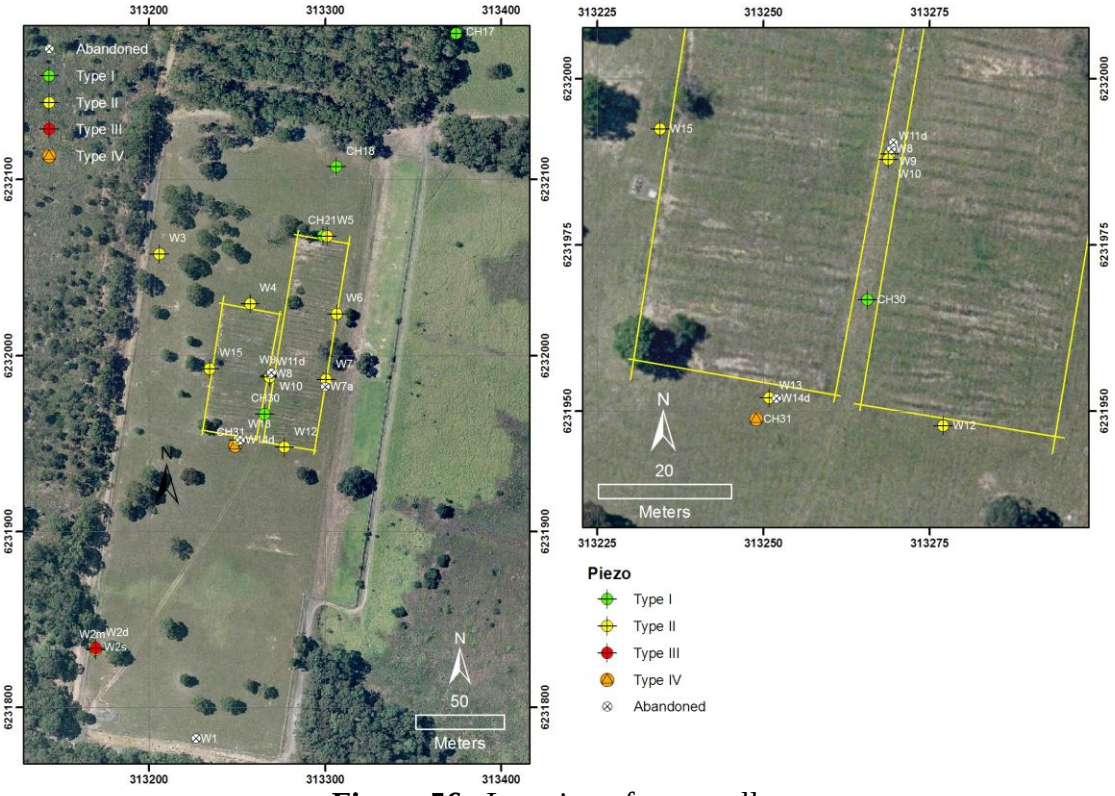

Figure 56. Location of new wells.

Generally, construction of the four Type I 'CH' and twelve Type II 'W' shallow piezometers proceeded according to specification, although a few problems with hole collapse of wet unconsolidated material were encountered in Type II 'W' wells as described in Section 3. These problems may have been avoidable with the use of wider diameter temporary casing to more closely match the hole size, although this would have required a larger rig capable of machine-emplacing such casing.

The Type III wells were designed to penetrate below the shale layer into the underlying sandstone. To prevent cross-contamination from the upper shallow groundwater, down through the shale, the contract required that the driller establish a dedicated casing with a seal within the shale layer, and demonstrate that the seal was effective prior to drilling deeper. This was not able to be accomplished for wells in the trench area. Significant difficulties were encountered with seal failure during first-stage construction of Type III 'W' deep piezometers W11d and W14d in the trench area. The second stage of installation of these wells was intended to penetrate the floor of the shale lens and to be continued into the Hawkesbury Sandstone, with the first stage upper seal preventing cross-contamination of aquifers. However, during testing of the seals, groundwater was observed mixing with the grout of the upper first stage seal preventing curing, with mixed water and liquid grout forcing its way to the standing water level. Because the seals were not effective, drilling did not proceed

below the shale layer and these wells were subsequently plugged and abandoned at the Stage I level, with the unsolidified grout cleared from the hole by air-blade, 'permanent' outer casing removed and the remaining hole filled with bentonite.

The upper seal of Type III W2d was placed in relatively dry conditions, and the second stage well construction continued according to specification. It was observed that due to the narrow casing diameters used, there is only space for a very small annulus of remaining seal between the outer casing (100mm ID) and air hammer diameter of 95 mm. It is possible that the upper seal was completely removed during second stage air hammer drilling.

W8, located in the middle of the trench area adjacent to W11d, also experienced seal failure. This well was originally intended to be screened within the parent shale as a Type II shallow piezometer, although due to recognition of the existence of a perched water table during the campaign, the design was modified to Type III in an attempt to obtain separation between the perched aquifer and deeper groundwater. Given the shallow position of upper seal emplacement, the permanent outer casing for W8 was capped and left in-situ.

The Type IV angle well design proceeded according to specification, despite being difficult to construct considering the unconsolidated and fractured material hanging over most of the hole. Well construction would not have been possible without the aid of machine placed and retracted temporary steel casing.

Future efforts to construct two-stage wells into the Hawkesbury Sandstone in the trench area may be more successful with the aid of a larger rig capable of wider hole diameters and/or machine emplacement of outer casings, similar to the procedure used for construction of CH31 angle hole. In addition, pressure injection of grout may assist with seal material emplacement, reduce dilution with formation water and allow the seal to cure and be proven water-tight. A wider diameter annulus will also be beneficial after second stage drilling and installation of inner casing, easing the introduction of second stage seal materials.

A record of the final turbidity measured at the end of 'W' series well development showed mixed success with final water quality. This result is possibly as good as could be expected given the fine and unconsolidated nature of the medium in which most wells were installed and the low transmissivity of the thin perched lens being sampled. The CH and W series wells are accessing a thin vadose zone water body perched within a clay system having very low yields, and will thus will not provide very low NTU samples similar that from a gravel-dominated aquifer. Type II wells W7, W3, W2m, W2s and W4 yielded the best results with final turbidity ranging between 5.8-13.9 NTU and no visible sediments, colour or cloudiness visible in purge water. Type III well W2d screened in the Hawkesbury Sandstone at the control site provided slightly cloudy water at 31.8 NTU, which may be attributable to the clayey nature of the uppermost Hawkesbury Sandstone, also reported during drilling of P1d (PPK, 2002). Type II wells W6, W13, W5, W15, W10 and W9 presented final turbidity between 39.3-83.2 NTU and displayed slight cloudiness or trace visible sediments in the final purge water. The worst results were obtained in W12 with a final turbidity of 430 NTU and sediment visible in the water, and this may indicate a problem exists with the screen or well construction of W12.

During well development, a gas build-up was noted in the field logs (Coffey, 2010) for well W5, observed each time the well was opened. No cause is suggested in Coffey Environments report, although it is noted that there were problems with hole collapse during well installation, and the well is built on top of 1.5 m of collapsed fill material at the base of the hole.

5 Conclusions/ Recommendations

This 2009-2010 campaign met the objectives of providing core samples and standardised groundwater wells in nearly all of the targeted areas, with the exception of deep wells and rock samples from the Hawkesbury Sandstone in the trenched area. The samples will allow detailed analysis of radiochemistry and transport mechanisms of waste related contaminants in close proximity to the trench area.

Much was learnt from the geophysical surveys, in addition to the intended purpose of helping define the trench boundaries. The 2009 shallow resistivity survey of the trench area showed patterns related to differing soil moisture inside and outside the trenched area, suggesting that the trenches may collect water during infiltration events and subsequently provide recharge to the weathered shale zone. The ground penetrating radar method was tested and proven to be ineffective at LFBG, most likely due to energy loss in the clay rich soil and weathered shale. The TDEM survey successfully mapped the position of the former trench marker posts, and was also proven to be an effective technique for detection of waste-related metal objects buried within the trenches.

The 2011 deeper resistivity survey showed variations in layering related to the weathering profile, stratigraphy and water content. Importantly, that survey also revealed a zone of differing resistivity traceable horizontally across six parallel survey lines, and vertically through the level of both shale and sandstone. It is unclear whether that pattern is caused by variations in lithology, or is a result of water content and chemistry. This zone could be further investigated by additional resistivity work and drilling.

The direct-push method provided the best-preserved core samples of the drilling methods used, but had however, refused penetration at variable depths ranging from 1 to 5 m requiring repeated attempts in some locations. Hollow stem auger drilling and sampling was possible to depths of at least 10 m. All auger holes were terminated due to the interception of water bearing zones rather than auger refusal.

Eighteen new groundwater observation wells were installed during the 2009-2010 campaign. Water quality monitored during well development was satisfactory for most wells, given the low-yield perched water body within a fine and unconsolidated weathered shale substrate, yielding a final turbidity range from 5.8 to 81.2 NTU, and one outlier of 430 NTU. This high turbidity result is from W12 and may indicate an unreported problem with construction of this well.

During this campaign, some opportunities were identified for improvement of well construction practices in the event of future drilling. Well construction was complicated in places by instability of the unconsolidated and wet weathered shale medium that sloughed into the borehole after drilling but prior to well construction. Such problems may be avoided during future well installation by the use of rig-installed temporary casing appropriate for the hole diameter, particularly a casing-advance system that can effectively seal off the wall of the borehole through the wet layer that was typically encountered at 2-3 m depth. Pressure injection of grout and a wider outer annulus may also assist with seal installation in two-stage Type III wells.

CONCEPTUAL MODEL

In addition to achieving most sampling objectives, the conceptual geological and groundwater framework of the site has been further advanced. The core, moisture and geophysical observations of this campaign combined with prior knowledge of the site and its neighbours tend to suggest subsurface water is located in three vertical zones at LFBG, similar to that predicted by Mumme (1974).

Near the trenches, perched water exists high in the leached shale zone at 2-3 m depth, and is encountered in multiple W series wells. This perched water may be recharged directly by rainfall. However, given that around 1 metre of clay was encountered during the drilling of every hole, the perched water may instead be being recharged laterally through the walls of the trenches. The patterns observed in the shallow resistivity survey appear to support the idea of lateral recharge from the trenches. The occasional overflow of boreholes in the vicinity of, but slightly downhill, from the trenches (OS2 and OS3), which is observed following major rainfall events, also supports this recharge mechanism. The deep resistivity survey suggests that the perched water occurs in disconnected pockets of limited lateral extent. This could be associated with the occurrence of the thin, hard siltstone layers encountered during drilling, assuming these represent a barrier to downward flow. Flow of perched water may be being diverted laterally some distance by the hard siltstone layers, where these are present, and also by the remnant laminated structure (fabric) variably present in the weathered shale. As the trench area occurs at the crest of a hill, the perched water may only exist during periods of recharge (‘wet years’) and may dry up altogether during ‘drought years’. Continued monitoring of water levels in the W series wells will demonstrate whether this occurs. The seepage observed in the areas of lower topography during heavy rainfall may be the partial surface expression of the perched water.

Unconfined aquifer water occurs in the lower leached shale zone, encountered in the first stage drilling of W8, W11d, W2d (screened in W2m) and in the Type IV angle well CH31. Several metres of dry weathered shale material were invariably encountered in between the perched water bearing zone and this lower unconfined aquifer water. This deeper unconfined aquifer may be perched by the relatively impermeable parent shale, although new wells were not able to be extended deep enough to test this assumption due to Type III well construction difficulties (seal failure), with the notable exception of CH31. Conceivably, the unconfined shale aquifer water may be in contact with immobile water trapped in the structures of the underlying parent shale. It is possible the unconfined aquifer water is recharged by leakage from the overhead perched water zone through breaks in the hard siltstone layers or through the ironstone gravel lenses observed for the first time in the direct-push and DDH cores. If the parent shale behaves as an aquitard, groundwater in the unconfined shale aquifer is likely to flow laterally and down-gradient through the leached zone southeast and north from the trenched area to the edge of the shale lens, expressed some distance offsite as surface water (for example at Turtle Ck). Given the position and relative level of the leachate extraction system in Harringtons Quarry, groundwater in the north-western portion of this aquifer may also be partially captured by Harrington’s Quarry leachate extraction. Groundwater in the southern portion of this aquifer may possibly be connected to, and preferentially flowing

through, fine sandstone lenses or interbedded shale/sandstone zones where these occur in connection with weathered shale.

Confined aquifer water occurs in the underlying Hawkesbury Sandstone. This aquifer is screened by wells P1D, P2D and W2D. Pump test data suggests this aquifer is most likely recharged from areas lateral to the shale lens, especially from the south-west according to the natural topography, and the SITA LH-II landfill is now in this pathway. The sandstone aquifer may be connected to the sandstone floor of Harrington's Quarry landfill. Toward the fringes of LFBG, the sandstone aquifer may also be connected to the shale aquifer in places via fine sandstone lenses or the interbedded shale/sandstone transitional zone.

Regarding older wells at the LFBG, given their uncased or full-length screen construction, most of the pre-existing deeper BH and MB series wells probably link topsoil with the perched water and unconfined aquifer water in the one screen interval. Groundwater samples from these wells therefore could be mixtures of both the upper perched water, lower unconfined aquifer water, with additional direct rainfall input through the near-surface vadose zone. Some of these older wells may provide a conduit to readily collect rainwater infiltration. The majority of the newly constructed W and CH series wells in the vicinity of the trenched area will provide unmixed groundwater samples from the perched water layer, with CH31 providing unmixed water from the unconfined shale aquifer. W2m and W2d will provide unmixed water from the unconfined shale aquifer and confined sandstone aquifer respectively, although these wells are some distance from the trench area. Completion of the proposed W8, W11d and W14d with an improved construction method would provide unmixed samples from various depths at the centre of the trenched area.

A conceptual geological model is compiled below at **Figure 57** taking into account the drilling and geophysics from this campaign, combined with prior site knowledge from geological logs and investigations on neighbouring sites.

RECOMMENDATIONS

1. Wenner-Sclumberger resistivity survey along parallel lines extended north and south beyond LFBG site boundary and in night soil area, to repeat interception of resistivity features in shale and sandstone. Data to 50m depth.
2. Auger/diamond drill coring at proposed site W11d (deep samples below trench area) and also near W7 (samples in resistivity feature if confirmed in repeat survey). Drilling by a combination of auger for the top 5 metres and continue to hole base using diamond drill coring to equivalent hole base as P2d at ~100m elevation, to describe geology beneath trench area and attempt repeat intersection of shale bands at 107m and 104m elevation.
3. Completion of two stage Type III deep well installation into Hawkesbury Sandstone at trench area at proposed sites W11d and W14d. Revisit the Type III well design, and work with potential contractors to ensure they have the equipment and experience required. Suggest the driller use a casing-advance method, or similar method for machine-placed outer casings, and pressure injected grout seals.

4. Complete mapping of trench area using EM-61 TDEM to locate buried metal drums and instruments.

5. Desktop study of SITA Lucas Heights II floor of landfill elevation model and piezometric surface projected to Little Forest.

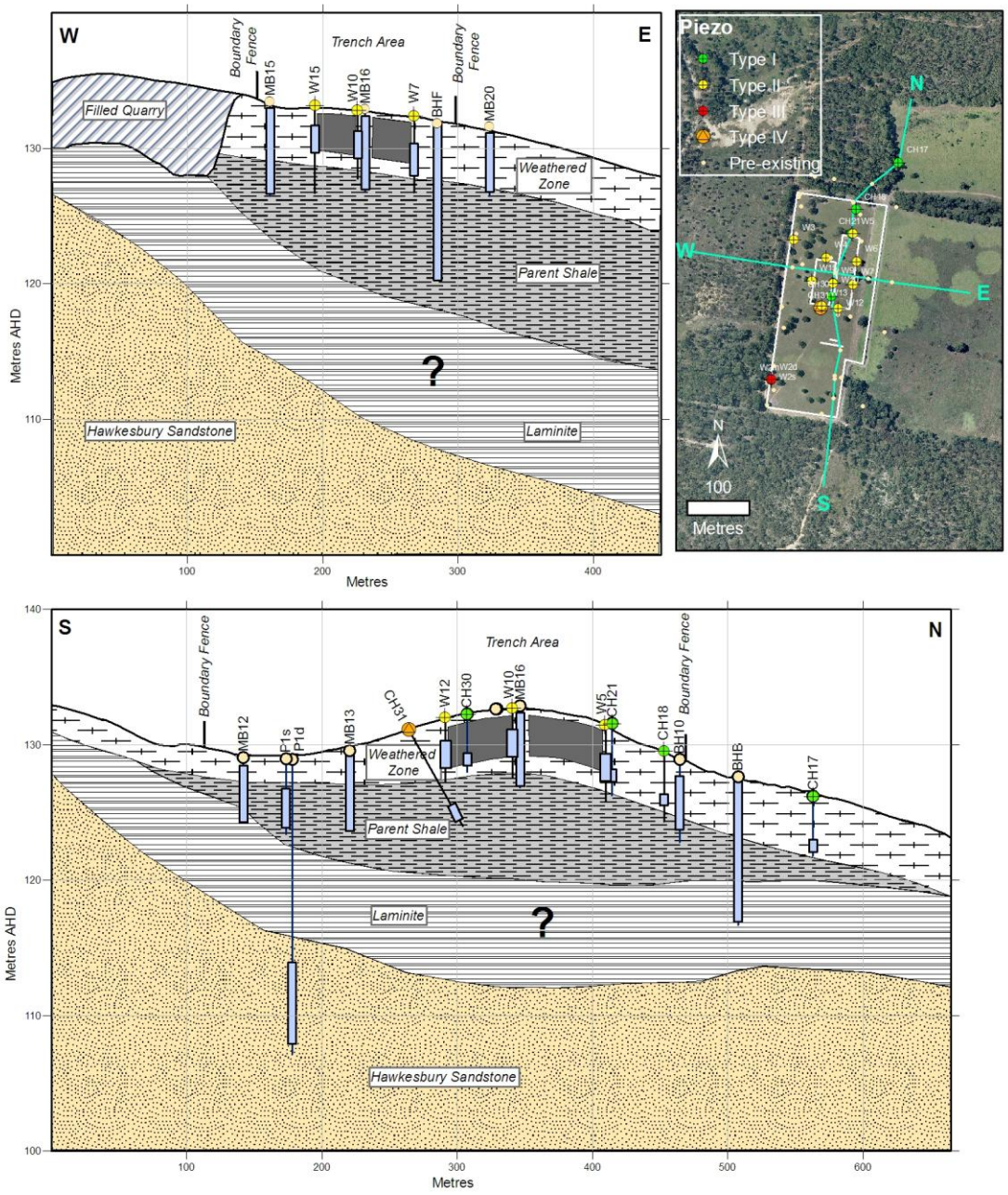

Figure 57. LFBG conceptual geological model.

6 References

AAEC, 1984, Little Forest Burial Ground, AAEC File LH87589.

AAEC, 1985, The Little Forest Burial Ground – an information paper, AAEC, DR19.

Adamson & Lloyd, 1961, Construction materials of the County of Cumberland, Geological Survey of NSW, GS1961/142.

ANSTO, 2002, Submission to ARPANSA on the site geological investigations for the replacement research reactor at Lucas Heights, Report RRRP-7500-3BEAN-002-A.

ARMCANZ, 2003, Minimum construction requirements for water bores in Australia. National minimum bore specifications committee, Agriculture and resource management council of Australia and New Zealand.

Bembrick C., Herbert C., Scheibner E. & Stuntz J., 1980, Structural subdivision of the Sydney Basin, In: *Herbert & Helby (Eds), A field guide to the Sydney Basin, Geological Survey of NSW, Bulletin 26.*

Bowman H.N. and Stewart T.R., 1974, Wollongong 1:50000 Geological Sheet Series 9029-II, Geological Survey of NSW.

Bowman, 1974, Geology of the Wollongong, Kiama and Robertson 1:50000 Sheets 9029-II, 9028-I & IV, Geological Survey of NSW.

Bradd, 2003, A report on the hydrogeology of the Little Forest Burial Ground, ANSTO/EM TN-01/2003.

Branagan D. and Packham, 2000, Field geology of NSW, NSW DMR.

Branagan D., 2000, Structural geology of the Hawkesbury Sandstone, with particular reference to the city of Sydney and nearby areas, *In: McNally G.H & Franklin B.J. (Eds.), 2000, Sandstone city, Sydney's dimension stone and other sandstone geomaterials, Environmental, Engineering and Hydrogeology Specialist Group, Geological Society of Australia, Monograph No 5.*

Clarke, Rev W.B., 1878, Remarks on the sedimentary formations of NSW, Royal Astronomical Society, Sydney.

C.M.S Surveyors Pty Ltd, 2010, Plan showing boreholes at Little Forest Burial Ground – Lucas Heights, (*Unpublished survey data*).

CPI (Coffey Partners International), 1991, Little Forest, Potential contaminated lands investigation, West Menai, Report E112/1-AC.

Conaghan P.J. and Jones J.G., 1975, The Hawkesbury Sandstone and the Brahmaputra: A depositional model for continental sheet sandstones, Australian Journal of Earth Sciences, 22:3, 275-283.

Conaghan P.J., 1980, The Hawkesbury Sandstone: gross characteristics and depositional environment, In: *Herbert & Helby (Eds), A field guide to the Sydney Basin, Geological Survey of NSW, Bulletin 26.*

Conway N.F. and Dudaitis A., 1972, Environmental survey at the A.A.E.C. Research Establishment Lucas Heights, results for the period January – July 1970, AAEC/E246.

Cook J.E., Dudaitis A., 1970, Environmental survey at the A.A.E.C. Research Establishment Lucas Heights, results for 1969, AAEC/E151 Supplement No 3.

Cooper & Richards Surveyors Pty Ltd, 2009, ANSTO Boreholes, (*Unpublished survey data*).

Dickson T.W., 1967, Extractive resources of the Menai area, Geological Survey of NSW, GS1967/209.

Domenico P.A. and Schartz F.W., 1990, Physical and chemical hydrogeology, John Wiley & Sons, Inc, Singapore.

Douglas and Partners and Coffey Partners International, 1992, (Joint) Report on hydrogeological investigation proposed extension regional waste depot Lucas Heights, Report CPI E156/1-CJ; DP 14780.

Douglas Partners Pty Ltd, 2006, Report on groundwater bore installation – Harrington's Quarry – Lucas Heights Waste Management Facility, Report 43626.

Douglas & Partners, 2007, Draft water balance study – Harrington's Quarry – Lucas Heights, Project 44628.

Ellis W.R., 1977, Possible methods of disposal of the AAEC's low and medium level solid radioactive waste and an environmental impact assessment of the reopening of an existing burial ground, AAEC/E421.

E.E.S. (Environmental & Earth Sciences Pty Ltd), 2001, Little Forest Night Soil Disposal Area, Lucas Heights, NSW, Report 101020.

Fergusson and Hosking, 1955, Industrial clays of the Sydney region, NSW: geology, mineralogy and appraisal for ceramic industries, Australian Journal of Applied Science, 6, No 3, pp 380-407.

Geological Survey of NSW, 1967, DM Camden DDH 85 lithological section, NSW Department of Mines.

Geological Survey of NSW, 1967b, DM Camden DDH 86 lithological section, NSW Department of Mines.

Geological Survey of NSW, 1972, DM Campbelltown DDH 4 geological log, NSW Department of Mines.

GHD, 2003a, Groundwater contamination assessment report for: Northern boundary – Harrington's quarry, Lucas Heights NSW, Report 2111350.

GHD, 2003b, Additional groundwater contamination assessment report for: Northern boundary – Harrington's quarry, Lucas Heights NSW, Report 2112062.

Giles M.S. and Dudaitis A., 1986, Environmental survey at Lucas Heights Research Laboratories.

Giles M.S., Foy, J.J., Hoffmann E.L., 1990, Environmental survey at Lucas Heights Research Laboratories, 1988, ANSTO/E689.

Guinea A., 2011, Electrical resistive tomography – Little Forest (*Unpublished*).

Harper, 1915, Geology and mineral resources of the southern coalfield, Geological Survey of NSW, Geology No 7.

Herbert C., 1979, The geology and resource potential of the Wianamatta Group, Geological Survey of NSW, Bulletin 25.

Herbert C. and Helby R. (Eds), 1980, A guide to the Sydney Basin, Geological Survey of NSW, Bulletin 26.

Herbert C. and Uren R., 1972, Duffys Forest shale deposit – proposed drilling programme, Geological Survey of NSW, GS1972/199.

Hoffmann, E., Loosz, T., Ferris, J., 2008, Environmental and Effluent Monitoring at ANSTO Sites, 2006-2007, ANSTO/E-762.

Isaacs and Mears, 1977, A study of the burial ground used for radioactive waste at Little Forest area near Lucas Heights NSW, AAEC/E427.

Jol H., 2009, Ground penetrating radar theory and applications, Elsevier B.V., Amsterdam.

Joplin G.A, Hall L., McElroy C., Noakes L.C., Perry J., 1952, Wollongong 4 Mile Geological Series Sheet I 56-9, Geological Survey of NSW.

Loke M.H. and Barker R.D., 1996, Rapid least-squares inversion of apparent resistivity pseudosections by a quasi-Newton method, Geophysical Prospecting, 1996, 44, 131-152.

Loke M.H, 1999, Electrical imaging surveys for environmental and engineering studies, Heritage Geophysics.

Loughnan et al, 1962, Weathering of some Triassic shales in the Sydney area, Australian Journal of Earth Science, 8:2, pp 245-257.

Lovering J.F., 1954, The stratigraphy of the Wianamatta Group Triassic system, Sydney Basin, Records of the Australian Museum 23(4):169-210.

Lovering J.F. and McElroy C.T., 1969, The Sydney Basin, Triassic system, Wianamatta Group, In: *The geology of New South Wales, Geological Society of Australia – Journal 16(1), 417-423*.

McKibbin D. and Smith P.C., 2000, Sandstone hydrogeology of the Sydney region. *In: McNally G.H & Franklin B.J. (Eds.), 2000, Sandstone city, Sydney's dimension stone and other sandstone geomaterials, Environmental, Engineering and Hydrogeology Specialist Group, Geological Society of Australia, Monograph No 5*.

McNeill J.D., 1990, Use of electromagnetic methods for groundwater studies, In *Ward S.H. (Ed),1990, Geotechnical and environmental geophysics, Society of Exploration Geophysics.*

McNeill J.D., 1996, Application of time domain electromagnetic techniques to UXO detection, Geonics Ltd Technical Note TN-32.

Mumme, 1974, Results of an early feasibility study of the Little Forest Burial Ground, AAEC ER/UN51.

Pells P.J.N, Mostyn G., Walker B.F., 1988, Foundations on sandstone and shale in the Sydney region, Australian Geomechanics, Dec 1988.

Pittman, 1903, Geological sketch map of the Sydney region, Geological Survey of NSW.

Rose G., 1966, Wollongong 1:250000 Geological Series Sheet SI 56-9, Geological Survey of NSW.

Sherwin L. and Holmes G.G., 1986, Geology of the Wollongong and Port Hacking 1:100000 Sheets 9029, 9129. Geological Survey of NSW.

SKM (Sinclair Knight Merz Pty Ltd), 2003, Little Forest Burial Ground – Boreholes (*Unpublished survey data*).

Slansky E., 1974, Notes on clay mineralogy of the Wianamatta Group, Geological Survey of NSW, GS1974/273.

Slansky E., 1974b, Xray identification of shales, Appin-Heathcote-Menai areas, Geological Survey of NSW, GS1974/284.

Slansky E., 1975, Clay mineral identification of five samples from Lucas Heights, Geological Survey of NSW, GS1975/334.

Standard J., 1964, Stratigraphy, structure and petrology of the Hawkesbury Sandstone, USYD PhD thesis.

Stroud W.J., 1974, The geology and low cost extractive resources of the Camden, Campbelltown, and Port Hacking 1:50000 sheet areas, Geological Survey of NSW, GS1974/193.

Stroud W.J., Sherwin L., Ray H.N. and Baker C.J., 1985, Wollongong – Port Hacking 1:100000 Geological Series Sheet 9029-9129, Geological Survey of NSW.

Stuntz J, 1971, Port Hacking Geological Series Sheet 9129, Provisional 1:100 000.

Van Heeswyck, 1978, Notes on operating and abandoned extractive sites on the Wollongong and Port Hacking 1:100 000 map sheets, Geological Survey of NSW, GS1978/299.

Willan T.L., 1925, Geological map of the Sydney district, Dept. of Mines NSW.